

VLA Test Memorandum No. 154

Tests and Recommendations  
for Tilt Sensors  
to Help Improve Pointing  
on the VLA

C. Janes and A. Sittler

December 1989

Table of Contents:

- I. Improving Pointing of the VLA
  - II. Description of the Tilt Sensor
  - III. Tests Performed on the Tilt Sensor Boxes
  - IV. Conclusions and Recommendations
- Bibliography
- Figures
- Documentation
- Appendix A: Manufacturer's literature



*TESTS AND RECOMMENDATIONS FOR TILT SENSORS  
TO HELP IMPROVE  
POINTING ON THE VLA*

I. Improving the pointing of the VLA.

Pointing of the VLA is about 15 arcseconds in practice (1 & 7). If the pointing must be accurate to at least 1/10 of the received signal beam width, the VLA is currently limited to a wavelength less than limitations imposed by, for example, the figure of the antenna. To observe efficiently at 43 GHz, the pointing must be improved to 1/10th beam width or 8 arcseconds for an 85' diameter antenna (4), and that is the immediate goal of the project to improve pointing.

Coefficients for pointing corrections are measured whenever an antenna is moved to a new pad. The corrections for tilt are expressed as follows:

$$\begin{aligned} \text{Tilt Y} &= (A1 \cos(AT) \sin(ET)/\cos(ET) + A2 \sin(AT) \\ &\sin(ET)/\cos(ET) + A6/\cos(ET) + A7) 60 \text{ arcseconds, and} \\ \text{Tilt X} &= (E1 \sin(AT) + E2 \cos(AT) + E3 \cos(ET) + E5) 60 \\ &\text{arcsec.} \end{aligned}$$

where Tilt Y = tilt parallel to elevation axle in arcsec.  
Tilt X = tilt perpendicular to elevation axle in arcsec.

AT = antenna position in azimuth, geographical  
ET = antenna position in elevation, geographical  
A1, A2, A6, A7, E1, E2, E3, and E5 are pointing coefficients

A list of coefficients current for the D array, December 1989, is shown in figure 1.

The equations and coefficients shown above correct for the bulk of repeating errors. Differential heating of the structure, wind loading, loose structural members, and encoder errors are some of the conditions that result in pointing errors not corrected by the coefficients.

Thermal expansion of structural members can cause 10's of arcseconds of pointing error (1) (figure 2). Insulation was applied to the antenna support in 1983 to 1985 to reduce temperature-induced tilts (4). Pointing, especially daytime pointing, was improved significantly.

Tilt sensors were tested by Dave Weber (7), Bob Newell (8), and Peter Dewdney (9), in an attempt to improve pointing further; 8 sensor boxes were made as a result of their studies. Four of these boxes have been mounted on VLA antennas, and various tests performed. The purpose of this paper is to describe the tilt sensors and tests, and offer recommendations for further studies.

## 2 Tilt Sensor Tests

### II. Description of the Tilt Sensor.

The sensor selected for the eight tilt measuring boxes is the Schaevitz LSOC-1. A pendulum inside the device is attracted by gravity. The torque current to servo the pendulum back to a reference position is passed through a precision resistor. The voltage generated across the resistor is the signal output. The sensor unit is filled with oil for damping; *maintenance personnel are cautioned against opening all ports except the one used for the signal connector.* Excerpts from the manufacturer's literature are included in Appendix A as well as interpretation of the specifications to arcseconds.

The tilt sensor is mounted inside a cast aluminum box on a tilt table (Dwg 1). The tilt table may be altered in tilt by means of a micrometer movement at the end opposite the ball bearing hinge. An adjustment of one micron on the micrometer results in a change of 2 arcseconds of tilt. There are two tilt sensors in the box, oriented orthogonally. A heating pad is mounted to the tilt table on the side opposite the tilt sensor. A thermistor also mounted to the tilt table provides the feedback for a temperature controller unit to servo control the temperature to setpoint near 40 C. Two heating control units are included in each box, one for each tilt table. A separate AD590JH temperature sensor provides a temperature readout to the Command and Monitor System.

The box mounts to the antenna by means of a mounting plate which is separated from the sensor box by an insulating pad and 4 stainless steel mounting posts through which pass the mounting bolts.

The box is connected to 120 VAC for the heating control, and the signal output is connected to a custom circuit board, the M24 module (Dwg 2 and 3). The M24 includes the instrumentation amplifiers used to scale and amplify the tilt and temperature signals. The signal cable also provides the DC power for the tilt sensors.

Though the resolution of the Schaevitz device is specified at 0.07 arcseconds and the range at  $\pm 1^\circ$ , the 7.2 gain of the instrumentation amplifier in the M24 module and the 12 bit analog to digital converter (ADC) in the data set limit the effective resolution to 0.5 arcseconds (LSB), and the range to 0.56 degrees ( $\pm 10$  VDC). The range and gain were conveniently selected so that 1 arcsecond = 10 mv at the output of the data set.

Dave Weber and others experimented with bubble tilt sensors, but found that the settling time was longer than for the pendulum-type devices. We are not aware of what search, if any, was conducted for other alternate tilt sensing devices. Schaevitz offers a sensor with an improved temperature coefficient, linearity, and sensitivity, but the manufacturer does not comment on long term stability nor, according to Neal Duffield, a design engineer for Schaevitz, do they even test for it. Judah Levine of the University of Colorado has conducted experiments to measure secular drift of tilt in the earth's crust with a sensor having

the sensitivity to measure nanoradians (4848.1 nradians = 1 arcsecond) of tilt (8). Levine agrees that the 1 arcsecond range of his device could be extended to 20 arcminutes for the NRAO design with a corresponding loss of sensitivity but points out the pendulum motion alone for his device costs \$5000.

The most expensive component of the boxes is the Shaevitz sensor. Here is a breakdown of parts costs:

Tilt Sensor Box total: \$3300 (2 per antenna)  
 Schaevitz LSOC-1 \$1000 each. (2 per box)  
 Oven Industries Temperature controller P/N 5C1-207P  
 and temperature sensor probe P/N TP30-1 \$100 (2 per  
 box)  
 Klinger Tilt Table #TG80 \$200 (2 per box)  
 Rose Enclosure, P/N 01.233318 \$150  
 Mechanical parts such as the mounting plate: \$250.  
 Connectors and other electrical components: \$300.  
 M24 module: \$700 (estimate) (1 per antenna)  
 Other:  
 Cable: \$150  
 Connectors: \$500

Total cost per antenna: \$7950

G. Hurst points out that each Klinger tilt table has to be rebuilt in his shop including the insertion of plugs in two large holes using a liquid nitrogen technique. It may be that we should build the tables ourselves. Hurst also has some ideas in improving the construction of the mounting plate to include heat treating to reduce stresses introduced from machining.

### III. Tests performed on the tilt sensor boxes.

#### A. Stability

##### 1. Description of setup.

We collected data over a period of several weeks to determine long term stability of the sensor boxes. The plots, shown in figure 3, typically show drift of a few arcseconds. Occasionally, a sensor output continues to drift in the same direction (an example is A2 in the figure); the problem has been corrected each time by tightening up the mechanical connections.

The stability tests were conducted by reading the tilt and temperature outputs every 10 minutes and recording the result on floppy disks with a PC and a Pascal program written by A. Sittler. The sensor boxes were located in the "shell" area of the AOC basement, on a concrete pier separated from the remainder of the basement concrete by fiber expansion joint material. The pier is 1' thick, as same as the remainder of the basement, but poured separately, according to Structural Drawing S13.

The data were plotted by importing the data to Lotus 1 2 3 R-3, removing DC biases by taking the average of all the data points, scaling, and using the 1 2 3 graph and print subroutines. The computer system used for graphing was a 286 PC clone with 2

#### 4 Tilt Sensor Tests

mbytes of memory and a dot matrix printer. The data show a long term stability of about 3 arcseconds, the error attributable in part to small changes in temperature of the tilt table as explained further in this section.

##### 2. Sensor noise.

A strip chart recorder shows that the sensors are sensitive to cultural and geological disturbances. The San Francisco earthquake of October 17, 1989, caused a peak-to-valley tilt of 15 arcseconds (figure 4). The other disturbance on the same chart is a train passing through Socorro on a track about 1 mile east of the AOC, according to NMIMT seismologist, Allan Sanford. The tilt caused by the train is 4.3 arcseconds p-p.

The periodic variation of the tilts in figure 3 appears to be a diurnal effect, perhaps from solar heating of the building or surrounding soil. The effect is as high as 1.8 arcseconds in amplitude, more than the 0.1 arcseconds to be expected from crustal tides induced by the moon (9). A. Perfetto of NRAO Tucson performed similar stability tests on the fifth floor of the Steward Observatory Building on the University of Arizona campus, and noted a diurnal shift of several arcseconds during the time when the south side of the building was heated by the sun.

The strip chart (figure 4) also shows a continuous short term variation of the sensor signal output which varies from sensor to sensor but is typically in the range of 0.4 to 0.8 arcseconds p-p. Since the envelope of the signal output is constant throughout the day, we assume that the peak-to-peak magnitude of the signal is a result of noise generated internally to the Schaevitz sensor. An alternate possibility is that vibration from the AOC air handling, which is operating 24 hours a day, contributes to the noise level. For example, A. Perfetto in Tucson noted in his tests that the signal envelope increased in amplitude starting at 6:30 am local time and subsided gradually from closing time at 5 pm until midnight when the janitors and the grad students go home. Presumably, the cultural disturbances are less noticeable in the AOC tests because the sensors were located on an isolated pier. A quick look with a low frequency spectrum analyzer shows a resonant peak in the sensor output at 2.5 Hz, just short of the 3 Hz specified limit of the sensor servo loop. The response does not seem to be filtered so that higher frequency outputs can be observed; another peak appears at 32 KHz.

J. Ruff tested the Schaevitz sensor in a mine shaft in an attempt to differentiate internal noise of the sensor from cultural disturbances (10). The tests were hampered by the difficulty of getting power to the sensor. This test should be repeated if the noise envelope from the sensor becomes a concern, and then the internal noise addressed if indeed it proves to be the dominant source of the noise envelope.

### 3. Temperature effects.

Temperature variations contribute significantly to sensor error. The temperature coefficient of the Schaevitz sensor itself is specified to be 1.37 arcseconds/C. We measured the coefficient to be 6 arcseconds/C with the sensor mounted in the box (figure 5). When the heater is first turned on, the tilt changes dramatically for the first few minutes while the temperature sensor on the tilt table is reaching its final value of about 40 C (11). Once the tilt table has had time to be uniformly heated as indicated by stability of the AD590 temperature sensor output, the tilt approaches a final value logarithmically over a period of up to 24 hours. The long time to stabilize is probably not a problem operationally, because a power outage long enough to cool down the tilt sensors would also warm up the Low Noise Receiver, so that the antenna would not be ready for observing for a number of hours after restoration of power for more reasons than the tilt sensors. The greater concern is contribution to tilt error of small variations of temperature within the sensor box. Though temperature sensor data taken during the stability test indicate a standard deviation of only 0.005 C and a p-p range of 0.05 C worst case, it may be that the 3 arcsecond p-p error in long term stability is a result of temperature variations of the tilt table not seen by the temperature probe, or that temperature differentials result from having two heaters in the same box with slightly different set points. Temperature data taken at telescope 6 and 22 over a 6 hour period show a worst case temperature range of 0.55 C. With the substantial temperature coefficient of the sensor box, a change of only 0.5 C will cause a tilt error of 3 arcseconds. It may be necessary to experiment with tilt sensors having better temperature coefficients and with tilt tables made with metals having lower temperature coefficients, if further tests show temperature variations to be a problem.

#### B. Box Tests

Peter Dewdney describes an antenna test called Box Test that can be used to compare measured tilts with pointing corrections (6). K. Sowinski performed three such tests for Antenna 22 (located at DE7) on November 13, November 16, and November 30, 1989; and one test on Antenna 6 (located at DN3) on November 30. For Box Test, the antenna is initially positioned at 135 degrees azimuth and a fixed elevation. For the tests described, an elevation near zenith was used. The Box Test automatically measures the tilt meter outputs a number of times at a given azimuth, then moves the antenna in azimuth 22.5 degrees for the next series of measurements. The test continues until the antenna reaches 585 degrees. The direction is then reversed, and the measurements repeated at the same azimuth positions back to 135 degrees. The test may be terminated at any time; all three of the November tests were stopped before the full reverse motion was completed.

## 6 Tilt Sensor Tests

We installed two tilt sensor boxes on each of the two antennas for the tests, one box on each side of the yoke mount just below the elevation axle (figure 6). The boxes are oriented so that two sensors measure tilt in the "Y" axis, parallel to the axle, and two in the orthogonal "X" axis. The sensors are reversed in sign, so that a given tilt of the antenna mount will cause a "+" tilt on one sensor and a "-" tilt on the sensor in the same axis on the opposite side of the yoke.

The sensors are read out by means of the M24 interface added to the B rack in the Pedestal Room, by Data Set 2 (Dwg 4), and by using the following multiplexer addresses on the VLA Command and Monitor System (12 ):

- '60: Encoder side, y axis (Ey)
- '61: Waveguide side, y axis (Wy)
- '62: Encoder side, x axis (Ex)
- '63: Waveguide side, x axis (Wx)
- '64: Ey temperature
- '65: Wy temperature
- '66: Ex temperature
- '67: Wx temperature

The time allotted by Box Test for the antenna motion to settle at each azimuth position is variable, as is the number of measurements made at each position. A settling time of 2 seconds was selected for Box Test 1, while 20 seconds was chosen for Box Tests 2 and 3. The number of data points at a given azimuth was selected to be 13 for Box Test 1, 37 for Box Test 2, and 25 for Box Test 3. The interval between data points is 5 seconds. Optimal values for the delay, number of data points, and sampling interval have yet to be determined.

The data are conveniently organized in columns of ASCII characters separated by spaces, so that importing a data file to Lotus 1 2 3 is straightforward. The data are printed out by entering the batch command LFI ,<filename> on the MONTY Modcomp computer, and may be transferred simultaneously to floppy disk using the DDS. There are four columns of instantaneous tilt readings in the data, one column from each of the four sensors on an antenna; and four columns of averaged data. The data are averaged using the formula (6):

$$x_{new} = 1/8 x + 7/8 x_{old}$$

MONTY will truncate the last two columns of data if the field width is not extended for the output command (13).

Because the first few data points are taken before the structure is stable, the Modcomp averaged data can be badly skewed if the settling time is too short (figure 7). For the data plots included with this report, we used only instantaneous values, and averaged with reduction routines. The reduction routine calculated the average for a given azimuth by adding together all the data points for that position and dividing by the number of points.

Figures 8 - 11 show the instantaneous values of tilt for Box Test 3 on antennas 6 and 22. Note that the x axis is shown in degrees azimuth; but, in fact, the plot is a chronological representation of the test. The antenna changes direction at 585 degrees azimuth, but the plot continues, repeating the azimuth positions. The predicted tilts are also shown on the figures, calculated from the coefficients and formula described in Part I, and with the antenna elevation set to 45° to simplify the calculations. The predicted tilts are calculated from geographical coordinates; whereas, the Box Test uses telescope coordinates which are phase shifted from the geographical coordinates by 180 degrees. To be strictly correct, the calculated tilts would have been phase shifted 180 degrees before plotting.

Though the instantaneous values vary as much as 25 arcseconds peak at a given azimuth, the standard deviation of tilts at a given azimuth is typically less than 8 arcseconds and an average of the instantaneous values agrees closely with the predicted values as shown in figures 12 - 19. C. Wade measured the DE7 pad for antenna 22 with a theodolite and found the 20 arcsecond error between measured and calculated values for that antenna is a result of pad movement; pad displacement is also the cause of the comparatively large 7 arcminute p-p tilt. When the difference is taken between residuals; i.e

$$\{E_y(\text{predicted}) - E_y(\text{measured})\} - \{W_y(\text{predicted}) - W_y(\text{measured})\} \text{ and} \\ \{E_x(\text{predicted}) - E_x(\text{measured})\} - \{W_x(\text{predicted}) - W_x(\text{measured})\},$$

the remaining tilt is about 5 arcseconds peak, with a standard deviation of 1.6 arcseconds.

Though the residuals from finding the difference between the averages of the tilt readings at a given azimuth are satisfyingly small, the same difference taken data point by data point show 10 arcsecond peak errors (figure 20). The data points are read out within a few milliseconds of each other, so that the differences appear to be a result of the sensor and not a synchronization problem. Neither do the spikes appear to be a result of noise in the readout electronics because temperature data read in over a period of 6 hours while the telescope is in use show no noise spikes. The instantaneous spikes in the tilt data must be understood further to make the tilt sensors useful for correcting short term disturbances introduced, for example, by wind.

Dewdney noted hysteresis in his measurements; i.e., the tilt measurements did not repeat when a given azimuth was approached in Box Test from opposite directions (6). In Figures 21 - 24, the plots for Box Test 3 were folded back at 585 degrees azimuth where the antenna changes direction, so that the averaged instantaneous tilt data for the two antenna directions overlay. The difference between  $E_y$  in increasing azimuth  $E_y(1)$  and decreasing azimuth  $E_y(2)$ ,  $W_y(1)$  and  $W_y(2)$ , and so on is shown in figures 25 - 28 as  $E_y$  hysteresis,  $W_y$  hysteresis, etc. The difference of the residuals; i.e.,

## 8 Tilt Sensor Tests

$\{E_y(1)-E_y(2)\} - \{W_y(1)-W_y(2)\}$  and  $\{E_x(1)-E_x(2)\} - \{W_x(1)-W_x(2)\}$ ,

are 7 arcseconds peak with a standard deviation of 1.5 arcseconds. Since the errors are comparable to the residuals for the difference between measured and calculated tilts, hysteresis in the measurements does not appear to be significant.

Finally, tilt measurements for all three box tests are compared in figures 29 - 32. The residuals are 5 arcseconds peak and the standard deviations are 1.7 arcseconds in Y, and 2.2 arcseconds in X, comparable with other residuals described. However, there is a tilt of 15 arcseconds between Tests 1 and 3 in the Y axis centered at 250 degrees azimuth. If this were a pad tilt, between tests 1 and 3, a similar tilt would be seen in the X axis, phase shifted 90 degrees; but at this azimuth, there is only a 5 arcsecond tilt in X. Axis Y for Box Test 2 also shows tilt with respect to Tests 1 and 3 in the same azimuth area. The antenna was removed from its mounting pad and returned between Tests 2 and 3, yet we are unable to fully explain the tilts between tests at this writing.

The residuals described; i.e., the difference between calculated and measured tilts, hysteresis, and drift, ideally would be straight lines. Some sources of the error are the following:

1. Deformations of the antenna structure from wind disturbances and differential heating. (D)
2. Gain differences and nonlinearities of the tilt sensors and their associated readout electronic circuitry. (G)
3. Noise internal to the sensor. (N)
4. Drift of the sensor caused primarily by small temperature differences. (T)
5. Error in measuring antenna position = LSB of position encoders. (E)
6. Errors in sensor positioning (misalignment of axes, etc) (6) (P)
7. Disturbances introduced by tracking errors and subreflector rotation. (C)

If we assign values to these errors as follows:

D = 4 arcseconds (representative RMS value of instantaneous tilt measurements taken with the antenna stationary during Box Test)

G = 0.1% est. or 2 arcseconds (from specifications of sensor, instrumentation amplifier, ADC)

N = 1.5 arcseconds (from Part II)

T = 3 arcseconds (from Part II)

E = 0 The position encoder LSB = 1.25 arcseconds (20 bit encoders), but the contribution to tilt error alone is insignificant.

P = 1 arcsecond (guess)

C = 0 for the box tests

A possible calculation of overall tilt measurement error is:

$$E = [ D^2 + S^2 + N^2 + T^2 + E^2 + P^2 + C^2 ]^{1/2} = 5.7 \text{ arcseconds,}$$

which compares favorably with the peak of residuals measured.



### C. Antenna stability test.

At J. Campbell's suggestion, the tilt meters on antenna 22 were monitored during the Thanksgiving shutdown period, 5 pm MST November 22, 1989, until 5 pm MST November 23. The data were plotted using the batch command MONPLT on MONTY (figures 33 - 37). The data points are 3 minutes apart.

The most dramatic phenomenon in the data is the tilt of both Y axis sensors in the same sign, indicating a deformation of the yoke. The yoke arms appear to have been spread apart possibly by thermal expansion of the elevation axle. The temperature differential over the same period is 20 C (dT). If we assume:

Temp coefficient of steel =	11.34 micrometers/m/C	(C)
Length of elevation axle =	7 m	(AL)
Length of yoke arm =	3.7 m	(YL)

We further assume the elevation axle will follow ambient temperature since it is hollow, uninsulated, and exposed to the wind, but the yoke arms will not, because they are insulated and because their hollow interiors are open to the temperature-controlled pedestal room.

Then, the axle will increase in length

$$dAL = dT * C * AL = 1.59 \text{ mm.}$$

The arctangent of  $1/2(dAL/YL) = 44.3$  arcseconds, which agrees favorably with the 40 arcseconds deformation in the figure. The noisiness of the tilt data in the figure during the daytime is presumed to be because of the wind which increased over the same period.

K. Sowinski noted deformation of the structure during the same time period by examining the output of the elevation position encoder. Though the structure was stationary, the servo off, and brakes on, the dish support structure moved with respect to the yoke (figure 38). No change in the azimuth encoder was found. Sowinski found similar elevation encoder motion in other antennas throughout the array over the same time period. Thermal expansion of the bull gear between the brake and the point where the gear connects to the dish support structure may explain this phenomenon as well.

The data show that changes in ambient temperature still deform the antenna structure. It may be necessary to characterize and improve the thermal performance as part of the pointing improvement project.

## 10 Tilt Sensor Tests

### D. Preliminary Operational Tests.

It is possible to plot tilt data while the telescope is in use, using MONTY and MONPLT, and even to down load data from the previous six days using MONLST. The Command and Monitor System permits recording simultaneously the tilts, the tilt sensor temperatures, position encoder outputs, drive motor currents, subreflector motion, temperature, and wind data.

Data taken for a 24 hour period starting 5 pm (00:00 UTC) December 17, 1989, on antenna 6, show spikes of hundreds of arcseconds from the tilt sensors in both axes. The spikes are apparently the result of vibration and not real tilts, since spikes of the opposite sign do not necessarily appear simultaneously in the "mating" sensor on the opposite side of the yoke (figures 39 and 40). The spikes can, however, be correlated with telescope motion (figure 41). When tilt data are discarded that were taken when the elevation or azimuth encoder position changed from the previous data point by more than 1000 LSBs (1 LSB = 1.25 arcseconds), the large spikes are all removed. However, the standard deviation of residuals, 7.9 arcseconds in Y tilt and 16.44 in X, show that the performance of the tilt sensors while the telescope is in motion must be better understood (figures 42 - 45). Decreasing the sensitivity of the tilt sensor with an electronic filter or a higher viscosity damping fluid may be necessary. Any correlation with tilt sensor temperature data and meteorological data are also left for a more sophisticated analysis (figure 46, 47).

The envelope of the tilt data during the first part of the "stability" test before the wind picked up was 5 arcseconds p-p, compared with 25 arcseconds p-p for tilt data during the box test when the antenna was stationary, and 50 arcseconds p-p when tilt data were taken while the antenna was tracking. Clearly, the tilt sensors are very sensitive to any motion of the antenna.

### IV. Conclusions and Recommendations.

The tests to date show that the tilt sensors on antenna 6 and 22 can be used to measure tilts of the yoke with a standard deviation of 2 arcseconds or better when the antenna is stationary, and with a long term stability of better than 3 arcseconds. Since a 1 arcsecond tilt in the same azimuth direction as the antenna is pointed can be expected to contribute approximately 1 arcsecond to pointing error, measuring tilt to an accuracy of 2 - 3 arcseconds appears to be a viable means of correcting the tilt contribution to pointing where the pointing error budget is 8 arcseconds. The preliminary operational tests indicate the performance of the tilt sensors while the antenna is in motion must be better understood, but we recommend that sky-tests move forward so that the results can be used to better characterize the dynamic performance.

We recommend the following:

1. Characterize the performance of the tilt sensors with the antenna in motion. Identify and solve any problems such as possible sensor instability introduced by antenna vibration.
2. Measure pointing on the sky using the tilt sensor outputs to adjust the corrections calculated from the pointing coefficients; i.e., change the pointing of the telescope as a function of the difference between the measured tilts and the predicted tilts, and measure the performance on the sky. Perhaps this test could be performed in conjunction with the beam offset tests established by P. Napier. The contribution to pointing error of antenna tracking and encoder errors will show up in a "sky test." Also, since the tilt meters only report on deformations of the yoke arms and below, such a test would show the affect on pointing of any deformations above the yoke, a potential problem area yet to be investigated on sky.
3. Investigate each antenna structure for loose members or other mechanical problems that would cause nonrepeating pointing errors. C. Wade has already begun this effort.
4. Investigate further the feasibility of reducing thermally-induced deformations of the yoke and elevation axle by adding insulation, reducing radiative coupling with sticky-back aluminum tape a la MMT (15), or by characterizing the deformation as a function of ambient temperature and actively correcting for it.
5. Examining correlations of tilt data with weather and telescope parameters while the telescope is in operation may also prove useful. The data can be easily ported to a downtown computer and a reduction routine using MONTY and the DDS. Note that Command and Monitor System data older than 6 days are recorded on magnetic tape, though a program does not yet exist to read the data back into MONTY. Lotus 1 2 3 may prove too limited for this effort.
6. The Box Test and Antenna Stability tests should be repeated, to verify the results so far, and to make an effort to look for systematic variations in the tilt data. Tests repeated while changing only one variable, such as the antenna elevation position, may uncover antenna characteristics that effect pointing. The tests may also reveal a long term drift in the sensors that may require a calibration technique, such as a pointing check every so often, or even an active offset on the tilt sensor that would permit looking for gain changes. Certainly, the Box Test and the Stability Test are the starting point when sensors are newly installed.
7. Investigate and experiment to determine if the antenna drive servo system can be used to actively correct for wind disturbances by inserting the tilt signal into the servo loop.
8. Investigate improvements to the pointing coefficient algorithm (14). It may be necessary, for example, to include a  $3\theta$  term in the sine and cosine functions to account for flexure in the azimuth ring and uneven loading of the bearing (16).
9. Investigate and improve the tilt sensor performance; i.e., reduce noise internal to the tilt sensor and reduce the temperature coefficient of the sensor box system.

## 12 Tilt Sensor Tests

### Bibliography:

1. VLA Test Memorandum No 129, VLA Pointing Errors: Preliminary Summary and Conclusions, Sebastian von Hoerner, January 1981.
2. Radio Astronomy, John Kraus, Cygnus-Quasar Books, 1980.
3. Interoffice memorandum, Antenna #6 Tiltmeter Tests, David Weber, May 6, 1981.
4. VLA Test Memorandum no 142, Discussion of VLA Pointing, R. Newell, February 1983.
5. Machinery's Handbook, 23rd Edition, Industrial Press, 1989.
6. VLA Test Memorandum No 148, Investigating the Use of Tiltmeters to Correct VLA Antenna Pointing, P. Dewdney, DRAO, Feb 1987.
7. VLA Test Memorandum No 138, Antenna Thermal Insulation, R. Newell, 1982.
8. Tilt Observations Using Borehole Tiltmeters, Journal of Geophysical Research, Vol 94, No B1, pgs 574-586, Judah Levine et. al., Jan 10, 1989.
9. The Tides of the Planet Earth, Paul Melchior, Pergamon Press, 1978.
10. Tiltmeter Investigations, Jim Ruff, Fall 1987, NMIMT Research Paper.
11. Notes, The Tiltmeter Assembly -- Some Thoughts, Dave Weber, undated.
12. VLA Technical Report No 44, An Overview of the Monitor and Control System, D. W. Weber, March 1980.
13. Notes, Format of tiltmeter data in Modcomp, B. K. Ravi, Nov 17, 1989.
14. Pointing and Tracking Algorithms for the Keck Telescope, Pat Wallace, Instrumentation for Ground-based Optical Astronomy, Lloyd Robinson, editor, Lick Observatory, July 1987.
15. Seeing Experiments with the MMT, J. Beckers et. al., SPIE Proceedings, 332, 16, 1982.
16. Some Notes on Pointing, Unsigned, Undated. (Sowinski and Janes have copies)

Figures:

1. Pointing Coefficients, December 1989, D Array
2. Approximation of effect on pointing of heating of a member on a VLA antenna.
3. Tilt sensor stability tests.
4. Strip chart showing San Francisco earthquake of October 1989.
5. Temperature stability tests.
6. Orientation of tilt sensors on an VLA antenna.
7. Box Test showing averaged tilt sensor outputs.
8. Box Test 3: Antenna 22, Instantaneous tilt measurements, Y axis.
9. Box Test 3: Antenna 22, Instantaneous tilt measurements, X axis.
10. Box Test 3: Antenna 6, Instantaneous tilt measurements, Y axis.
11. Box Test 3: Antenna 6, Instantaneous tilt measurements, X axis.
12. Box Test 3: Antenna 22, Instantaneous tilt, averaged, Y axis.
13. Box Test 3: Antenna 22, Instantaneous tilt, averaged, X axis.
14. Box Test 3: Antenna 6, Instantaneous tilt, averaged, Y axis.
15. Box Test 3: Antenna 6, Instantaneous tilt, averaged, X axis.
16. Box Test 3: Antenna 22, Tilt Residuals, Y axis
17. Box Test 3: Antenna 22, Tilt Residuals, X axis
18. Box Test 3: Antenna 6, Tilt Residuals, Y axis.
19. Box Test 3: Antenna 6, Tilt Residuals, X axis.
20. Box Test 2: Antenna 22, X Tilt Residuals.
21. Box Test 3: Antenna 22, Hysteresis, Y axis.
22. Box Test 3: Antenna 22, Hysteresis, X axis.
23. Box Test 3: Antenna 6, Hysteresis, Y axis.
24. Box Test 3: Antenna 6, Hysteresis, X axis.
25. Box Test 3: Antenna 22, Hysteresis residuals, Y axis.
26. Box Test 3: Antenna 22, Hysteresis residuals, X axis.
27. Box Test 3: Antenna 6, Hysteresis residuals, Y axis.
28. Box Test 3: Antenna 6, Hysteresis residuals, X axis.
29. Antenna 22 Box Tests, Comparison of tests 1, 2, and 3, Y axis.
30. Antenna 22 Box Tests, Comparison of tests 1, 2, and 3, X axis.
31. Antenna 22 Box Tests, Residuals between tests 1 and 3, Y axis.
32. Antenna 22 Box Tests, Residuals between tests 1 and 3, X axis.
33. Antenna 22: Ey Tilt, Nov. 23 to Nov. 24.
34. Antenna 22: Ex Tilt, Nov. 23 to Nov. 24.
35. Antenna 22: Wy Tilt, Nov. 23 to Nov. 24.
36. Antenna 22: Wx Tilt, Nov. 23 to Nov. 24.
37. Wind Speed / Temperature, Nov. 23 to Nov. 24.
38. Antenna 22: El Encoder Study.
39. Antenna 6: Y Tilts while antenna in operation, Dec. 17.
40. Antenna 6: X Tilts while antenna in operation, Dec. 17.
41. Antenna 6: Telescope Position for test, Dec. 17.
42. Antenna 6: Y Tilts while antenna is tracking, Dec. 17.
43. Antenna 6: X Tilts while antenna is tracking, Dec. 17.
44. Antenna 6: Y Tilt residuals while antenna tracking, Dec. 17.

14 *Tilt Sensor Tests*

- 45. Antenna 6: X Tilt residuals while antenna tracking, Dec. 17.
- 46. Array temperature and wind speed, Dec. 17.
- 47. Antenna 6: Tilt sensor temperatures, Dec. 17.

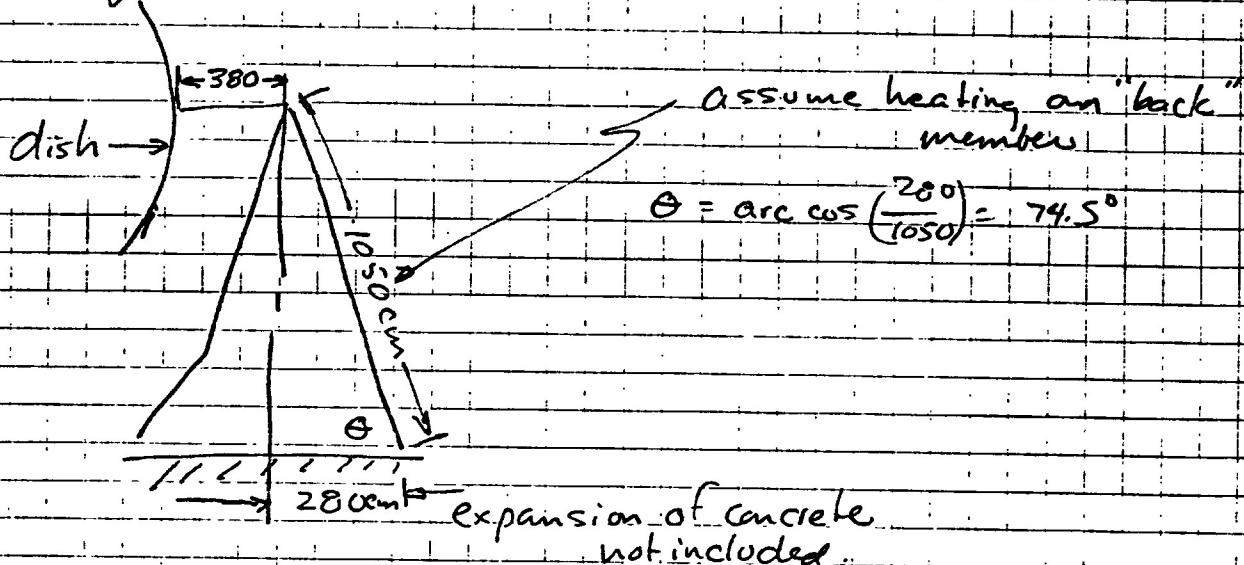
Drawings:

- 1. NRAO Dwg No D13721P68, 2 sheets, Tilt Meter Mount Assembly, Feb. 1989.
- 2. NRAO Dwg No C13720S26, 1 sheet, Tiltmeter Schematic, Dec. 1988.
- 3. NRAO Dwg No C13720S30, 1 sheet, Wiring Diagram, April 1989.
- 4. NRAO Dwg No D13720S29, 2 sheets, M24 Schematic, March 1989.



Approximation of effect on pointing of heating of the "back" member. VLA

10/20/8  
CCJ



$$\text{expansion of member} = .1134 \mu / \text{cm} / ^\circ\text{C} \times 1050 \text{ cm} = 119.1 \mu / ^\circ\text{C}$$

$$\text{effect of expansion vertically} = 119.1 \mu / ^\circ\text{C} \sin \theta = 114.7 \mu / ^\circ\text{C}$$

Pointing desired for 43 GHz =  $7 \mu$  (pg 19)

$$1 \mu \text{ at base of dish} = \frac{1 \mu}{360^\circ} (2 \pi 380 \text{ cm}) = 18.4 \mu$$

$$\text{Vertical deflection of dish} = \frac{18.4 \mu}{\mu}$$

$$\text{per } ^\circ\text{C} = \frac{114.7 \mu / ^\circ\text{C}}{18.4 \mu / \mu} = 6.23 \mu / ^\circ\text{C}$$

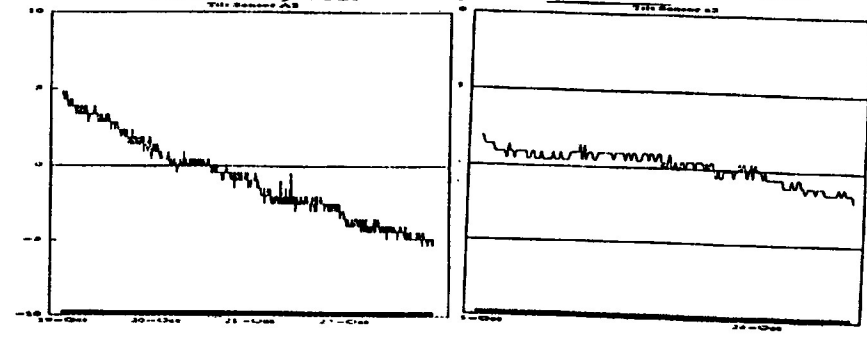
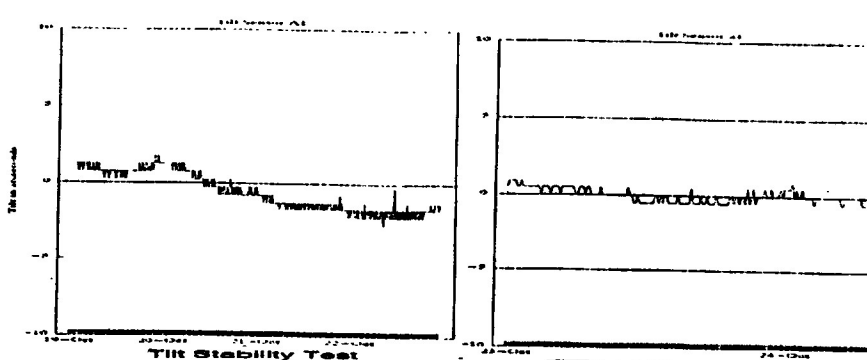
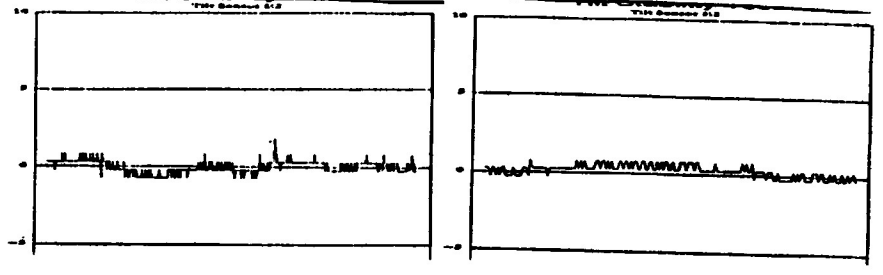
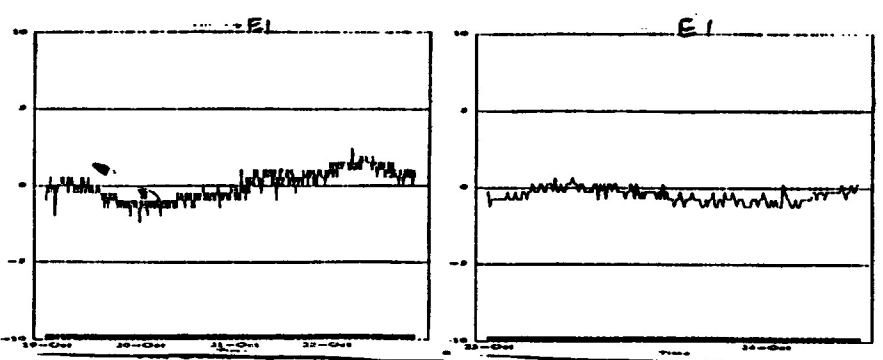
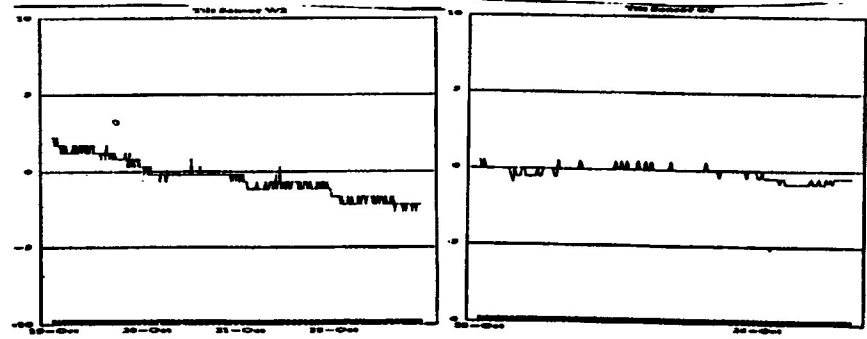
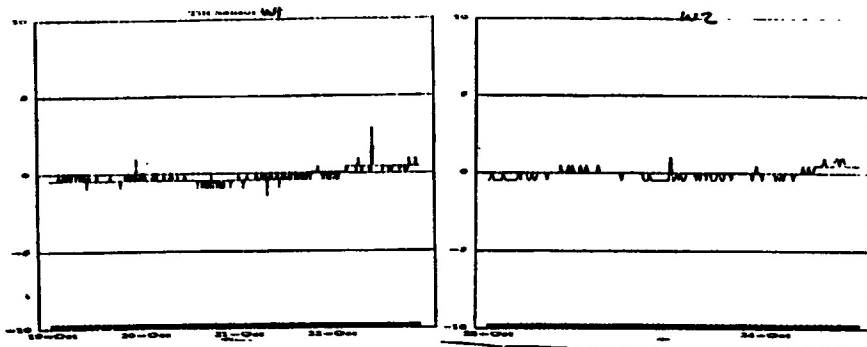
For  $\Delta C$  of  $5^\circ$ , vertical deflection of antenna

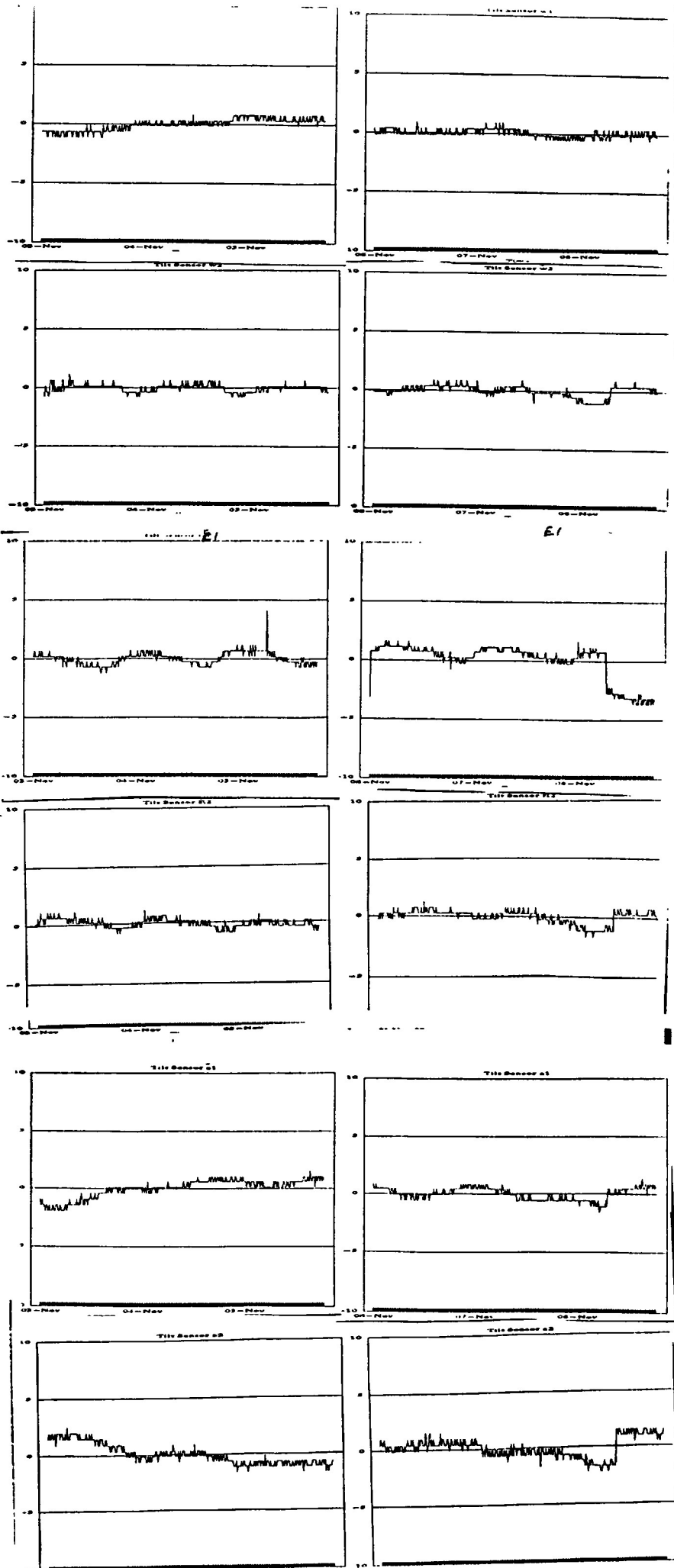
$$\approx 30 \mu$$

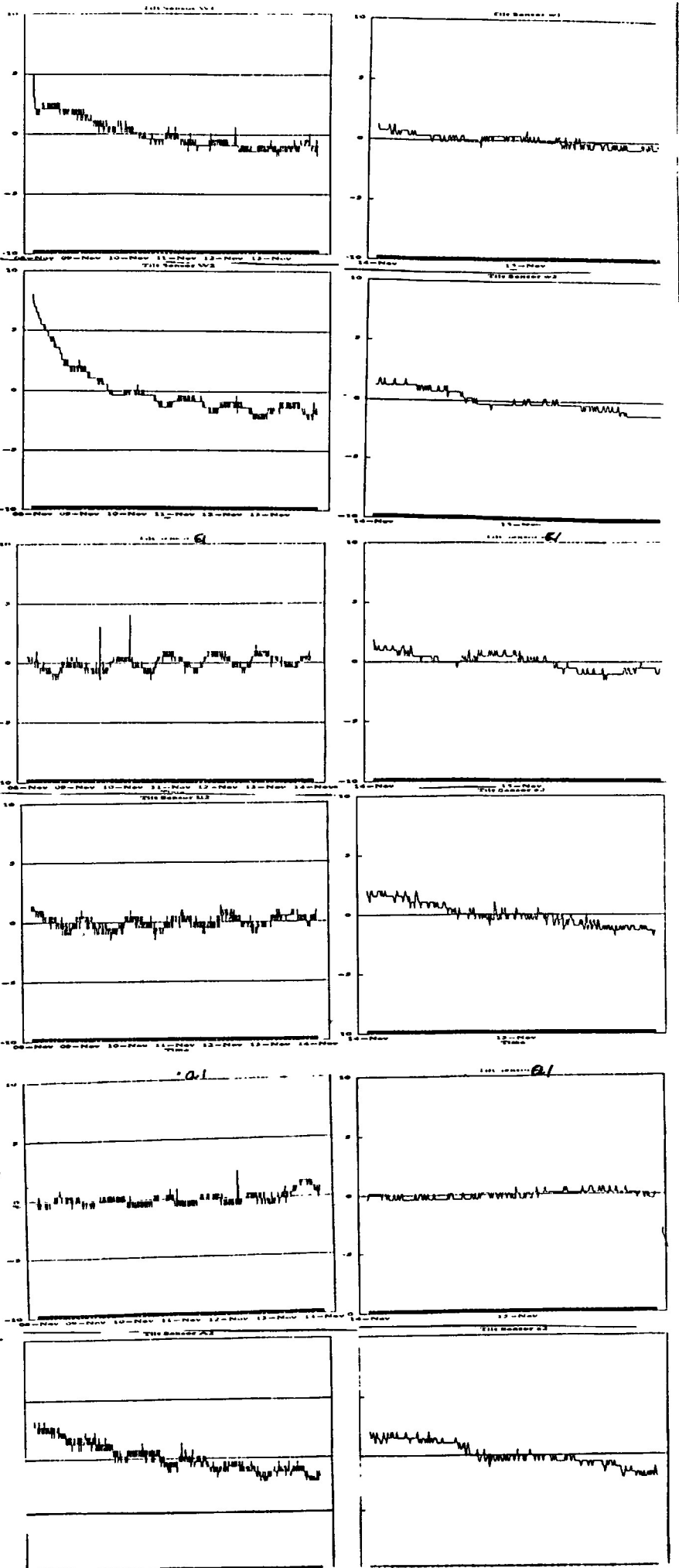
2

want  $7 \mu$  max.  
Continued pg 39









10/17/89 SAN FRANCISCO EARTHQUAKE J

2:10 pm

4:20 pm

6:40 pm

8:40 pm

9:40 pm

TICRAN

EW ORIENTATION

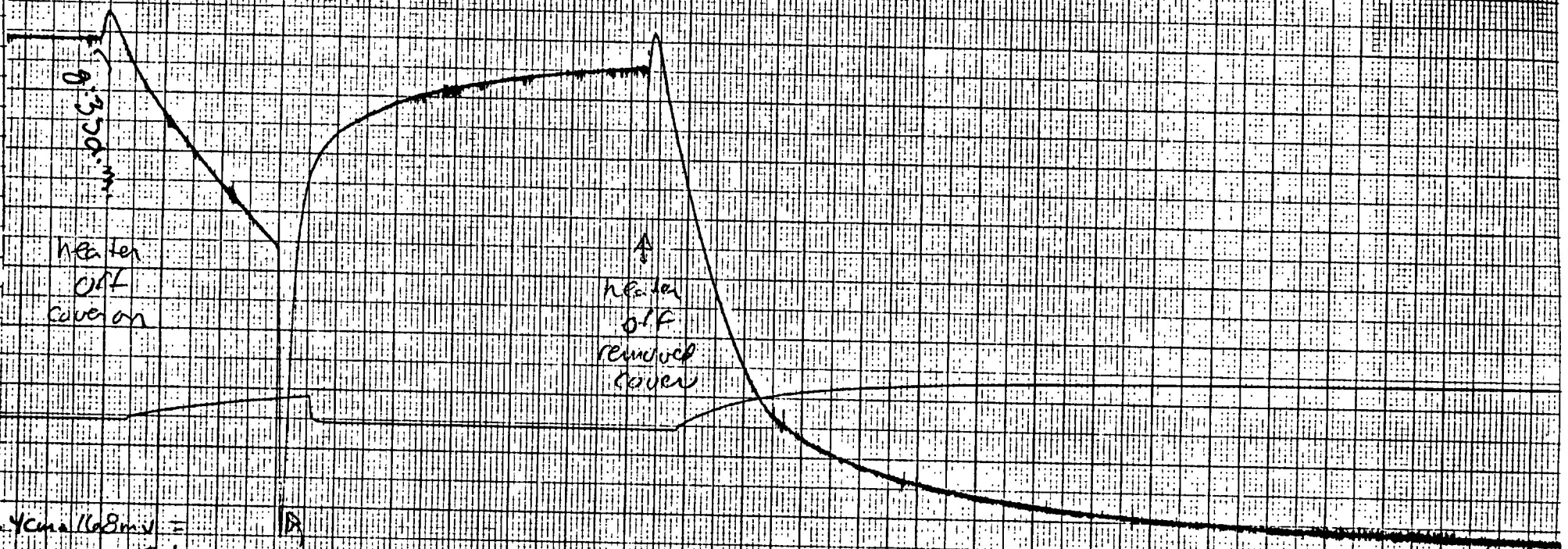
CHART SPEED 5CM/IN

SCALE: 5CMV FULL DOWN 1 INCH

AREA 1 INCH = 100 CM

NIS ORIENTATION

91



0.4 cm / 0.8 mV = 1/2 increase  
 1/2 increase in heater on  
 (0.37 increase)  
 SENSOR A2 PC

Chart speed = 2.5 cm / 100  
 500 mV / 1 cm  
 BOTH PENS  
 10/22/89

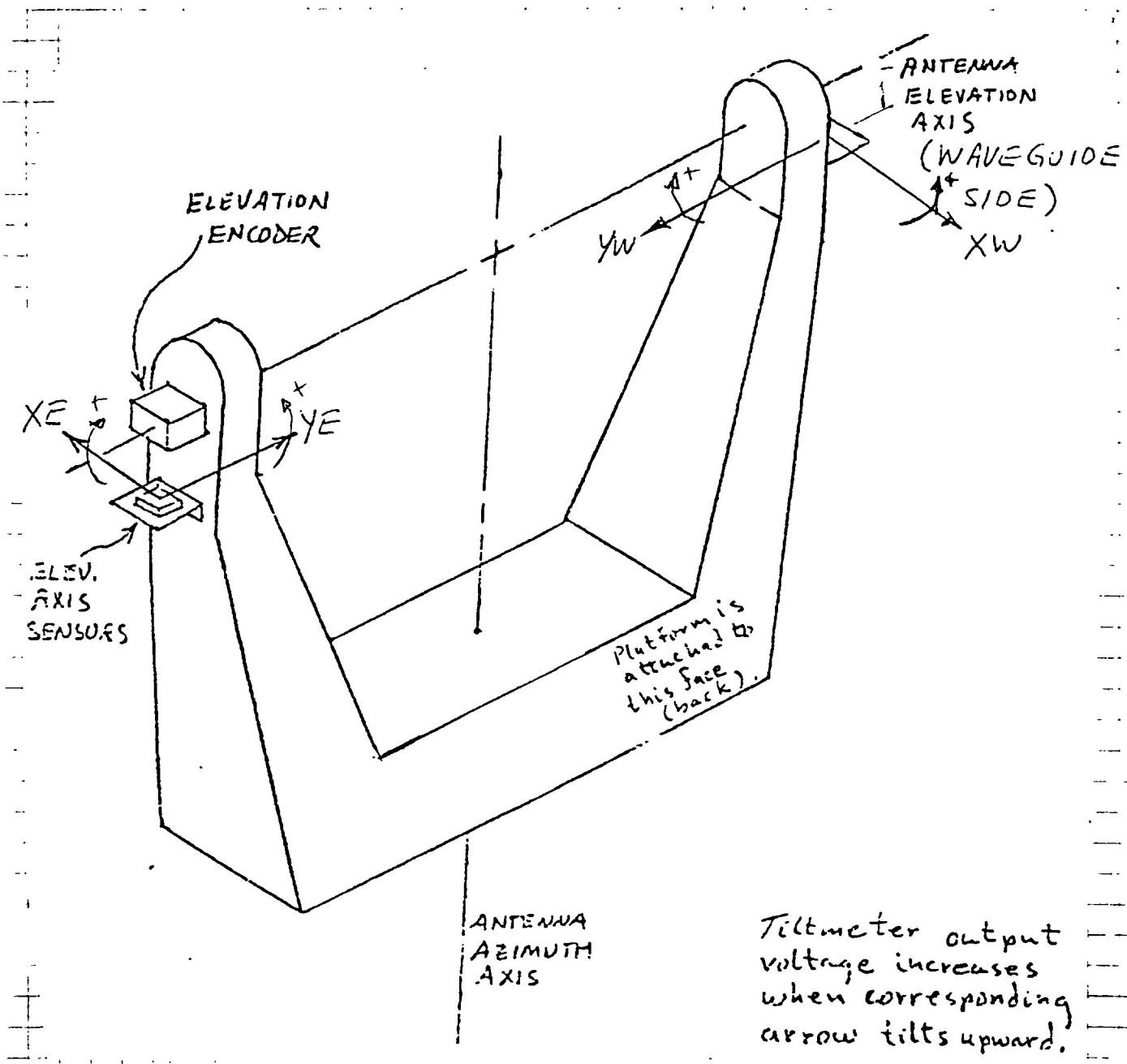
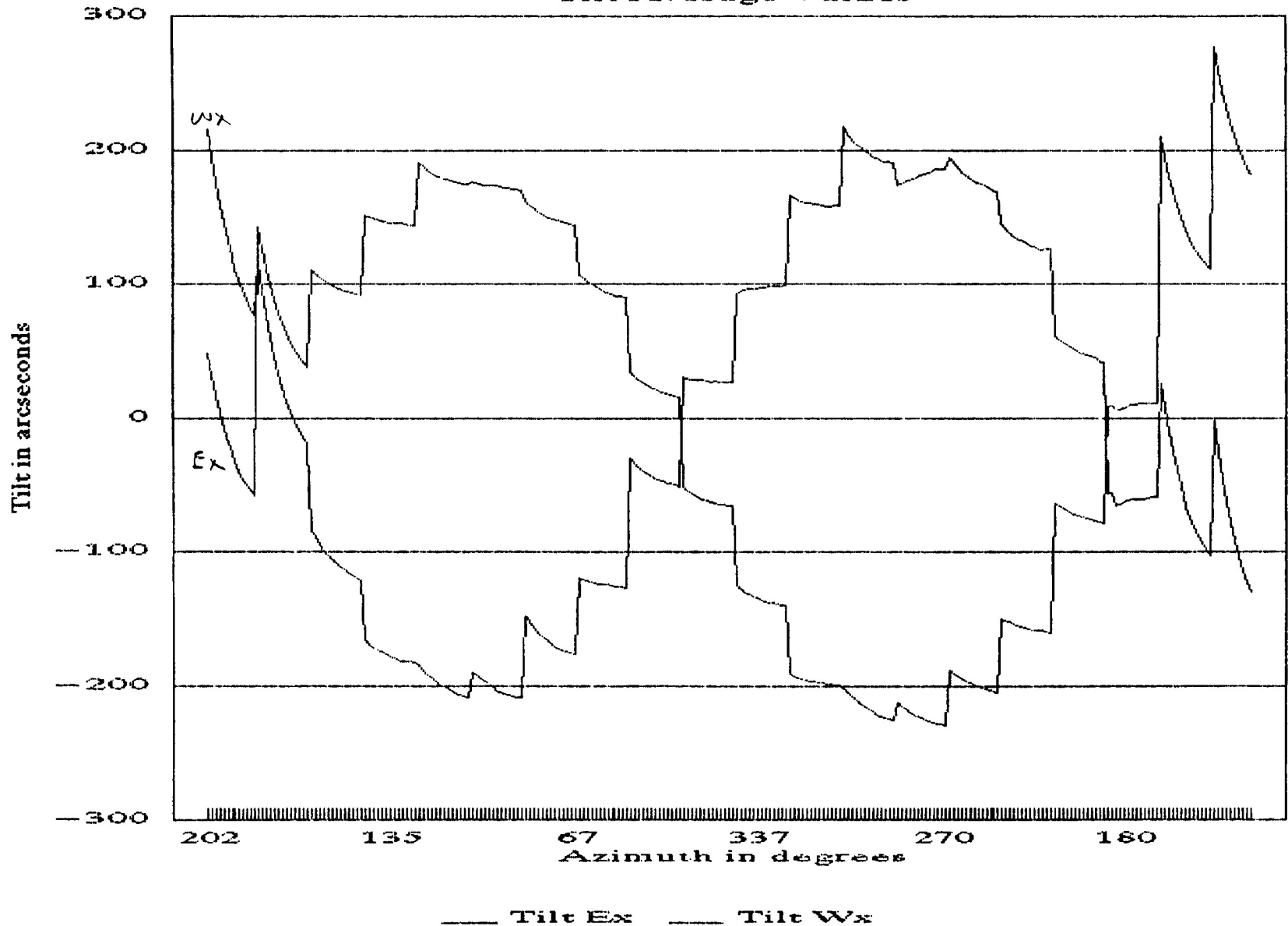


Figure 1: The antenna yoke showing the mounting points of the pairs of tiltmeters. In the diagram the back face of the yoke is shown (i.e. the antenna is facing away from the reader). The X tiltmeters measure tilt angles in a plane perpendicular to the elevation axis. The Y tiltmeters measure tilt angles in a plane containing the azimuth and elevation axes. The pair mounted near the elevation encoder are denoted E tiltmeters; the pair mounted near the waveguide are denoted W tiltmeters. The E pair and W pair respond in the opposite sense to the same tilt.

# Box Test 1: Antenna 22

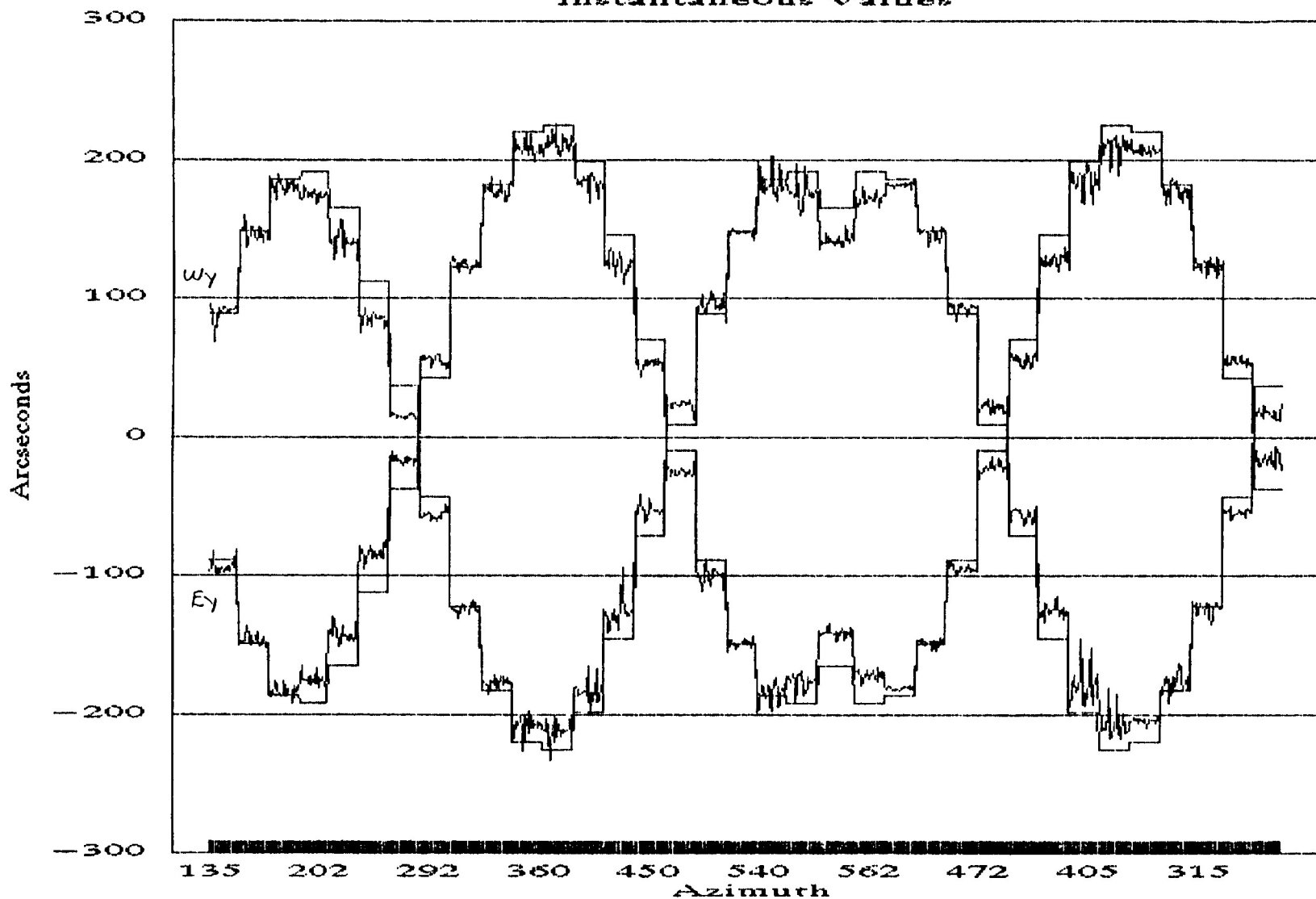
Tilt Average Values



Test 1, Nov 16, 1989  
C. Jones

# Box Test 3: Ant 22

Instantaneous Values

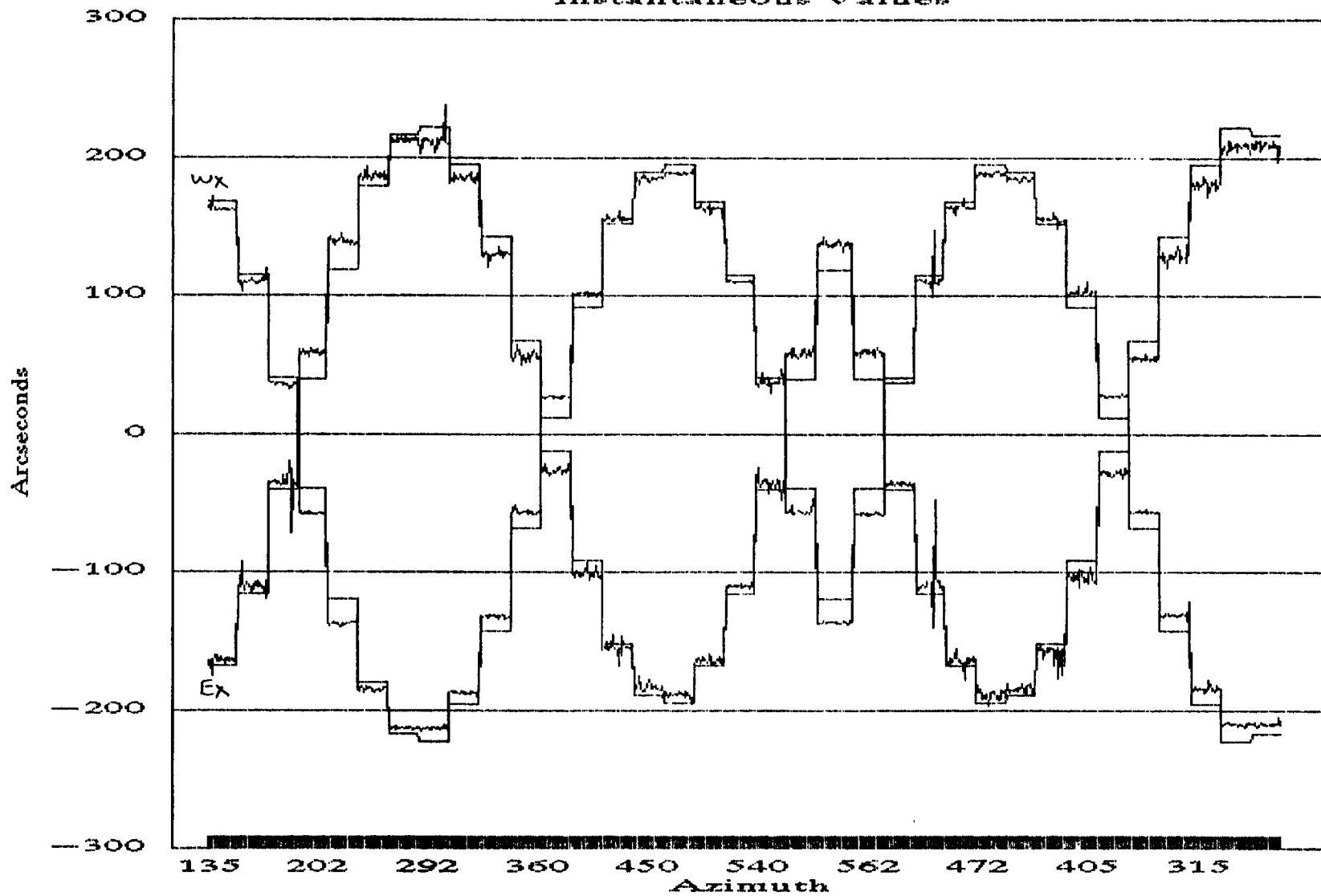


Test 3, Nov 30, 1989  
C. Jones



# Box Test 3: Ant 22

Instantaneous Values

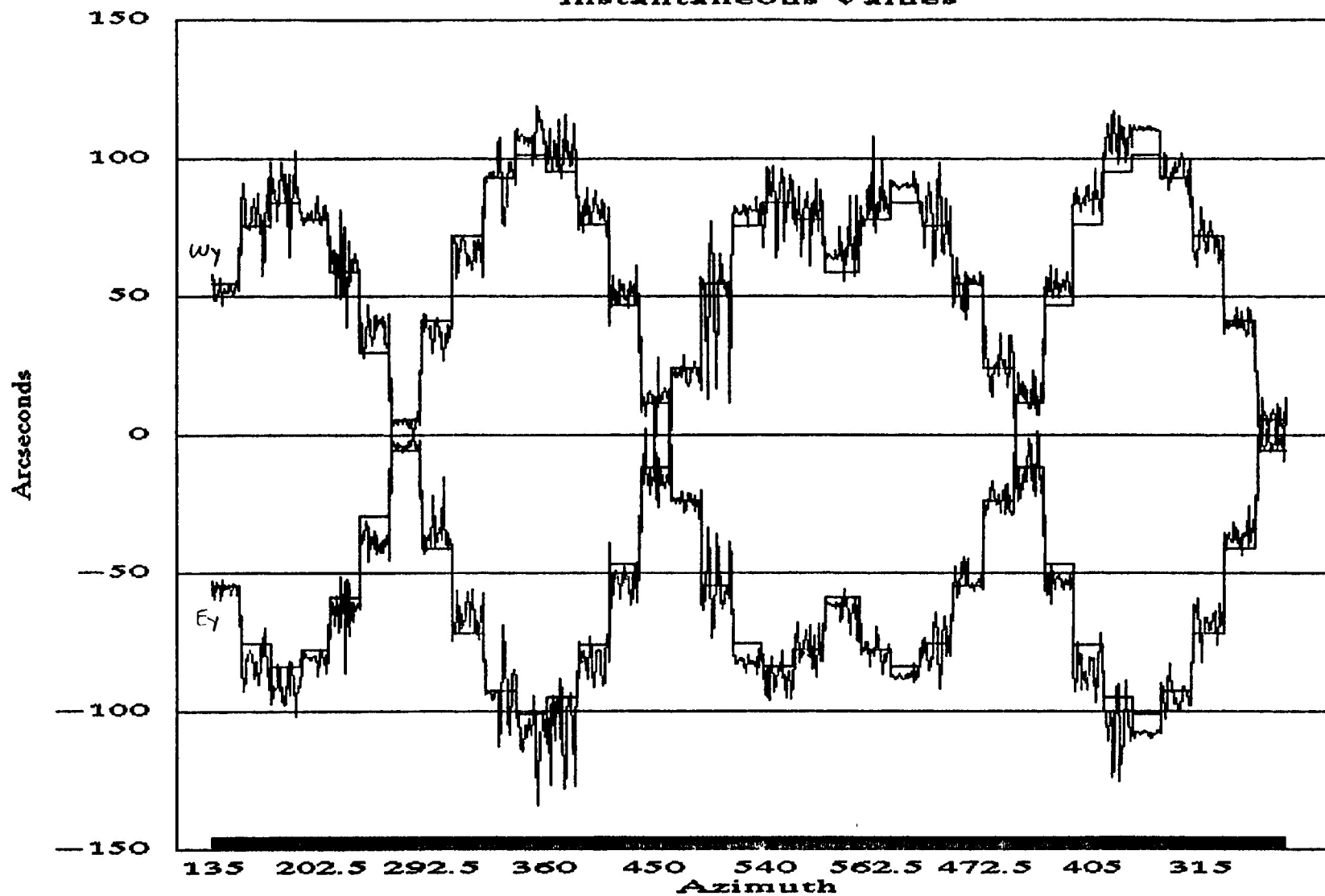


— Tilt Ex    - - - Tilt Wx

Test 3, Nov 30, 1989  
C. Jones

# Box Test 3: Ant 6

Instantaneous Values

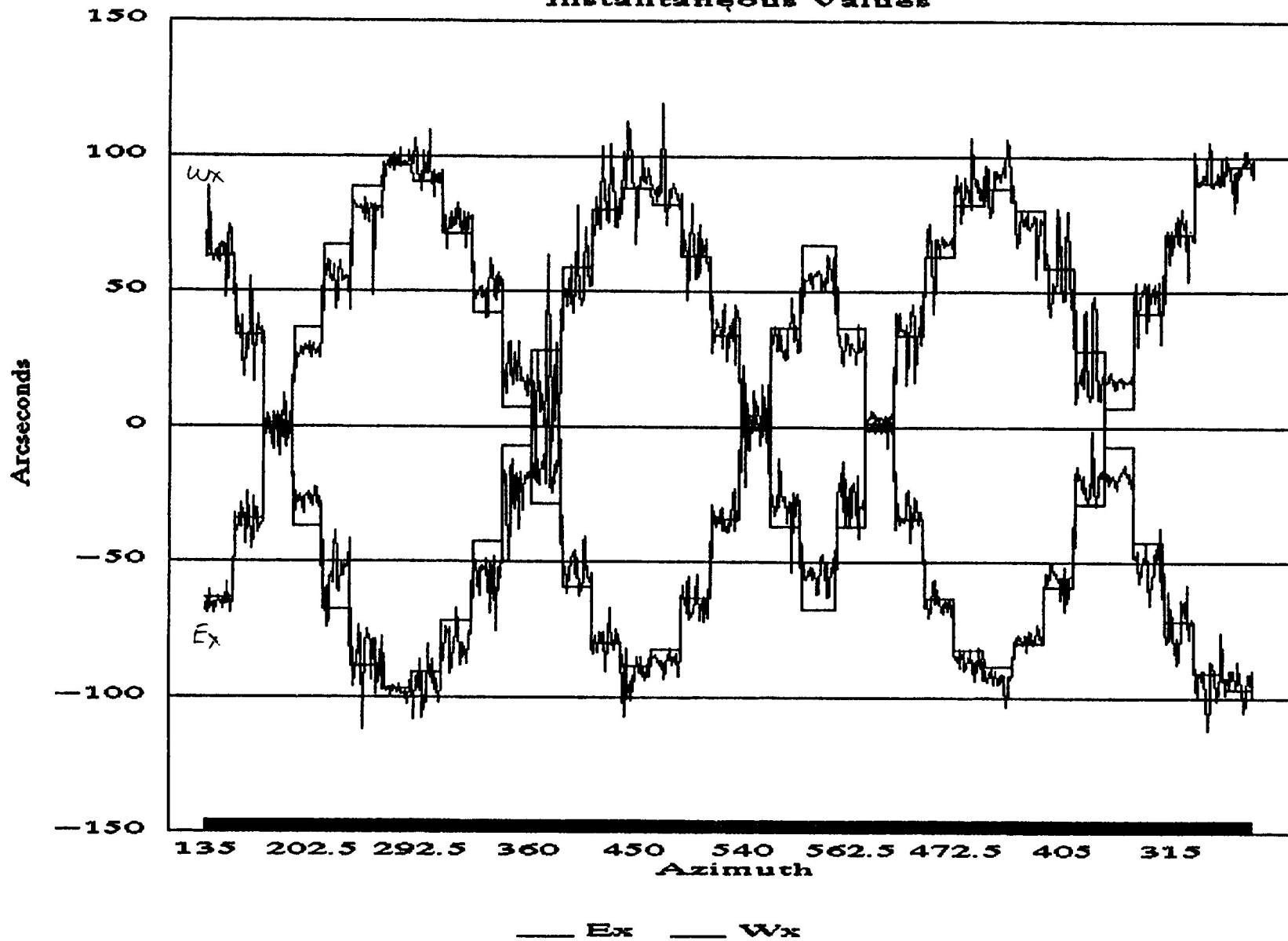


Test 3, Nov 30, 89  
C. Janes

—  $E_y$  —  $W_y$

# Box Test 3: Ant 6

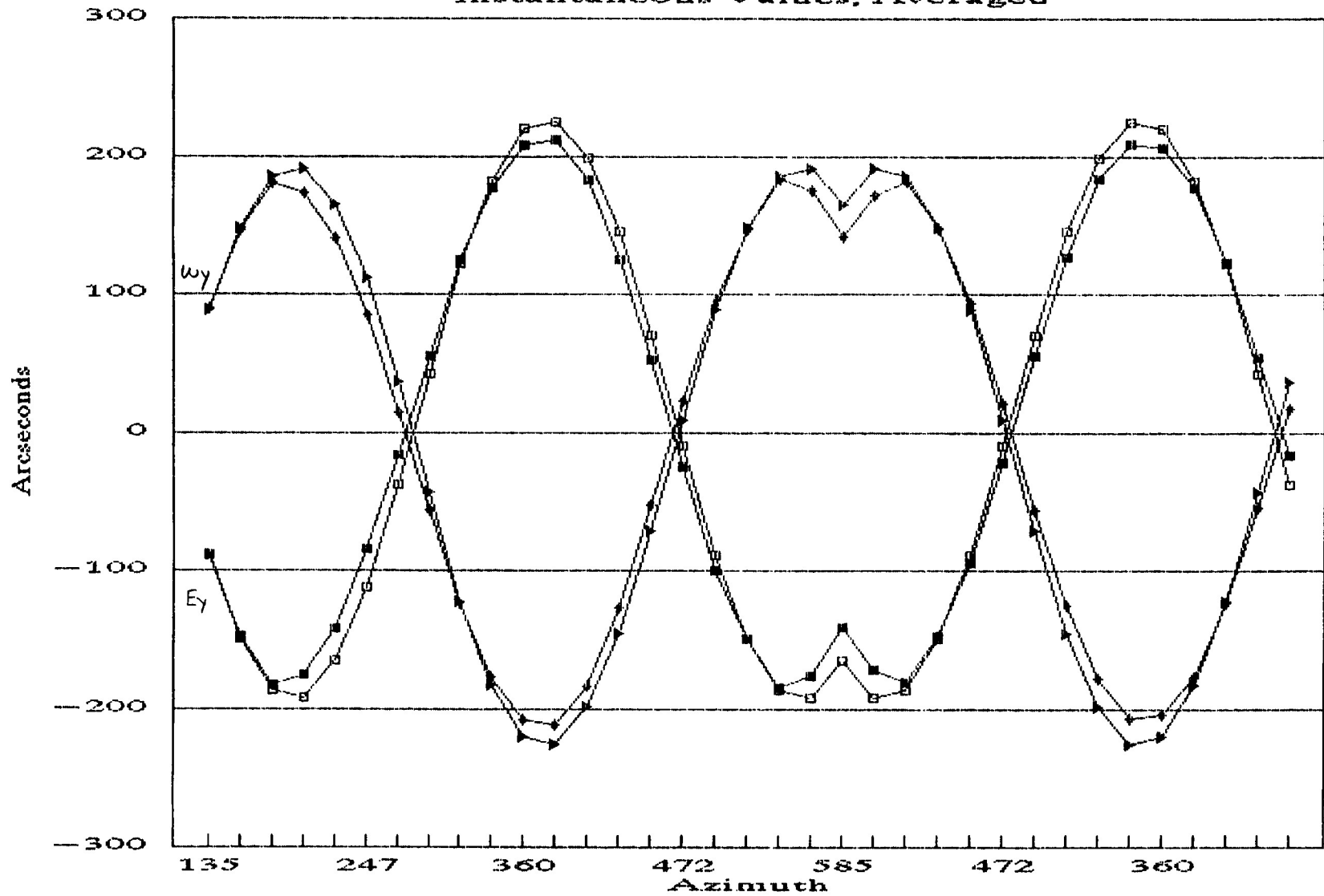
Instantaneous Values



Test 3, Nov 30, 89  
C. Janes

# Box Test 3: Ant 22

Instantaneous Values, Averaged

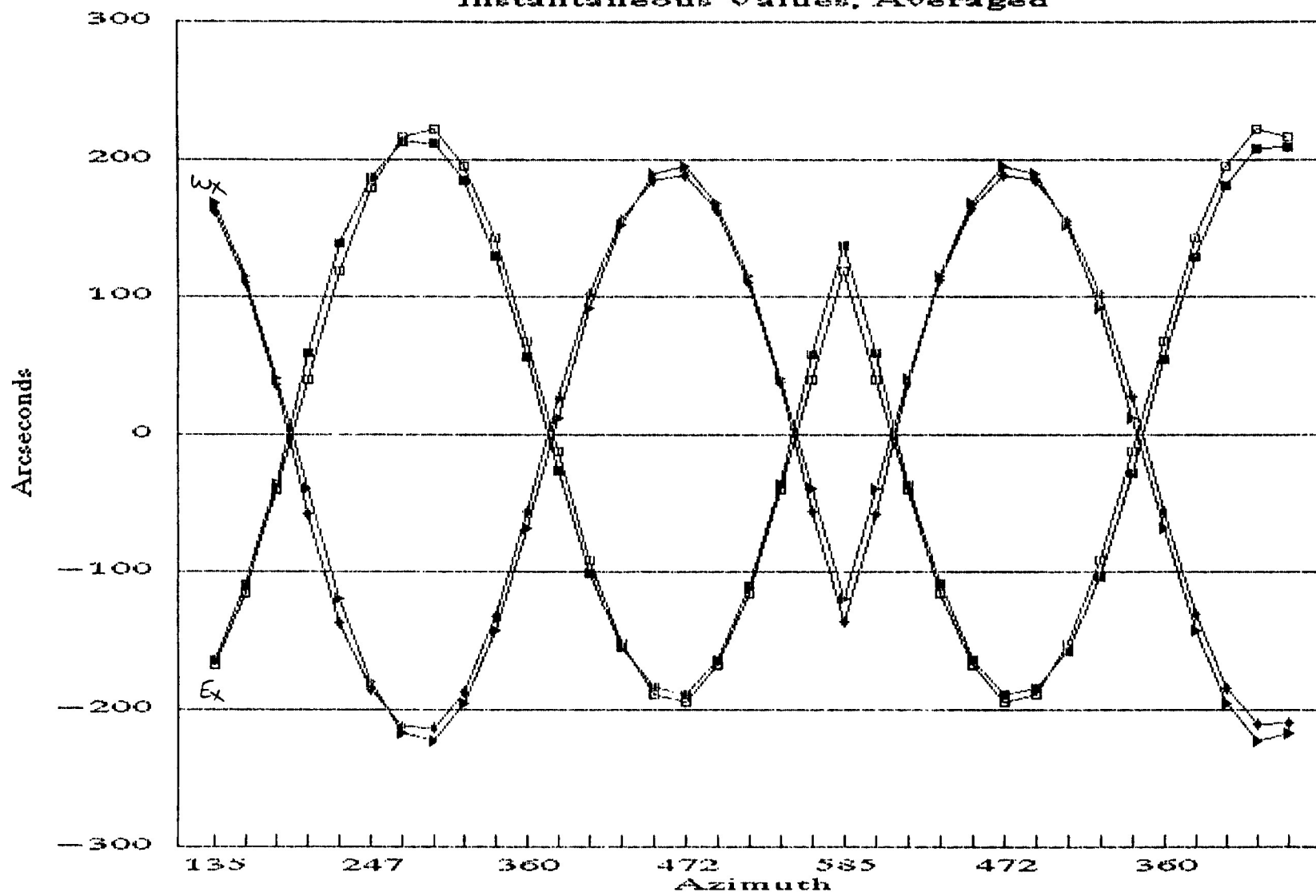


Tilt Ey   
  Tilt Wy   
  Coeff   
  Coeff

Test 3, Nov 30, 1989  
C. Janes

# Box Test 3: Ant 22

Instantaneous Values, Averaged

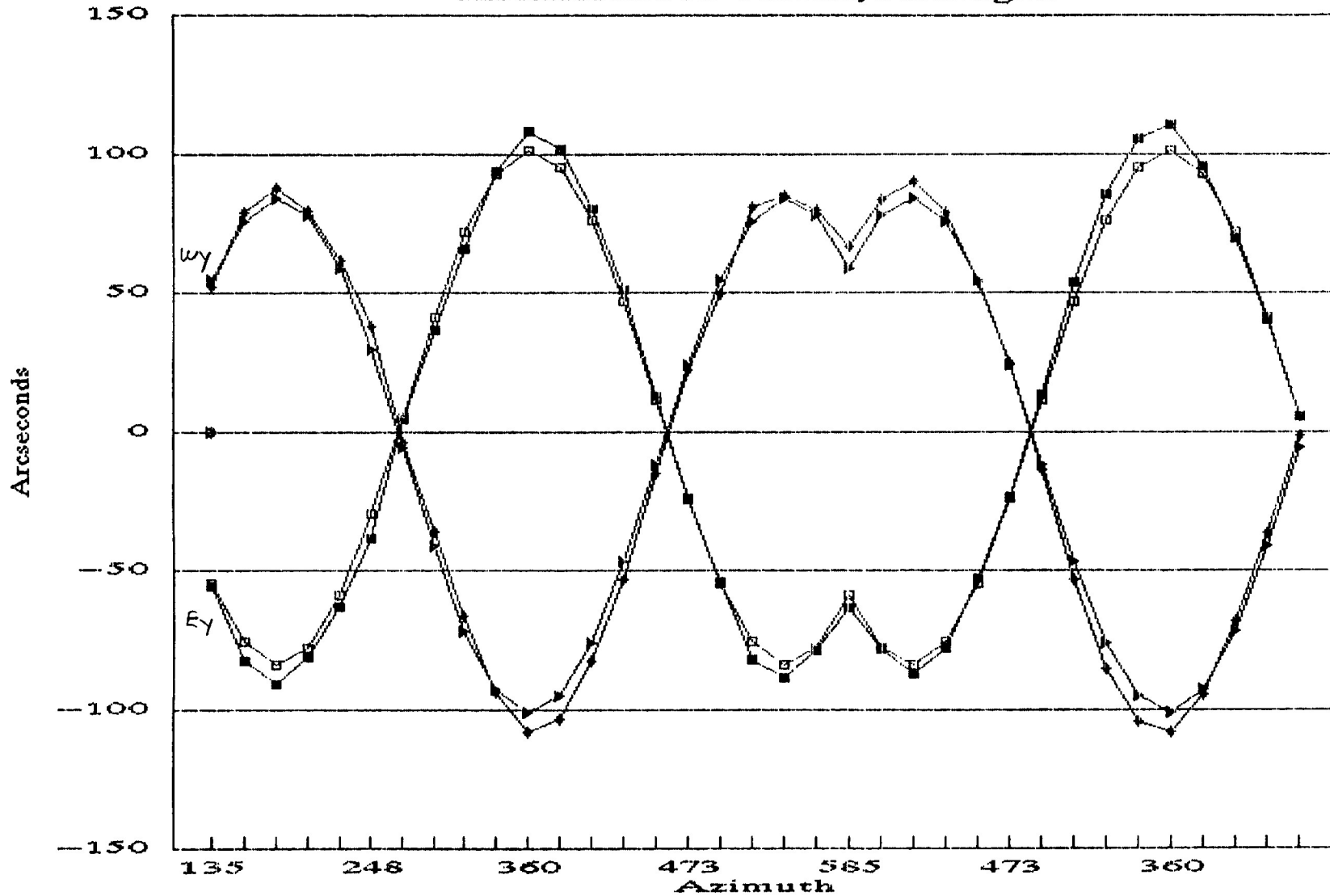


Tilt Ex   
  Tilt Wx   
  Coeff   
  Coeff

Test 3, Nov 30, 1989  
C. Janes

# Box Test 3: Ant 6

Instantaneous Values, Averaged

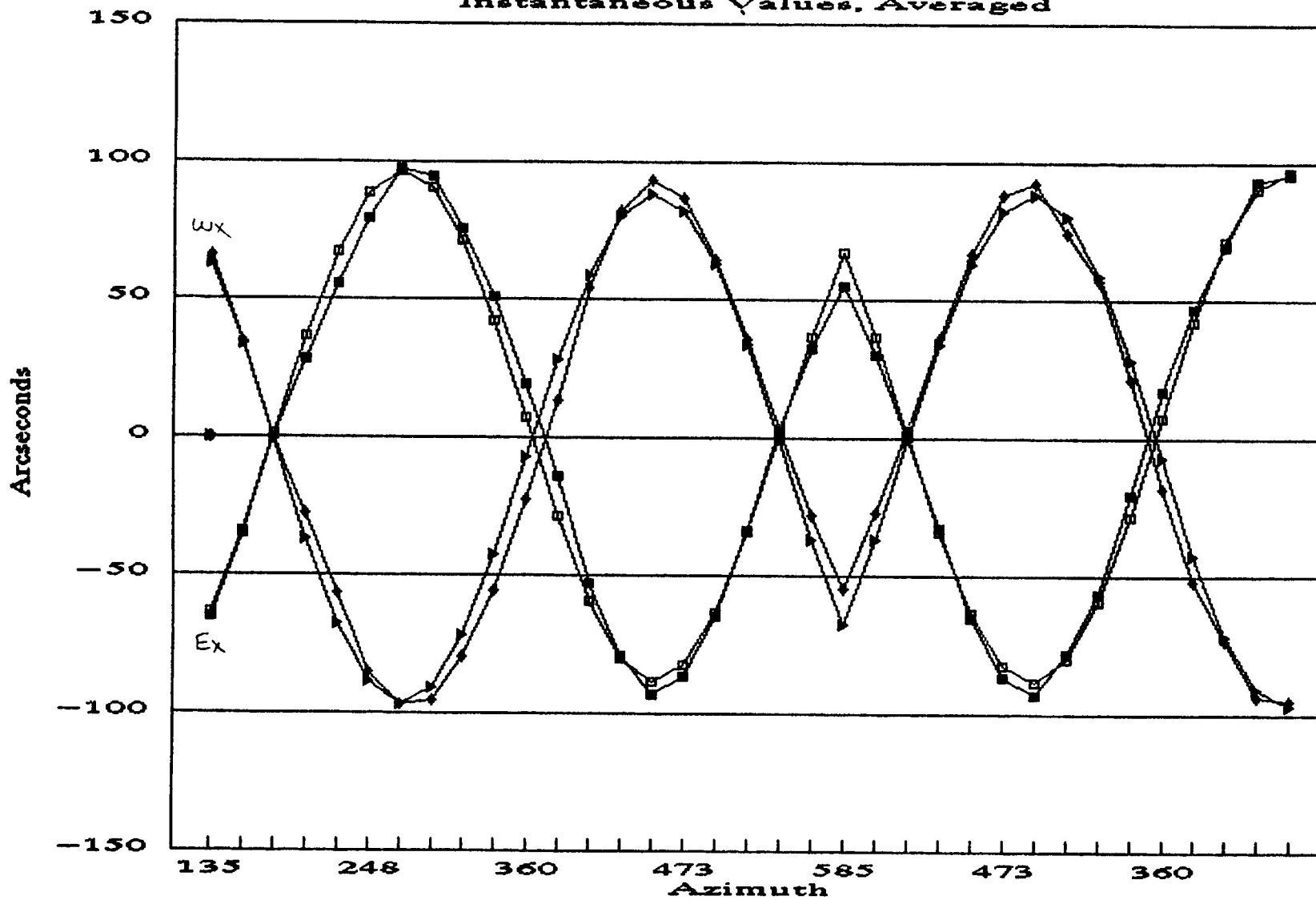


—■— Tilt Ey    —▲— Tilt Wy    —▶— Coeff.    —□— Coeff.

Test 3, Nov 30, 89  
C. Jones

# Box Test 3: Ant 6

Instantaneous Values, Averaged

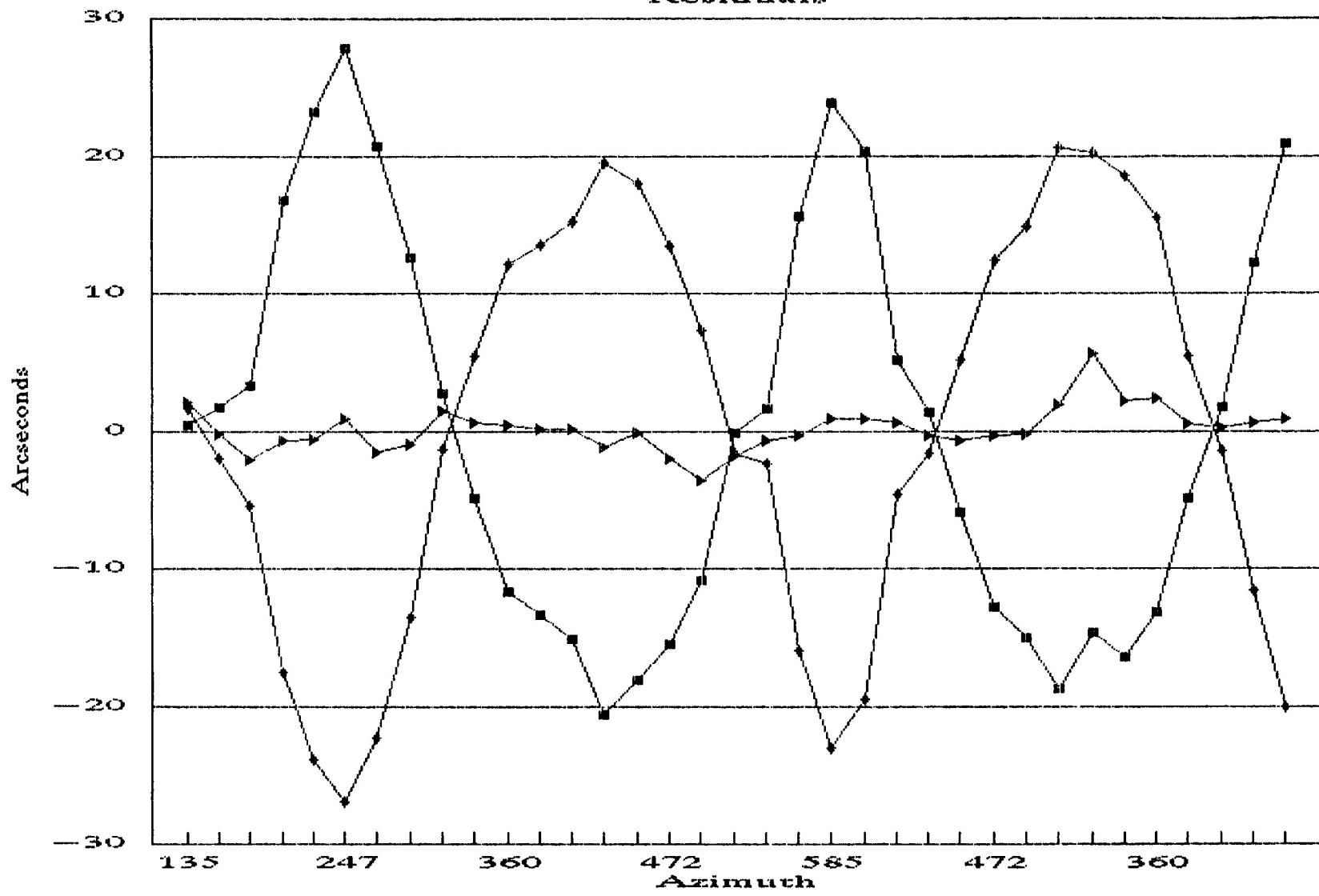


—■— Tilt Ex    —▲— Tilt Wx    —▶— Coeff.    —□— Coeff.

Test 3, Nov 30, 89  
C. Janes

# Box Test 3: Ant 22

Residuals



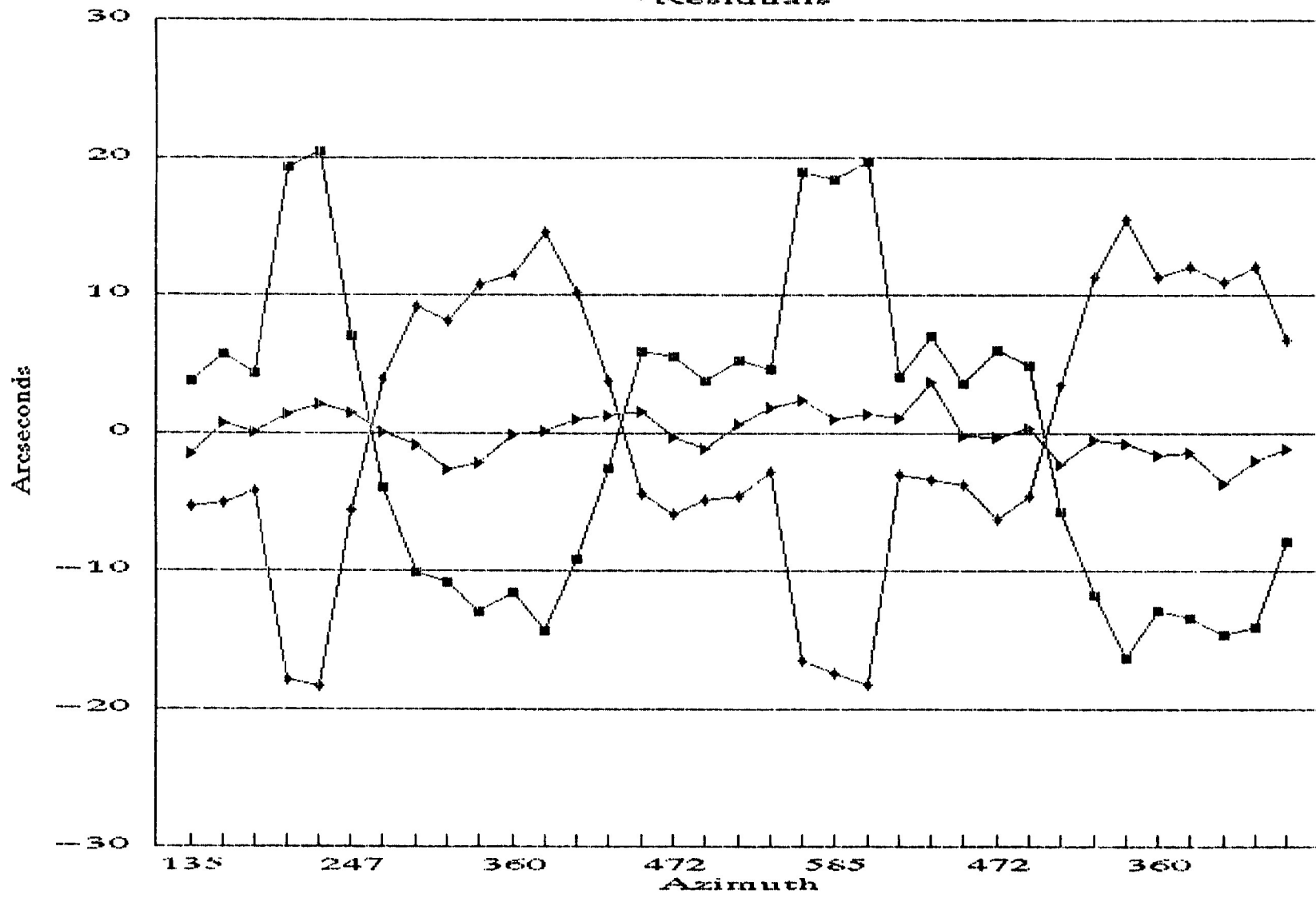
—■— Res Ey
—▲— Res Wy
—▶— Residual

Test 3, Nov 30, 1989  
C. Janes



# Box Test 3: Ant 22

Residuals

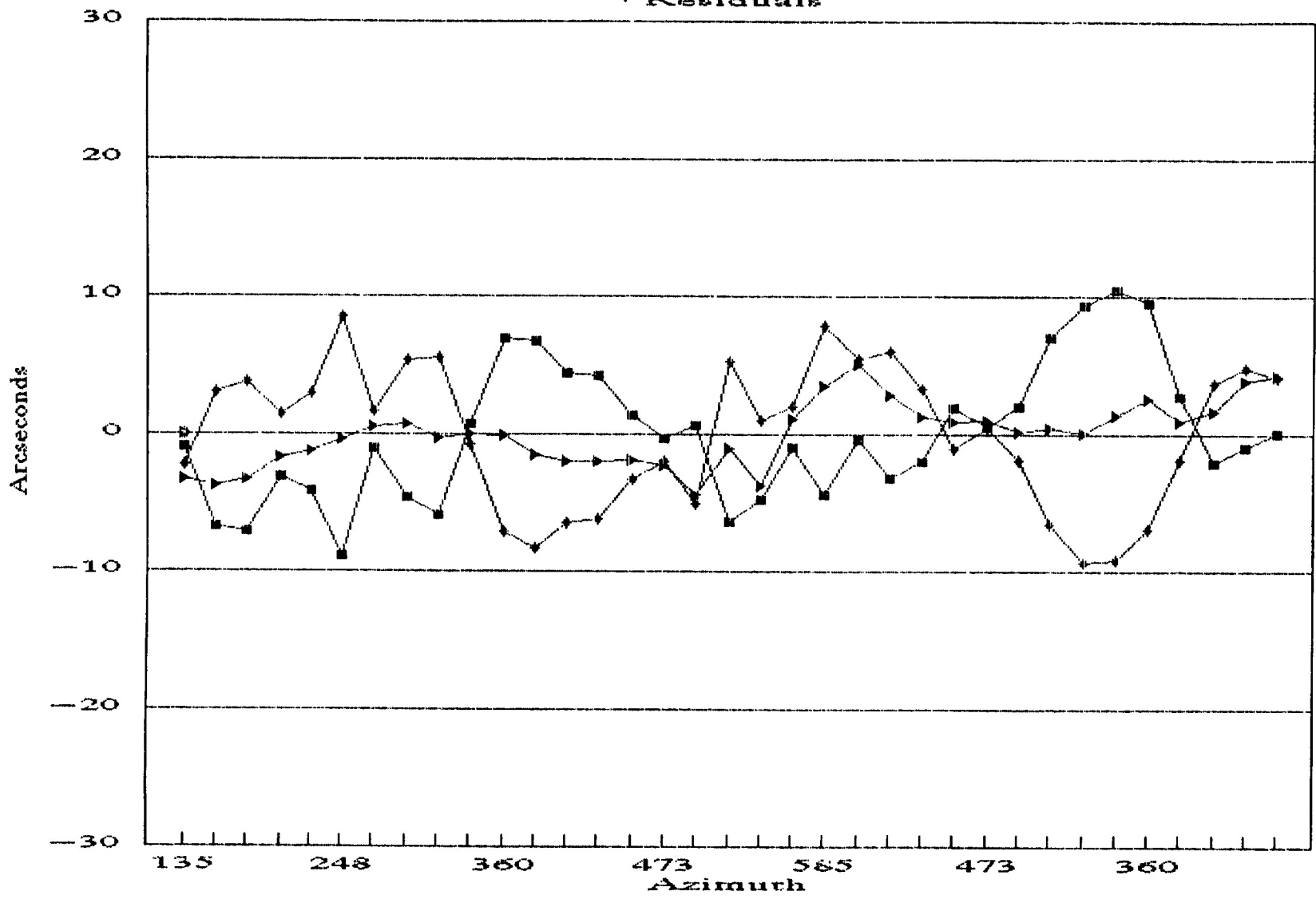


■ Res Ex    ◆ Res Wx    ▲ Residual

Test 3, Nov 30, 1989  
C. Jones

# Box Test 3: Ant 6

Residuals

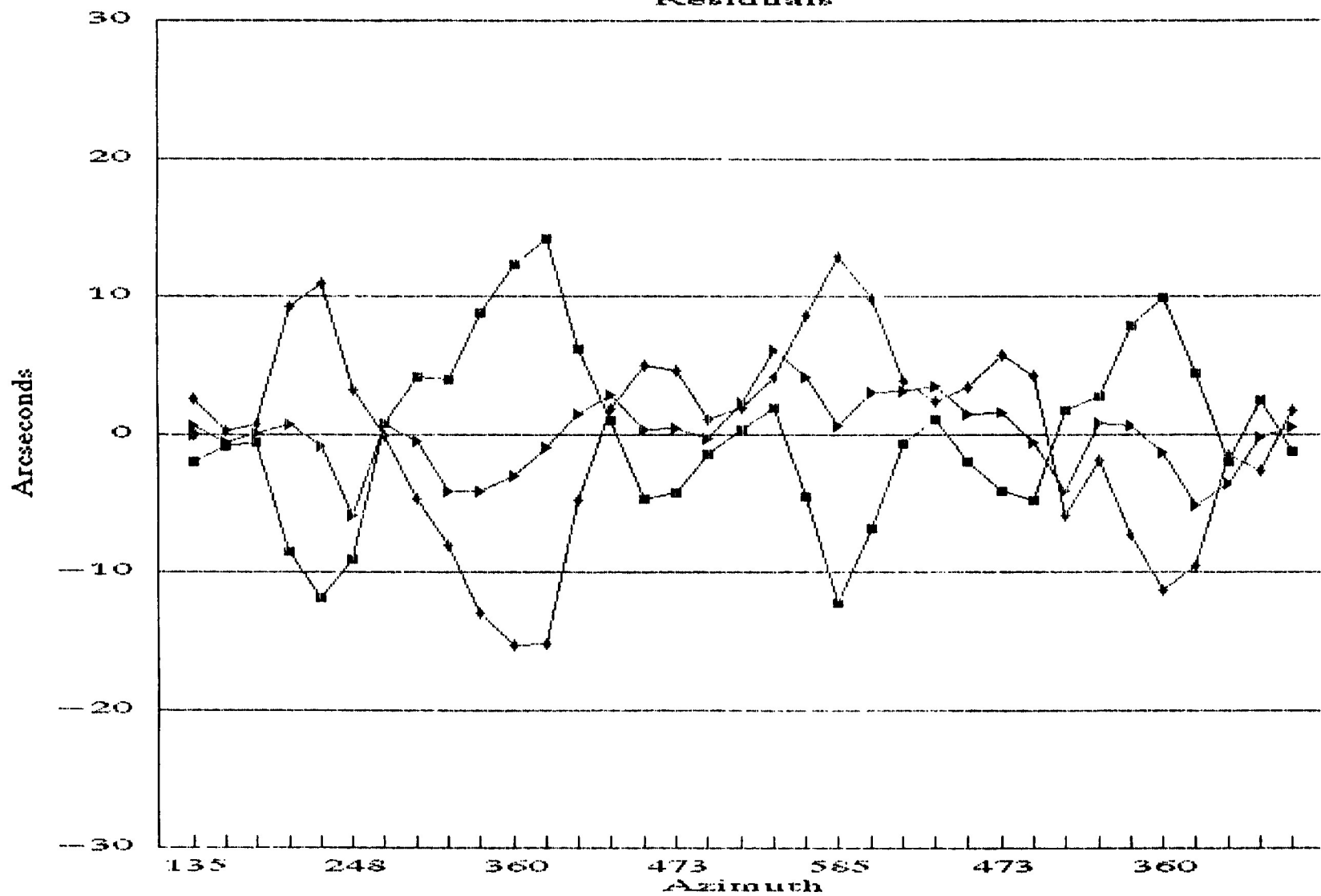


■ Res Ey    ▲ Wy Res    ▲ Residual

Test 3, Nov 30, 89  
C. Janes

# Box Test 3: Ant 6

Residuals

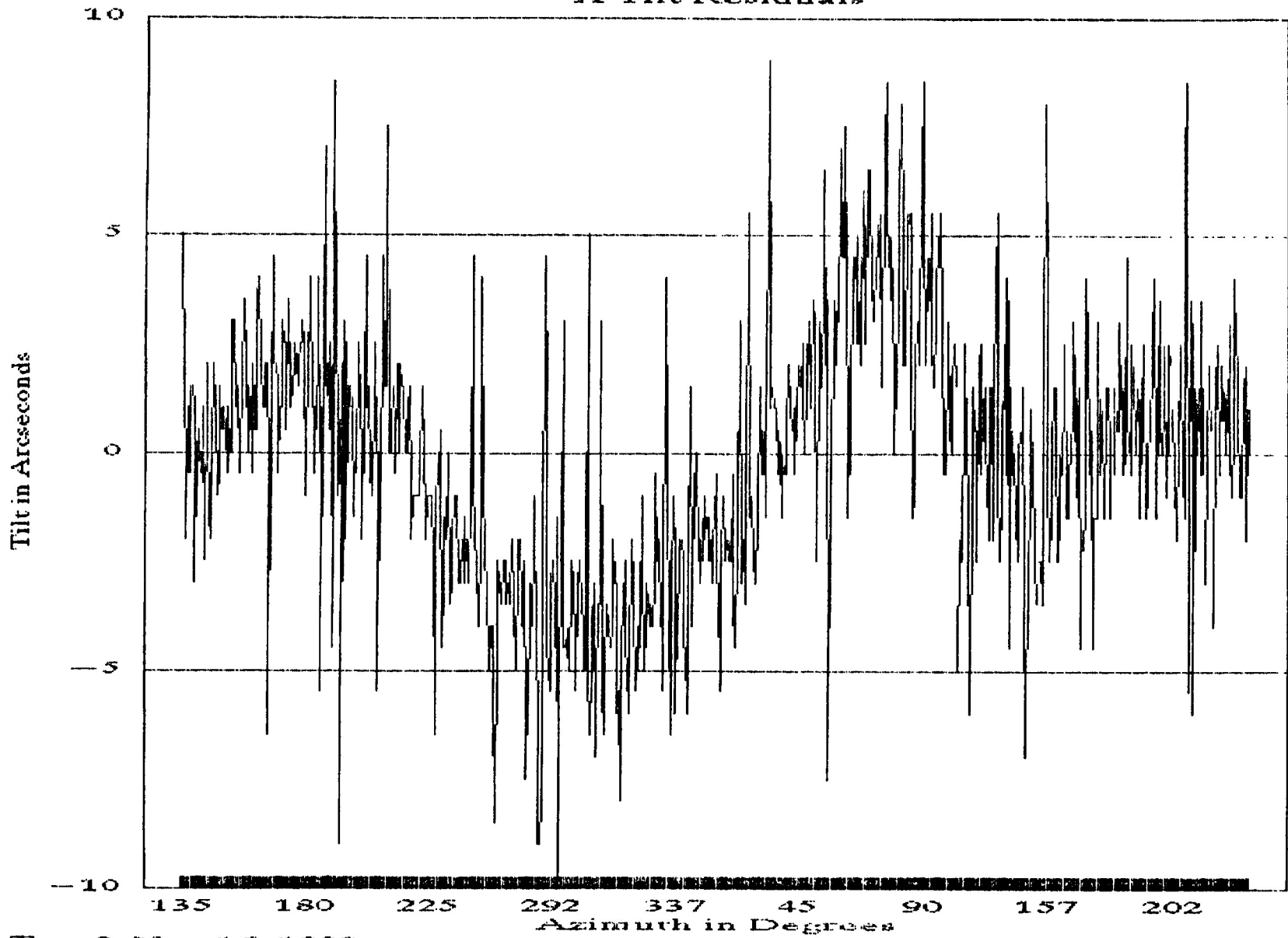


—■— Res Ex    —▲— Res Wx    —◆— Residual

Test 3, Nov 30, 89  
C. Jones

# Box Test 2: Antenna 22

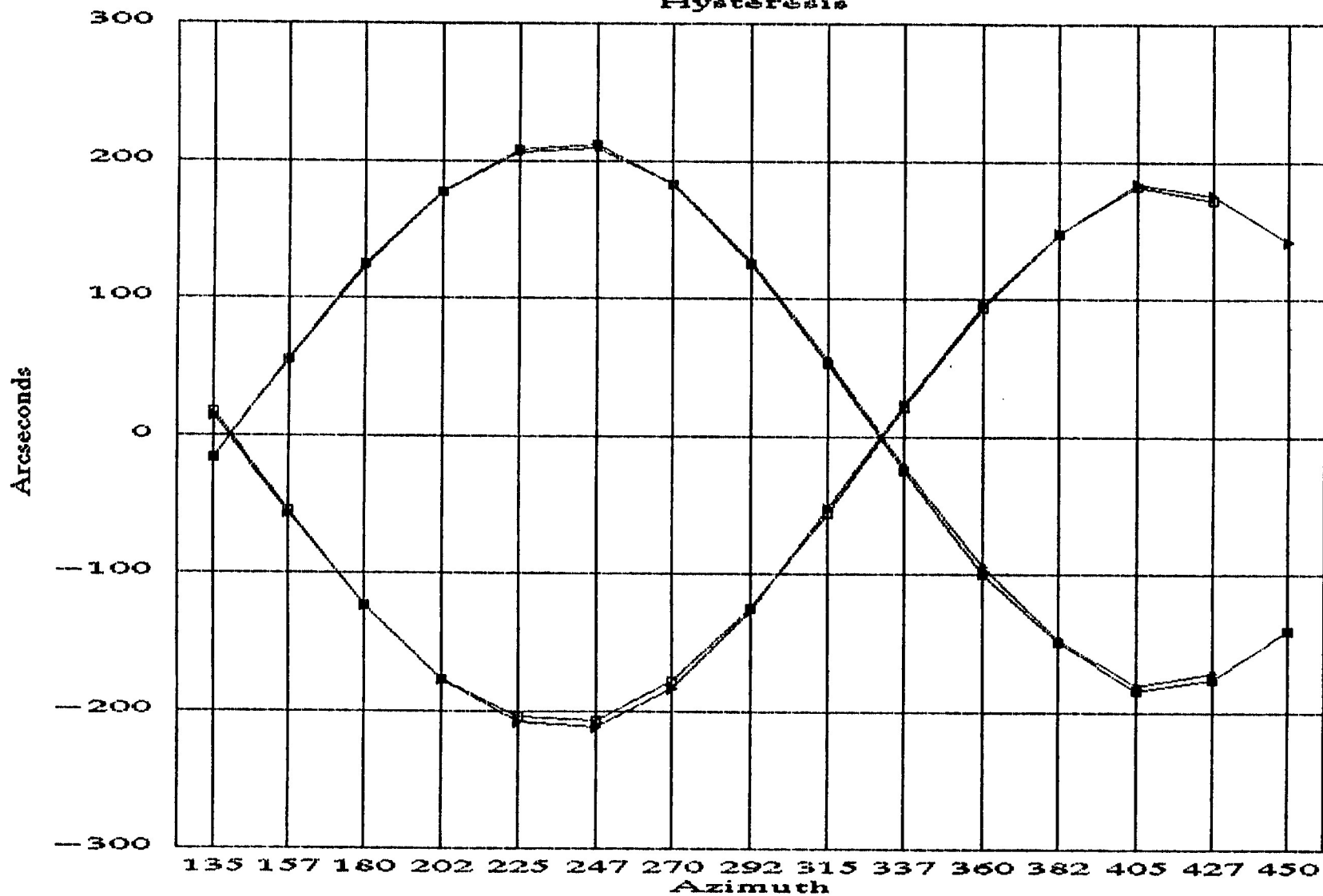
X Tilt Residuals



Test 2, Nov 16, 1989  
C. Jones

# Box Test 3: Ant 22

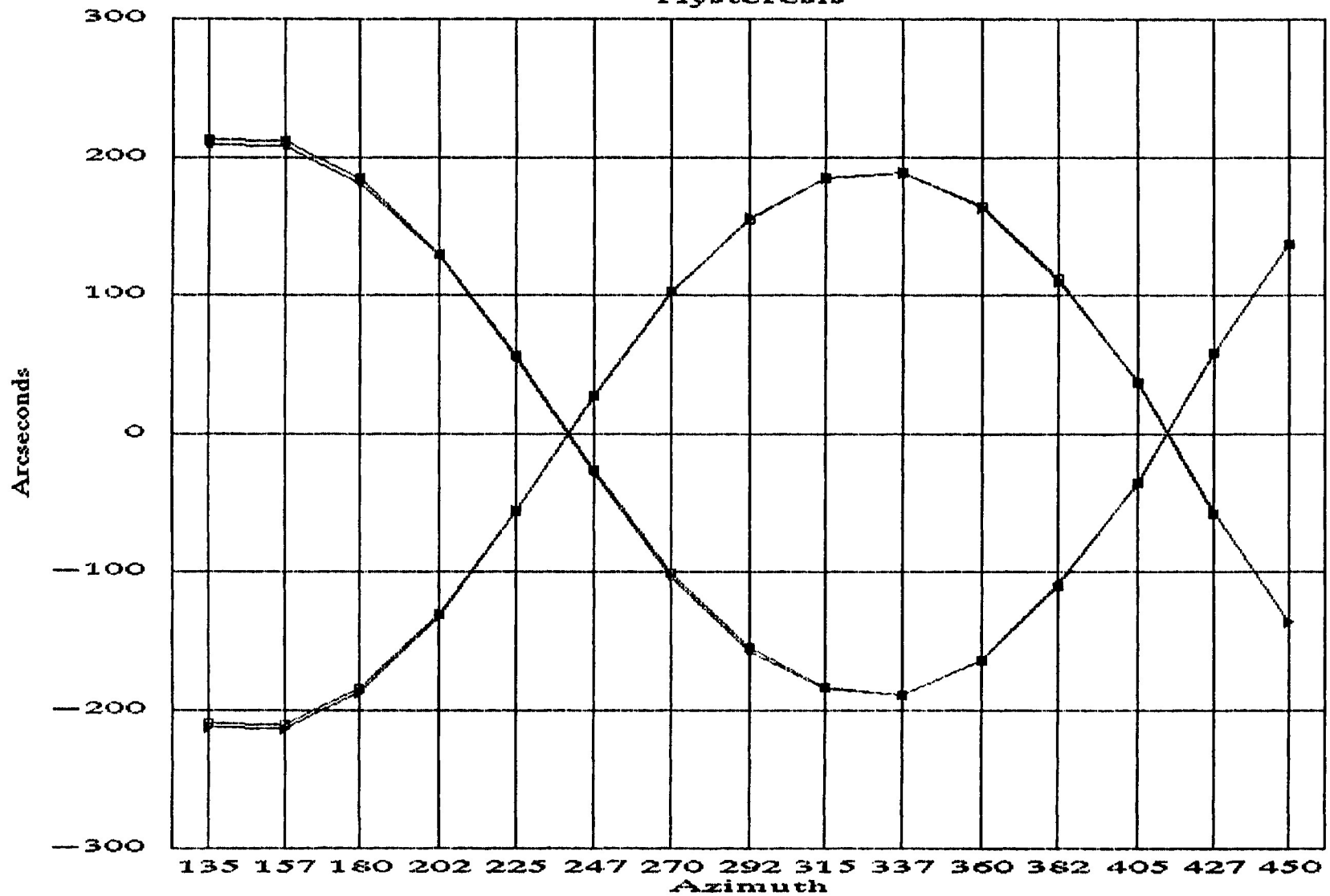
Hysteresis



● Tilt Ey (1)    ◻ Tilt Ey (2)    ▲ Tilt Wy (1)    ◻ Tilt Wy (2)  
Test 3, Nov 30, 1989  
C. Jones

# Box Test 3: Ant 22

Hysteresis

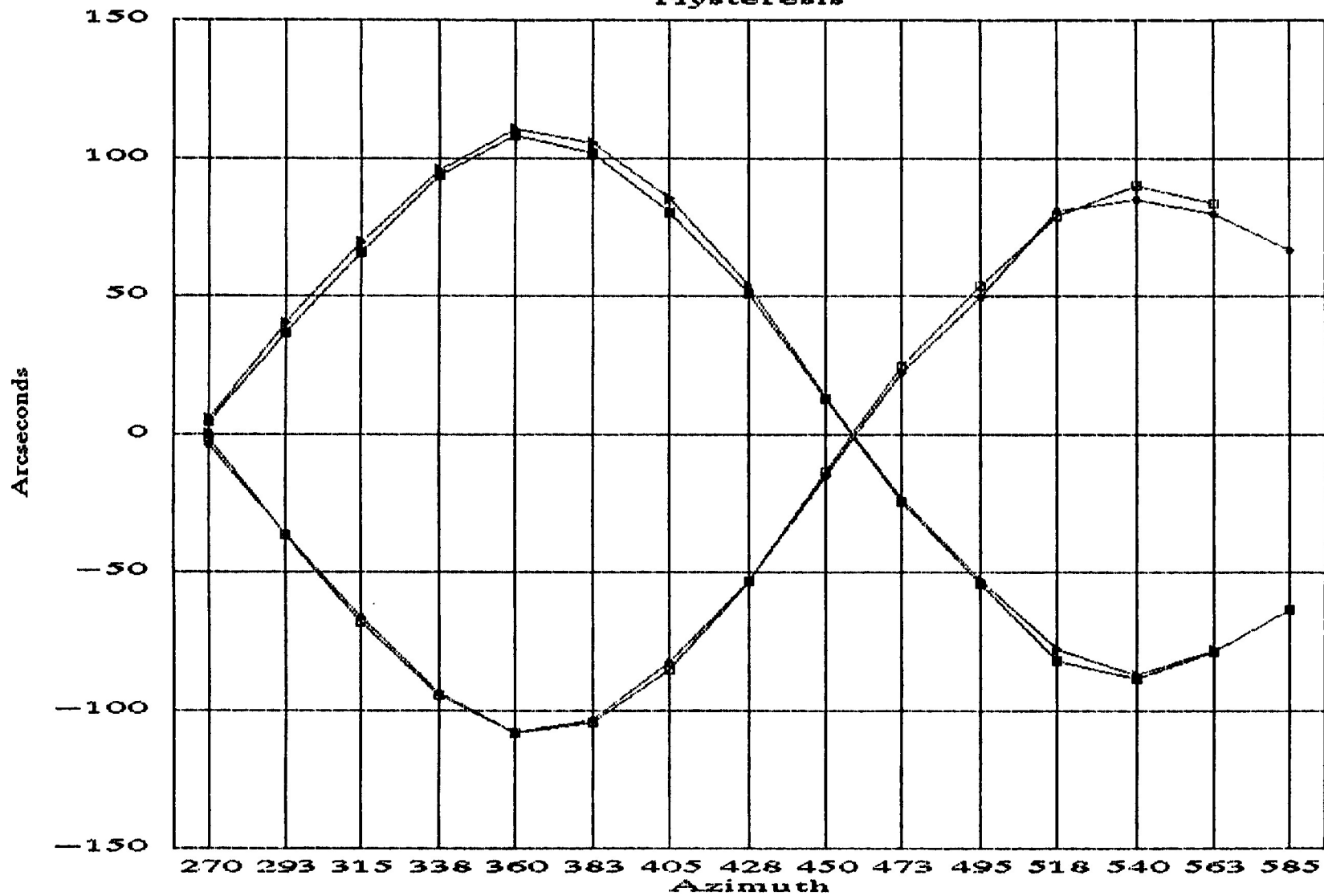


—■— Tilt Ex (1)    —▲— Tilt Ex (2)    —▶— Tilt Wx (1)    —□— Tilt Wx (2)

Test 3, Nov 30, 1989  
C. Janes

# Box Test 3: Ant 6

Hysteresis

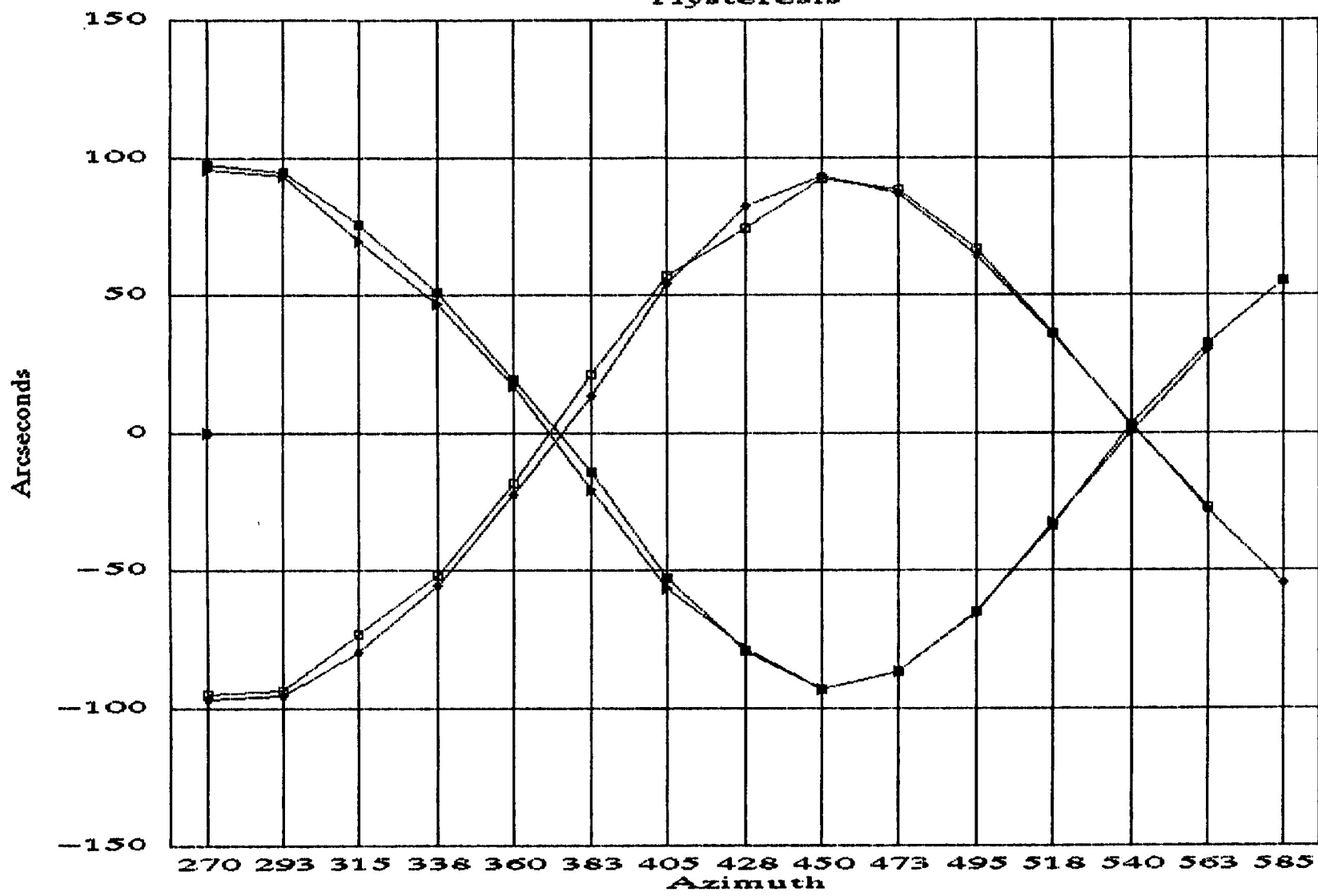


■ Tilt Ey (1)    ● Tilt Wy (2)    ▲ Tilt Ey (2)    □ Tilt Wy (2)

Test 3, Nov 30, 89  
C. Janes

# Box Test 3: Ant 6

Hysteresis



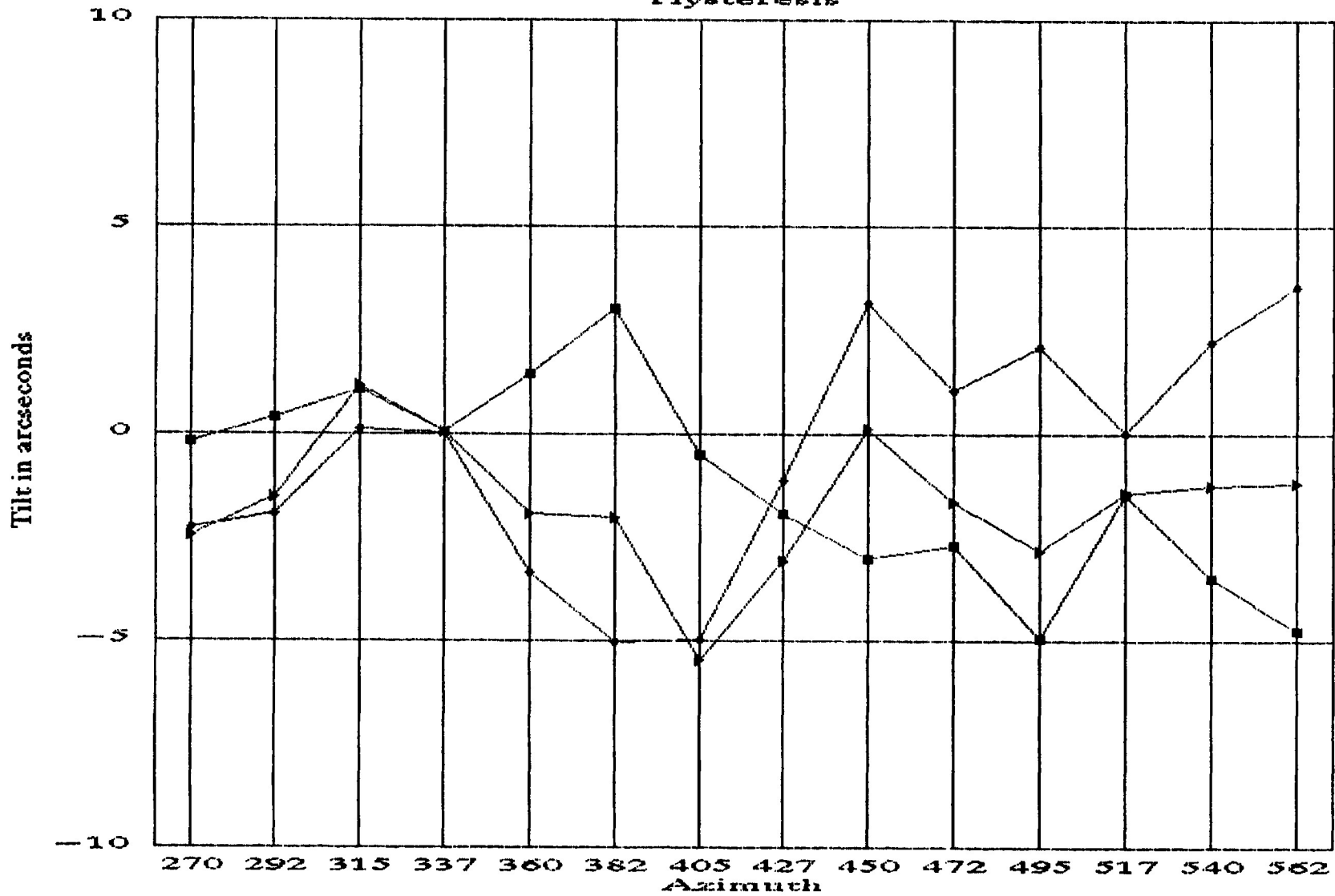
Tilt Ex (1)   
  Tilt Wx (2)   
  Tilt Ex (2)   
  Tilt Wx (2)

Test 3, Nov 30, 89  
 C. Jones



# Box Test 3: Ant 22

Hysteresis



—■— Ey Hyst.

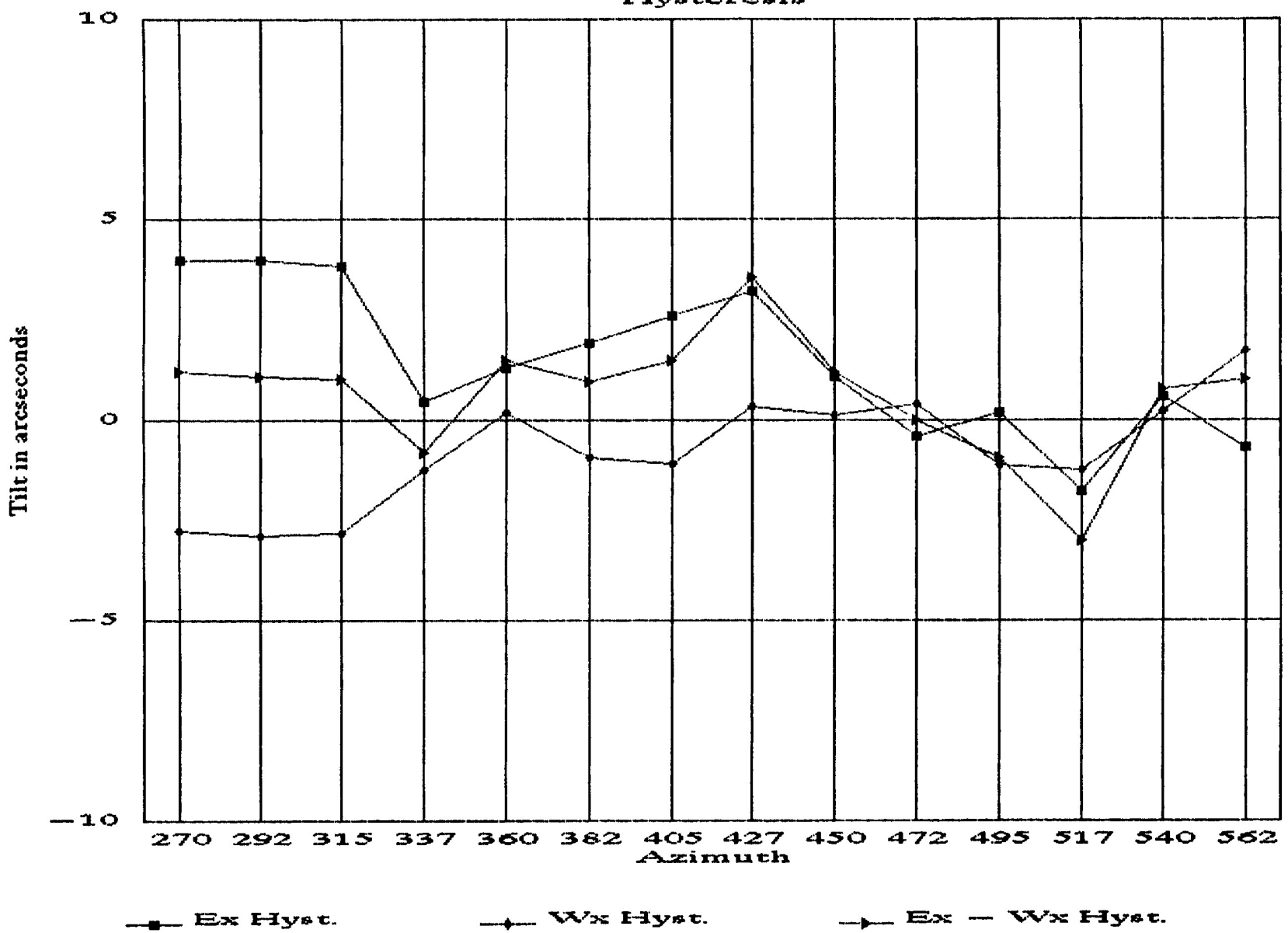
—+— Wy Hyst.

—▶— Ey - Wy Hyst.

Test 3, Nove 30, 89  
C. Jones

# Box Test 3: Ant 22

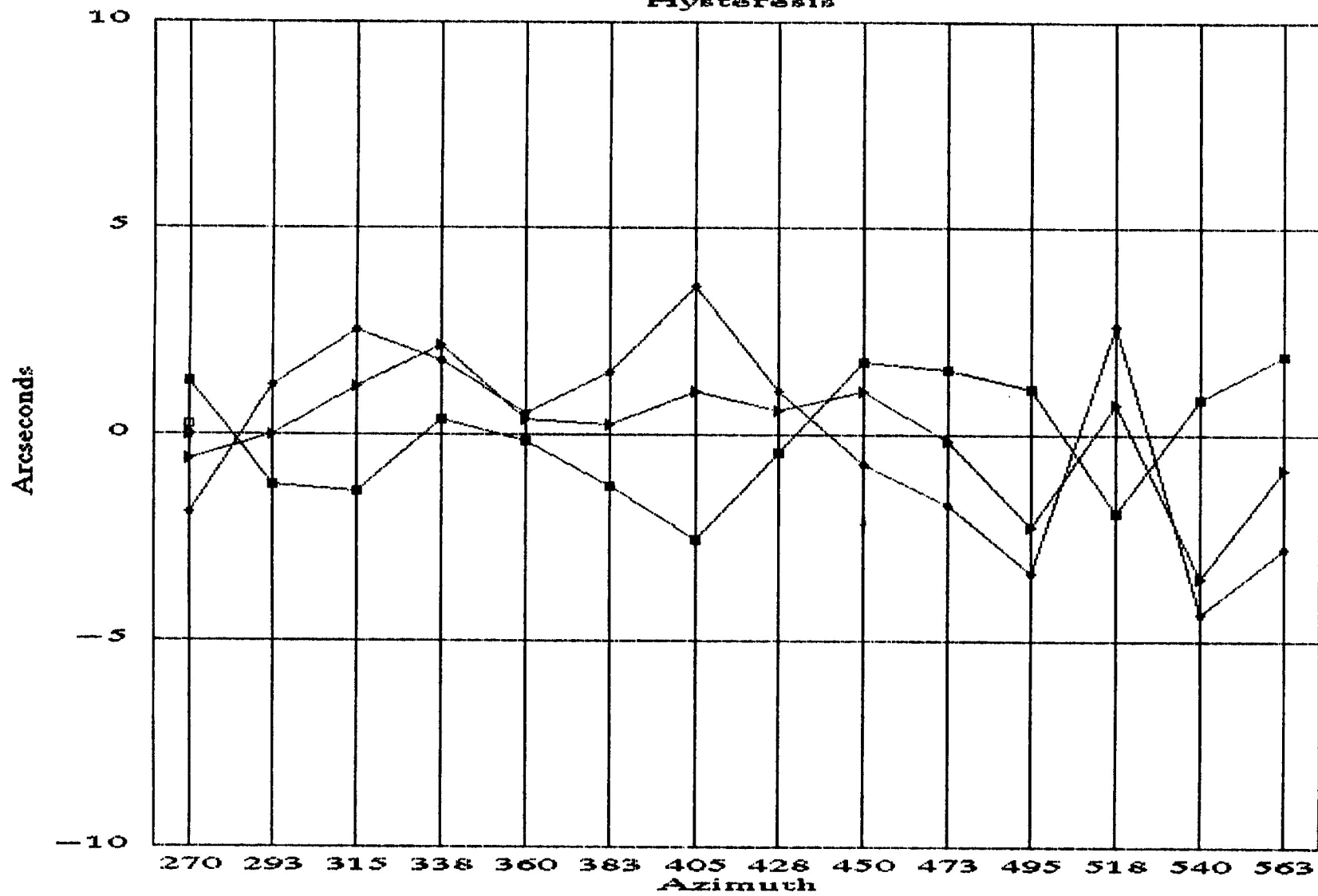
Hysteresis



Test 3, Nov 30, 89  
C. Jones

# Box Test 3: Ant 6

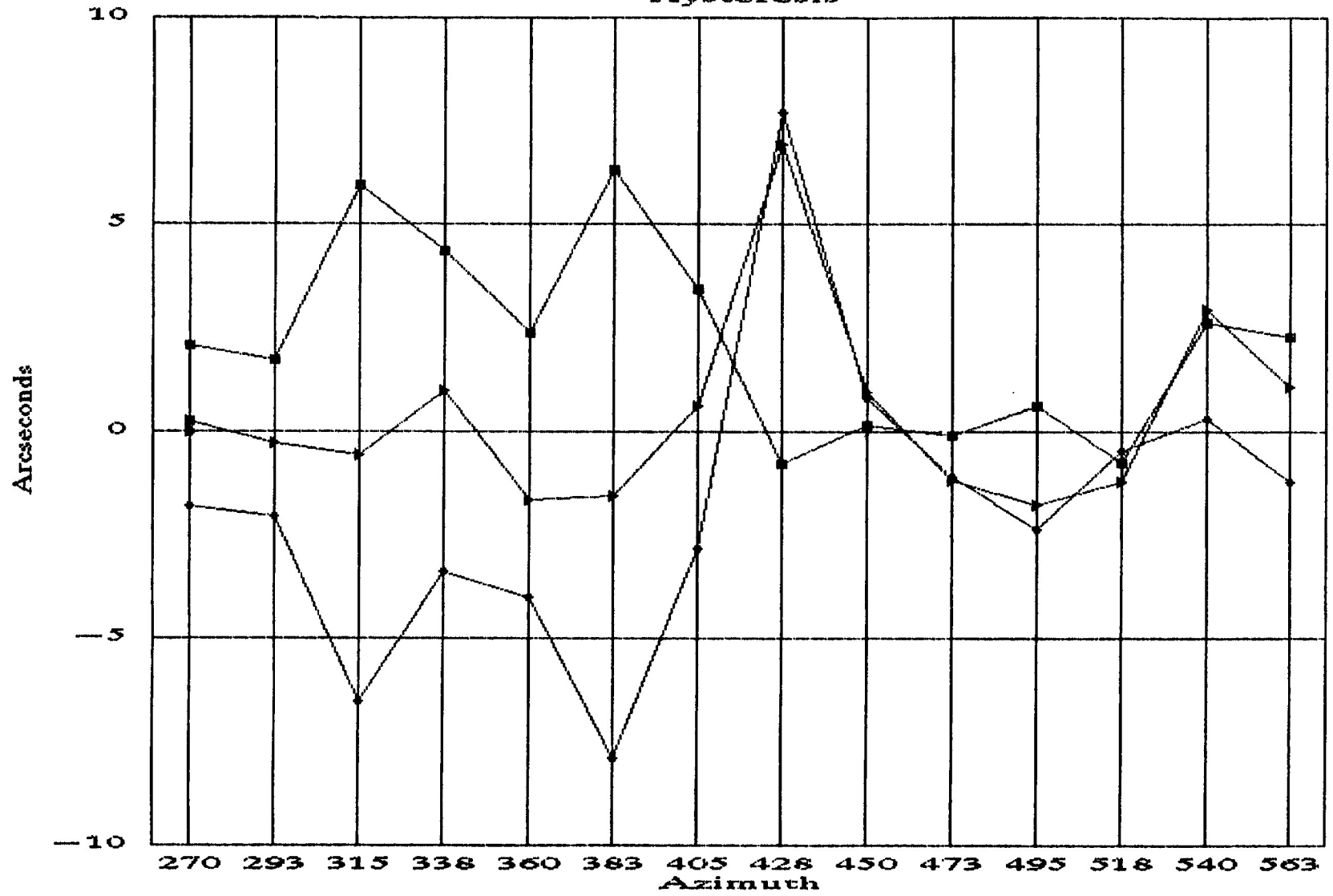
Hysteresis



■ Ey Hyst.      ◆ Wy Hyst.      -+ - Ey - Wy Hyst.  
 Test 3, Nov 30, 89  
 C. Jones

# Box Test 3: Ant 6

Hysteresis



Ex Hyst.

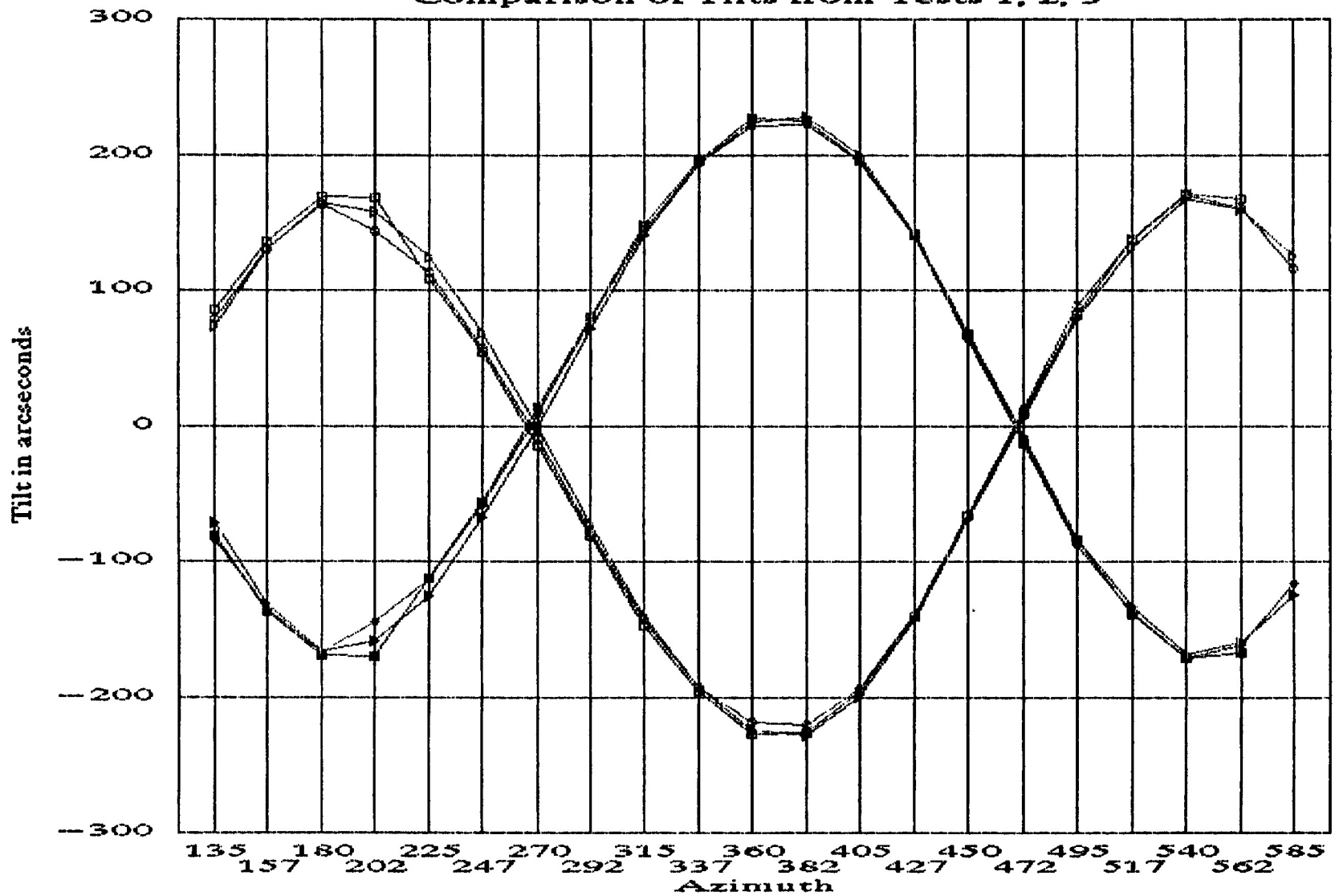
Wx Hyst.

Ex - Wx Hyst

Test 3, Nov 30, 89  
C. Janes

# Antenna 22 Box Tests

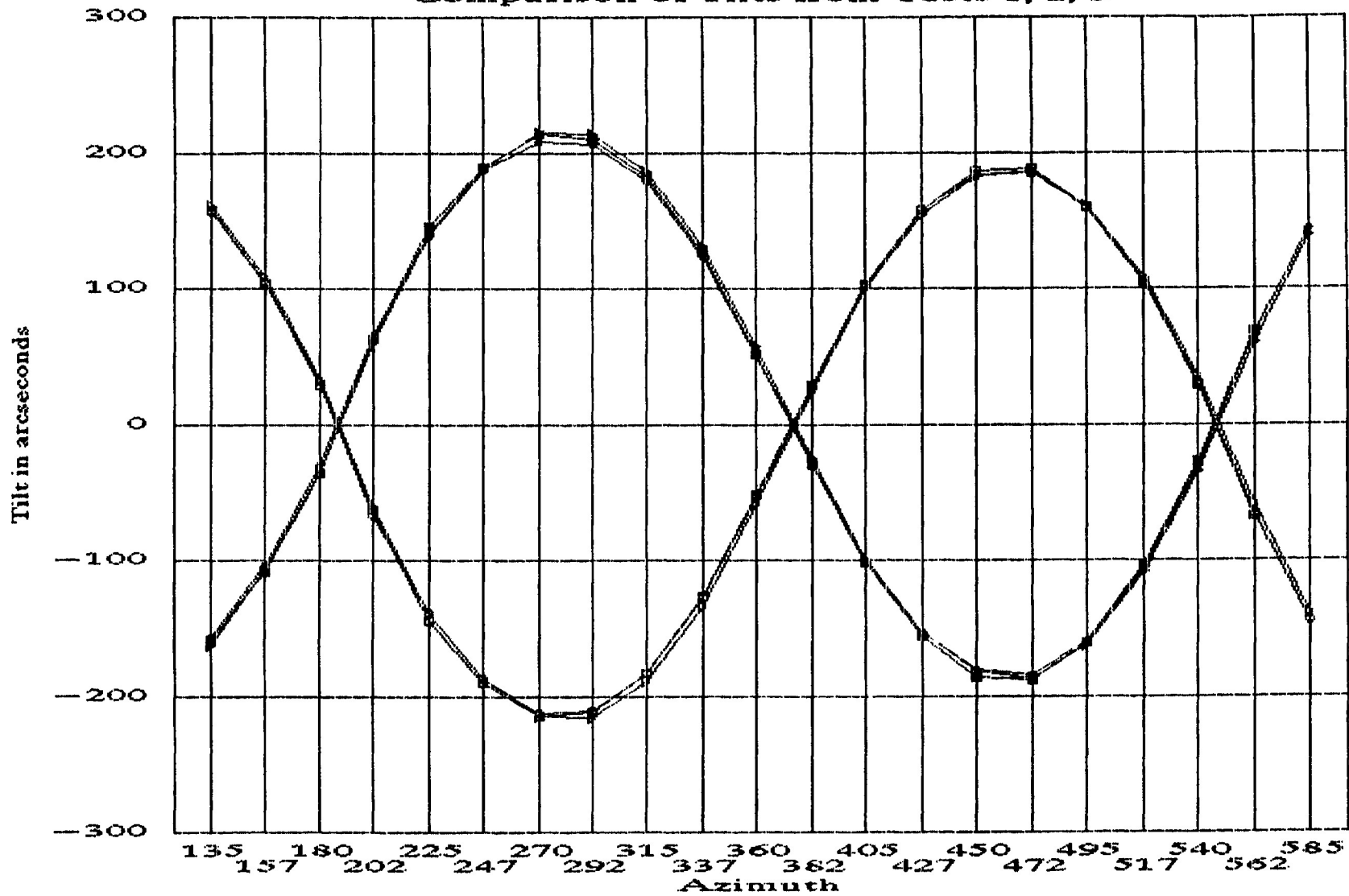
Comparison of Tilts from Tests 1, 2, 3



—■— Ey (1)    —▲— Ey (2)    —▼— Ey (3)    —□— Wy (1)    —◆— Wy (2)    —→— Wy (3)  
 1: Nov13; 2: Nov16; 3: Nov 30, 89  
 C. Janes

# Antenna 22 Box Tests

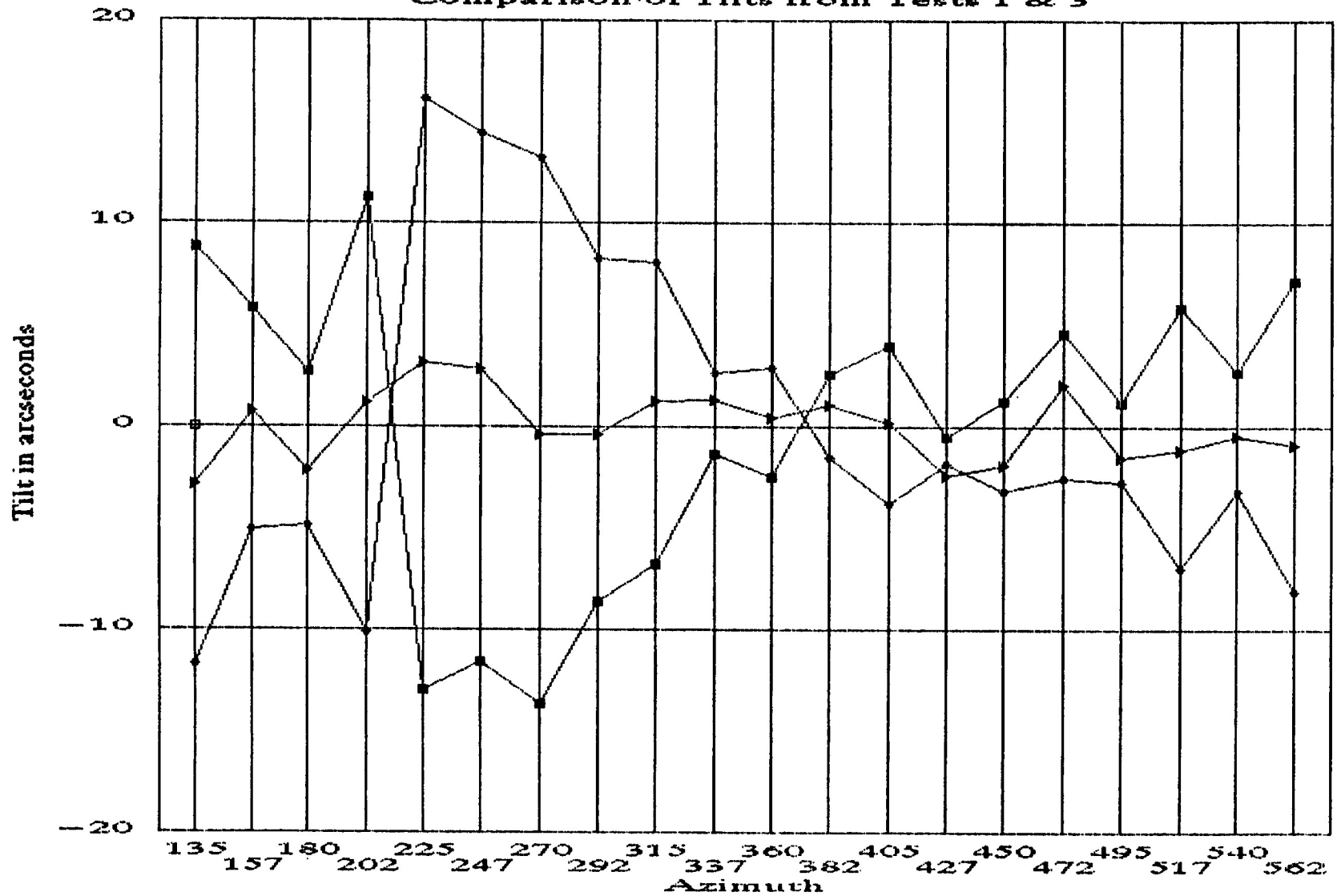
Comparison of Tilts from Tests 1, 2, 3



—■— Ex (1)    —◆— Ex (2)    —▲— Ex (3)    —■— Wx (1)    —◆— Wx (2)    —▲— Wx (3)  
 1: Nov 13; 2: Nov 16; 3: Nov 30, 89  
 C. Jones

# Antenna 22 Box Tests

Comparison of Tilts from Tests 1 & 3

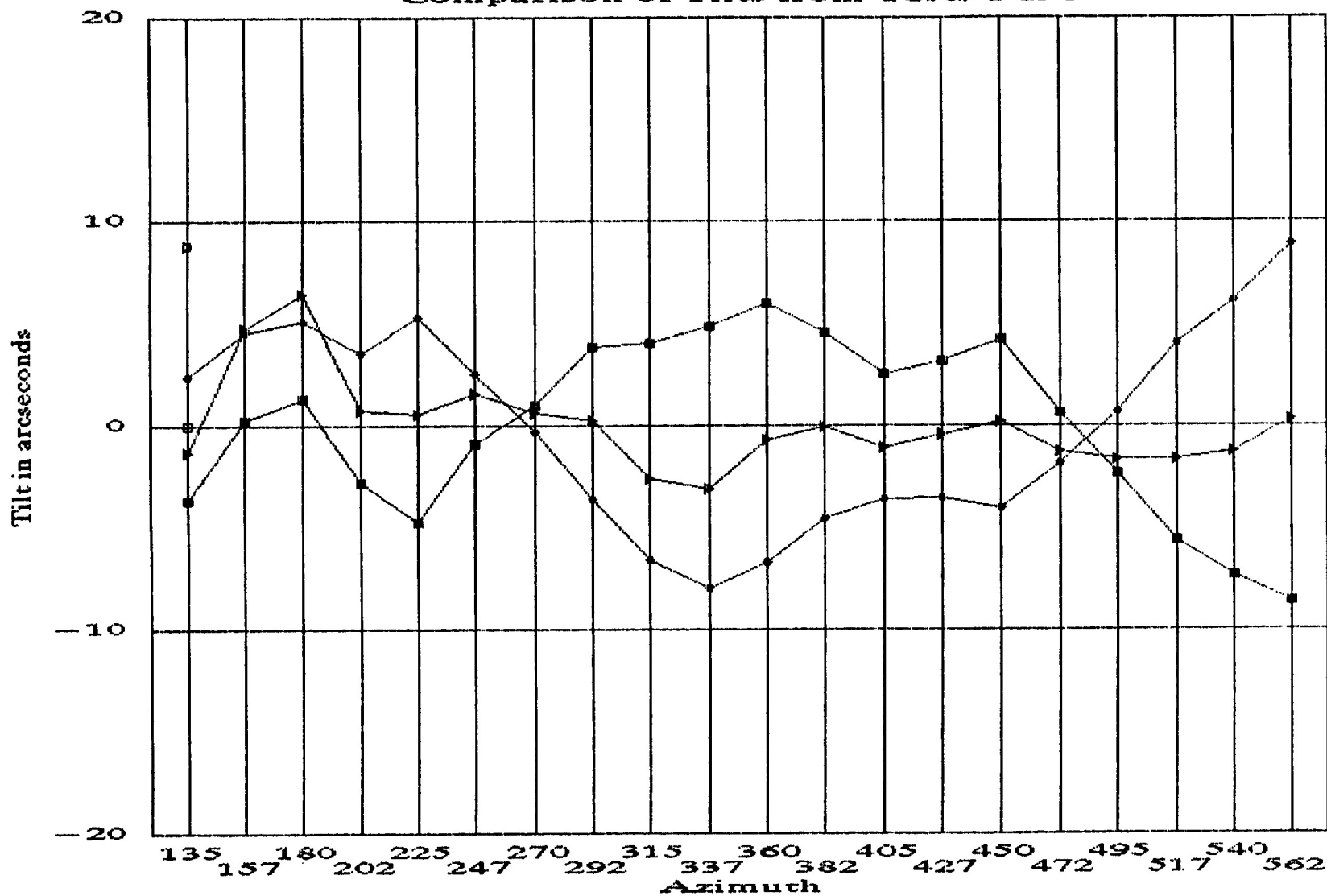


Ey(3) - Ey(1)    
  Wy(3) - Wy(1)    
  Ey - Wy

1: Nov 13; 3: Nov 30, 89  
C. Jones

# Antenna 22 Box Tests

Comparison of Tilts from Tests 1 & 3



■ Ex(3) - Ex(1)

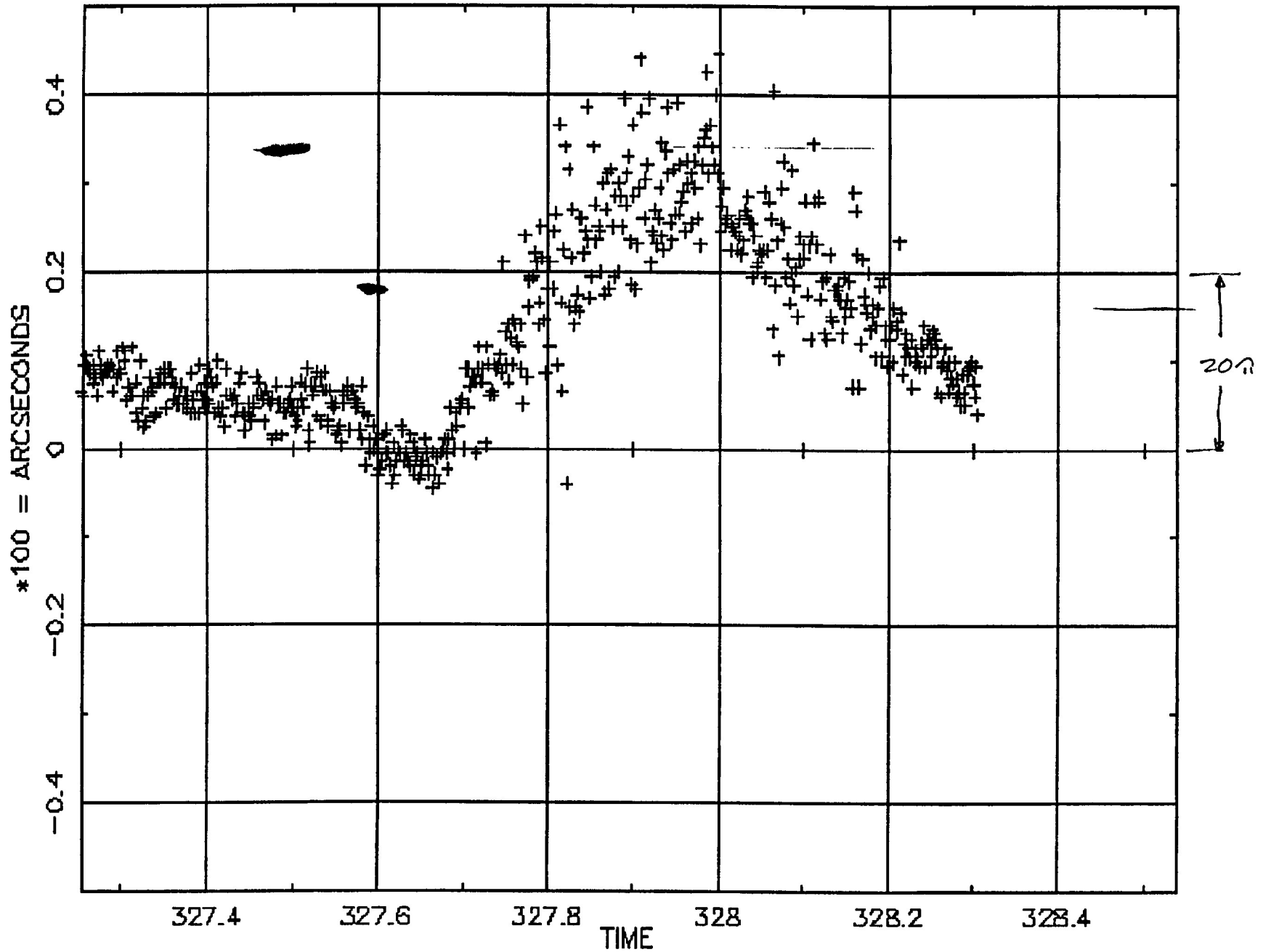
◆ Wx(3) - Wx(1)

▲ Ex - Wx

1: Nov 13; 3: Nov 30, 89  
C. Jones



ANTENNA 22: EY— —  
89NOV23 06:20:11 TO 89NOV24 07:40:11



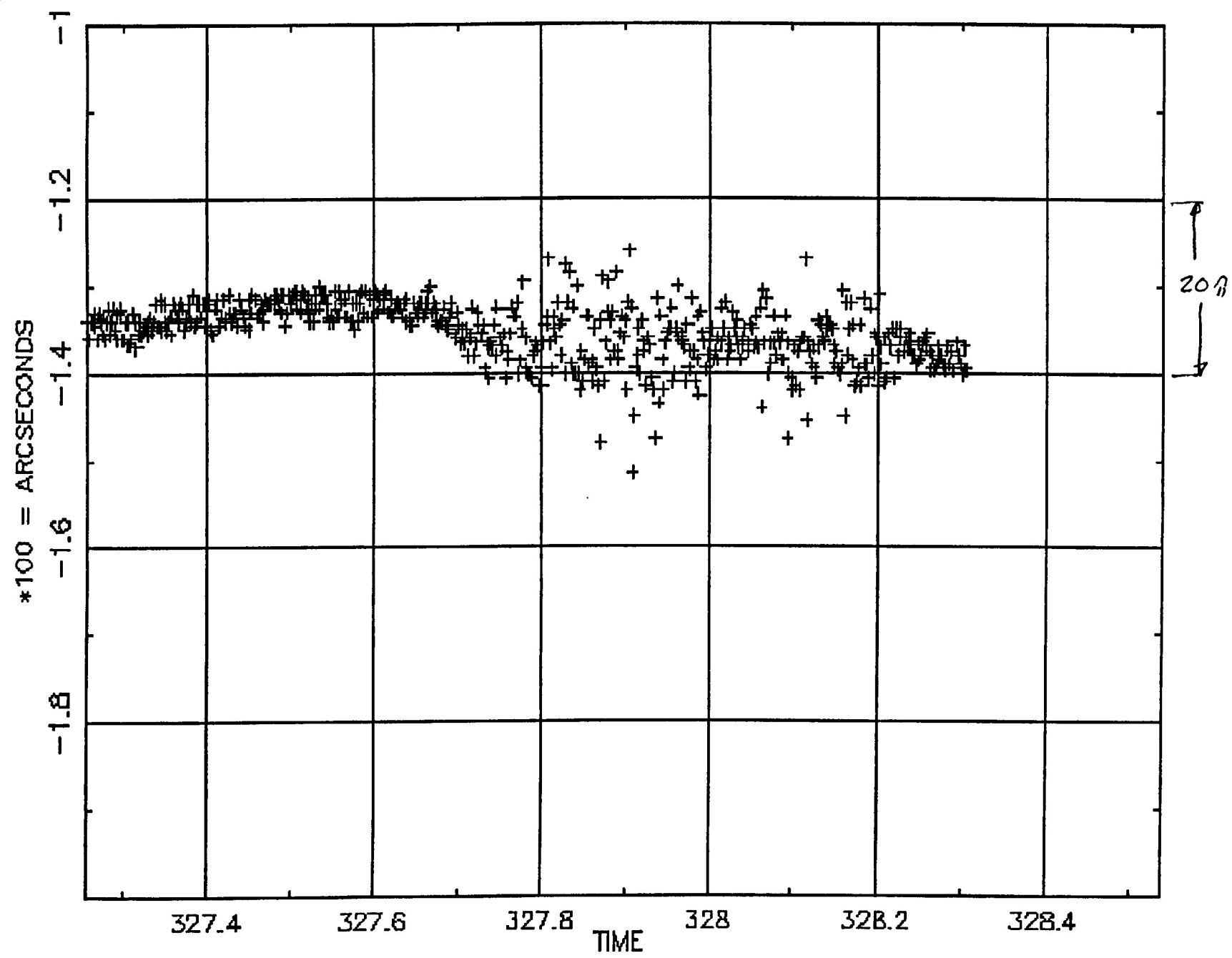
1:22:2:6D:V^

27 NOV 89 22:55:40

33

ANTENNA 22: EX  
89NOV23 06:20:11 TO 89NOV24 07:40:11

\*



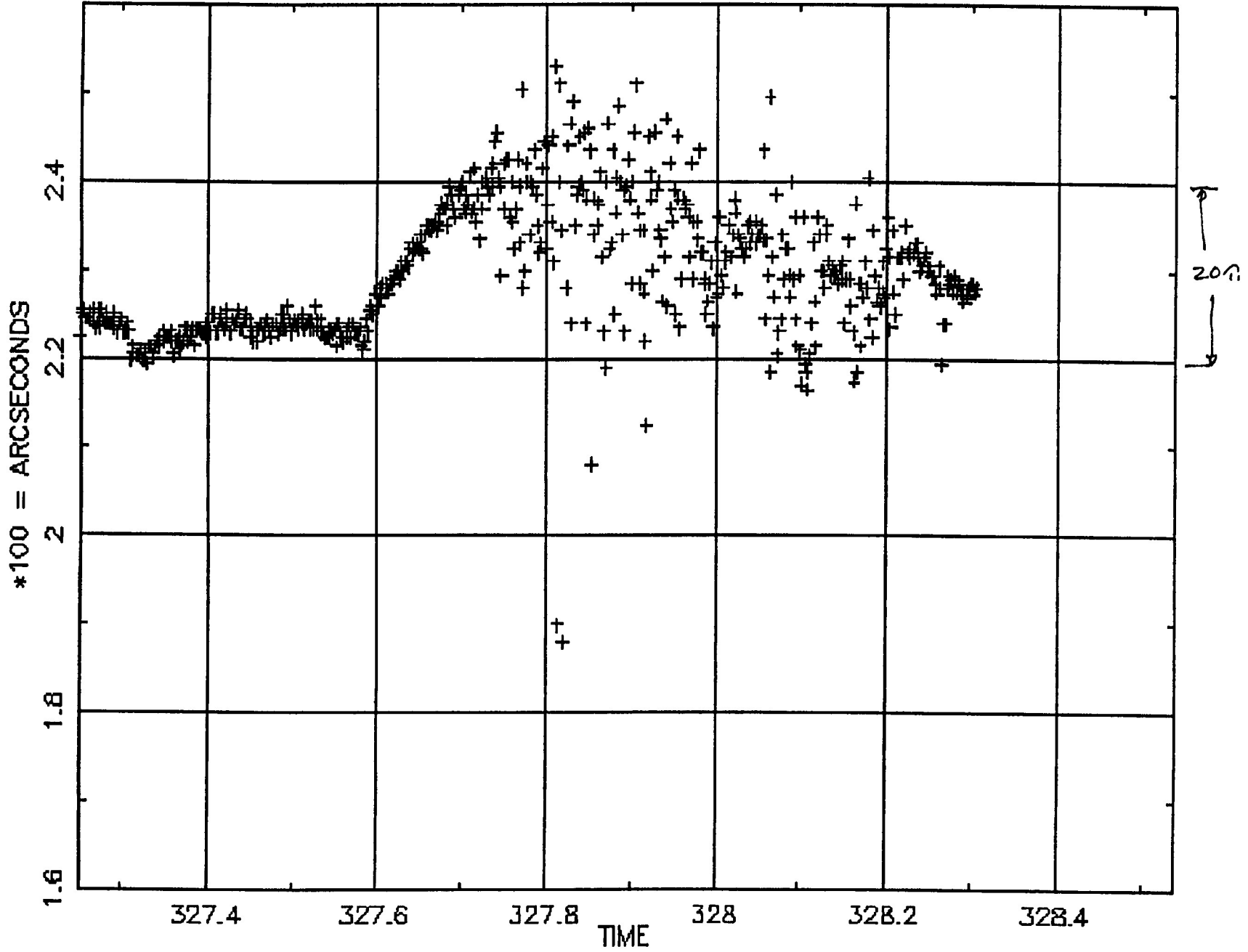
1:22:2'61:V

27 NOV 89 22:07:08

31

\*

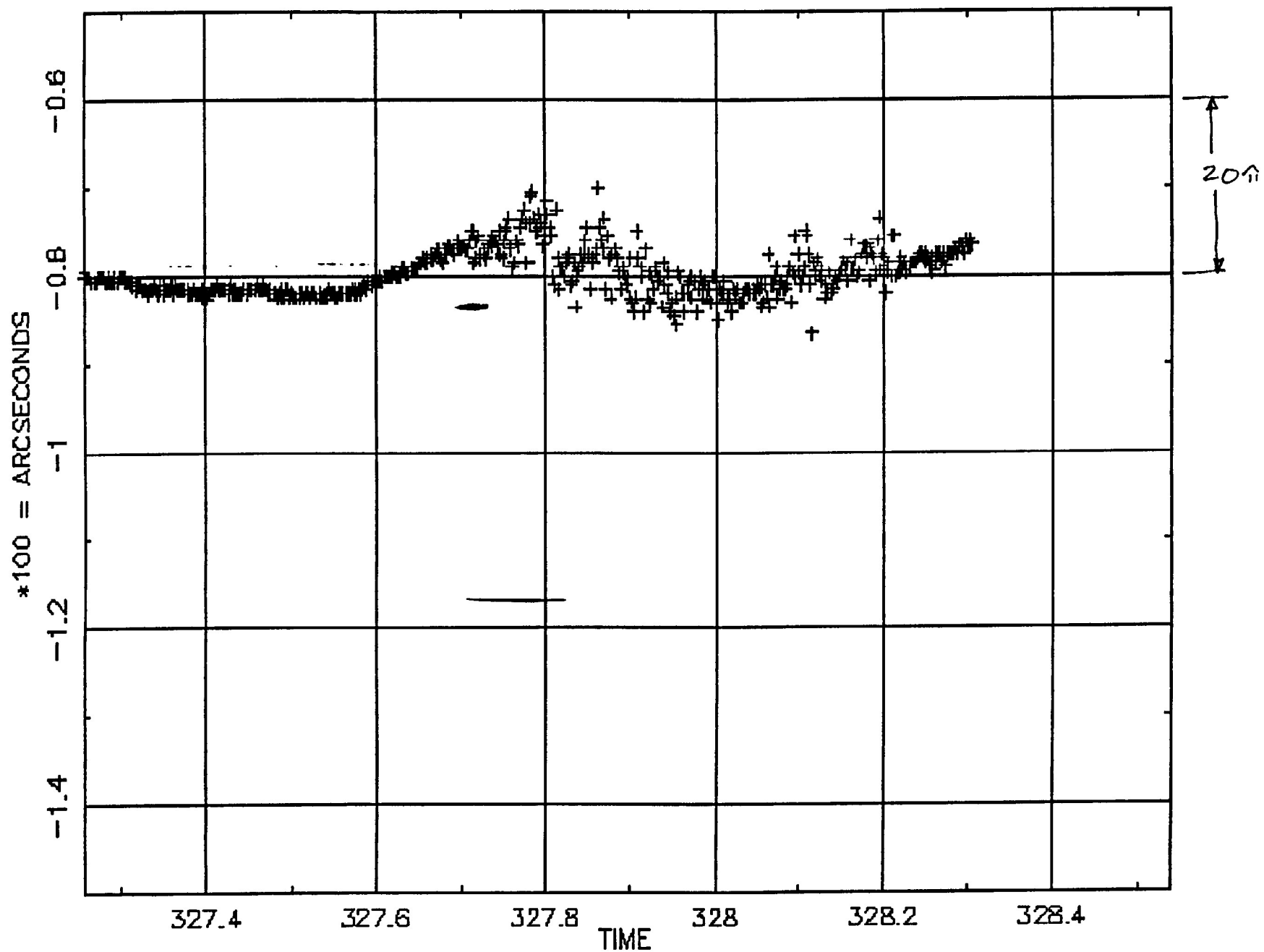
ANTENNA 22: WY  
89NOV23 06:20:11 TO 89NOV24 07:40:11



1:22:2'62:VA

27 NOV 89 22:17:24

ANTENNA 22: WX  
89NOV23 06:20:11 TO 89NOV24 07:40:11

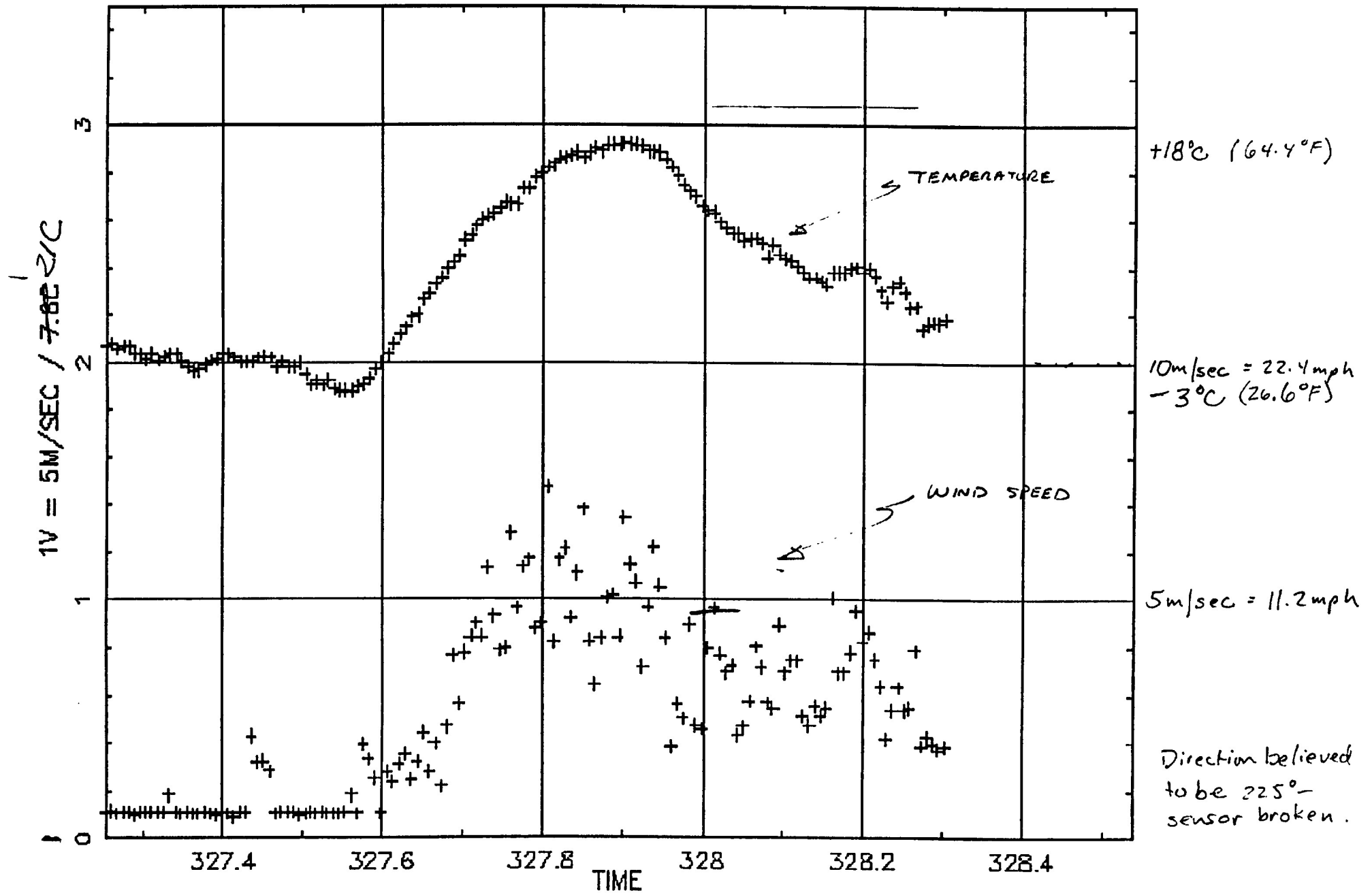


1:22:2:63:V^

27 NOV 89 22:40:14

3

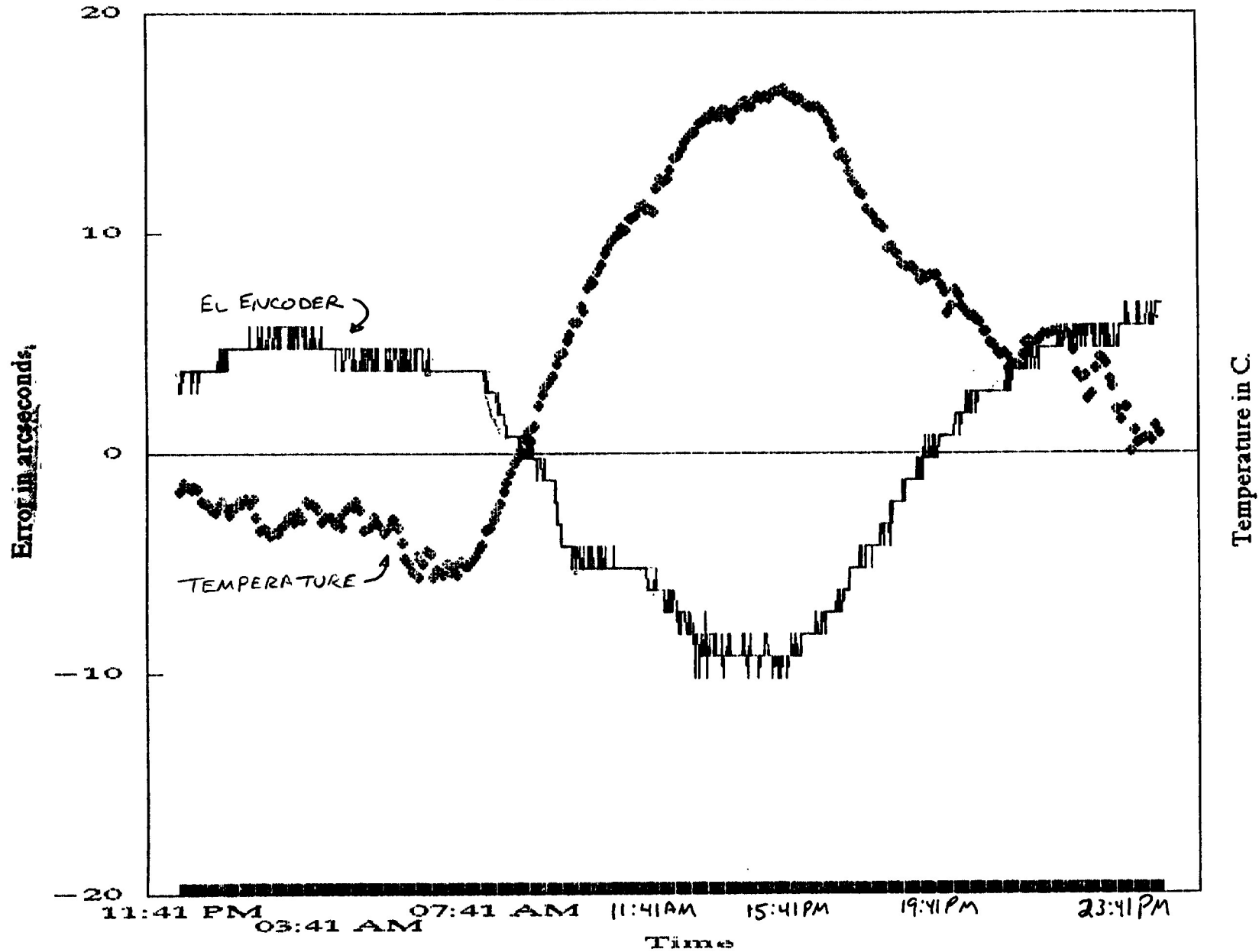
WIND SPEED/TEMPERATURE  
 89NOV23 06:21:31 TO 89NOV24 07:41:31



1:0:0:2;V^2:0:0:4;V^A

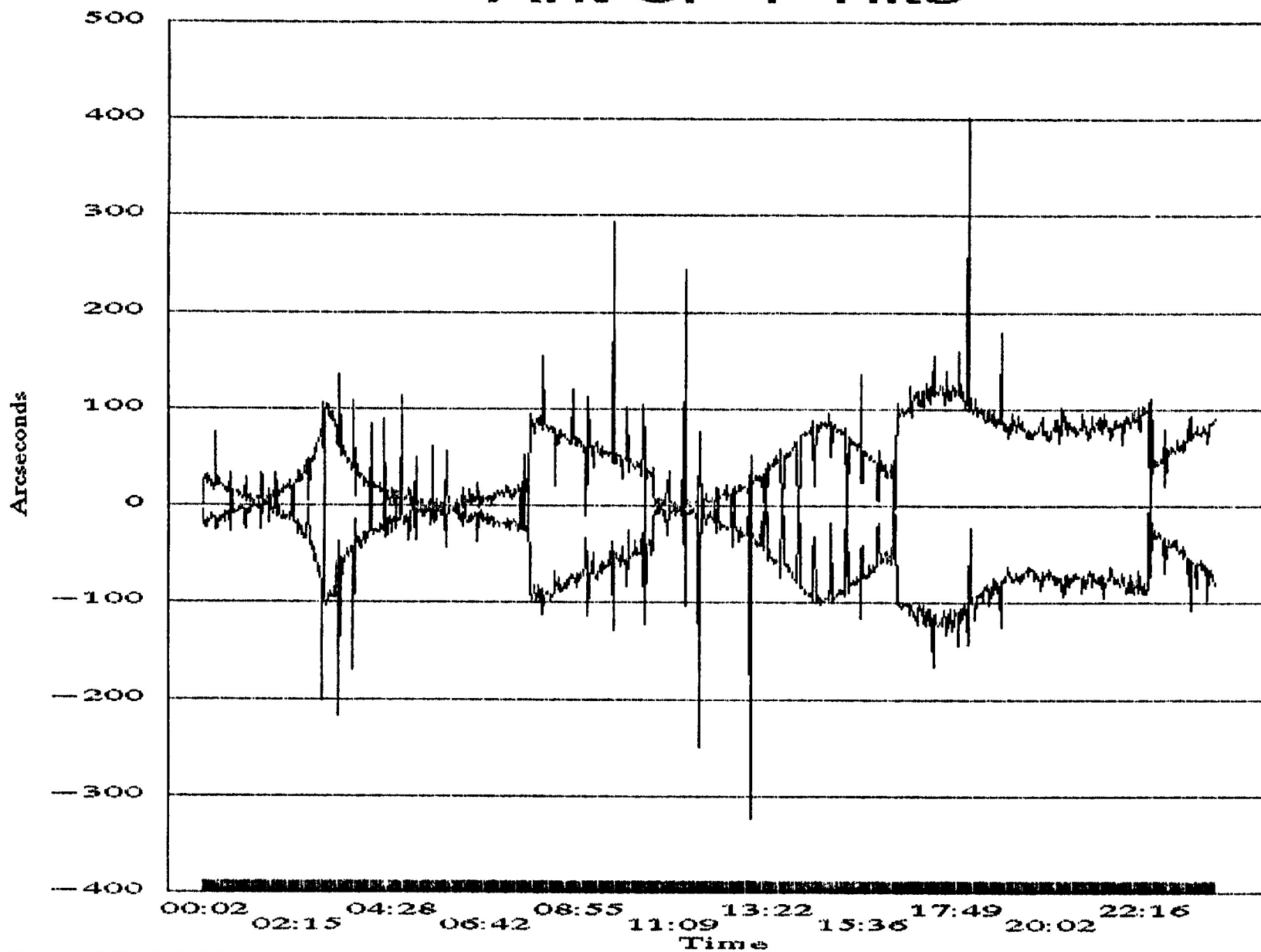
# Antenna 22: El Encoder Study

Variation of El at stow



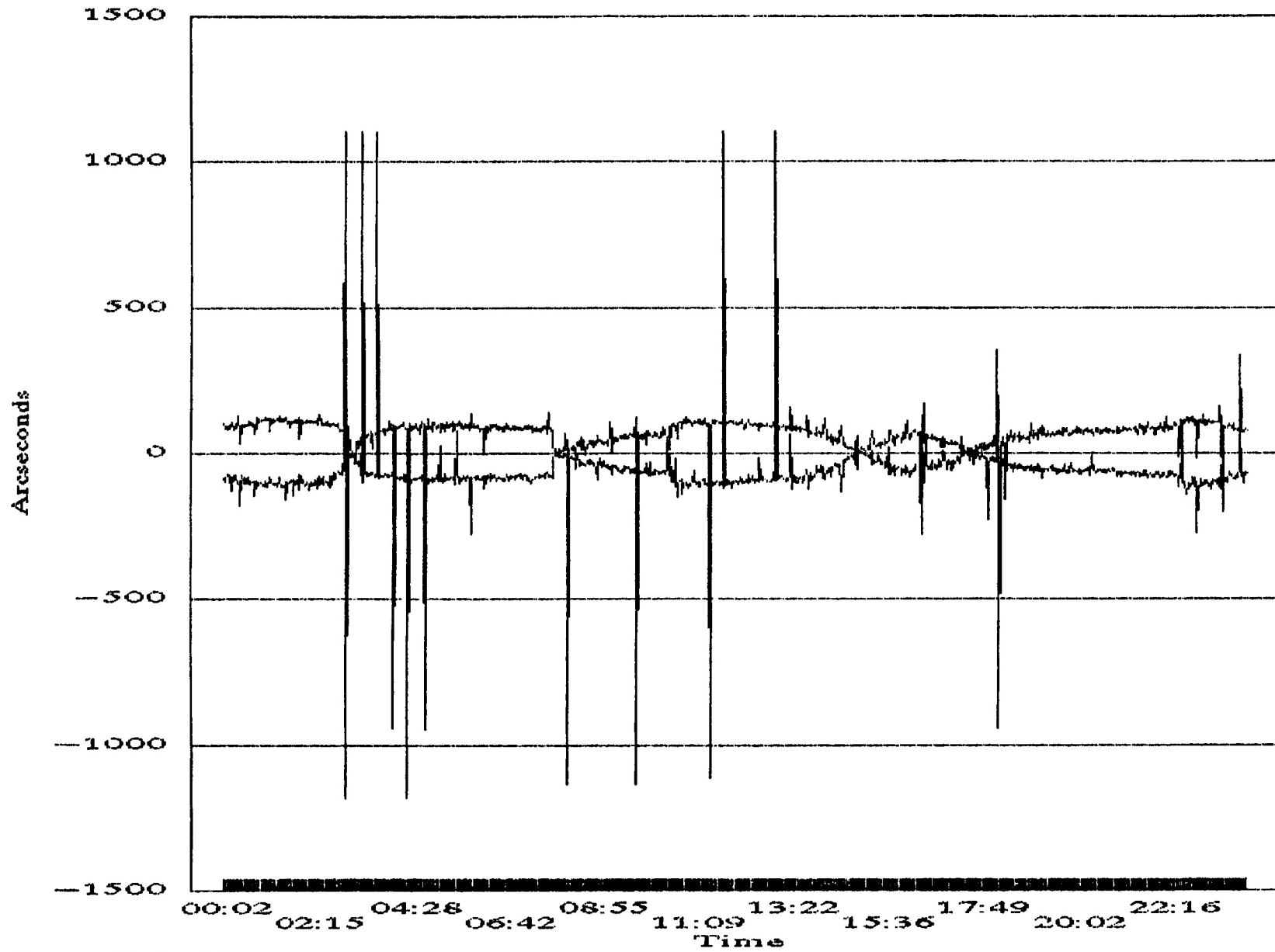
DATA TAKEN 23-24 NOV WITH  
SERVO OFF, BRAKES SET.  
AZ DID NOT CHANGE  
C. JAMES 28 NOV 89

# Ant 6: Y Tilts



Dec 17, 1989  
C. Janes

# Ant 6: X Tilts

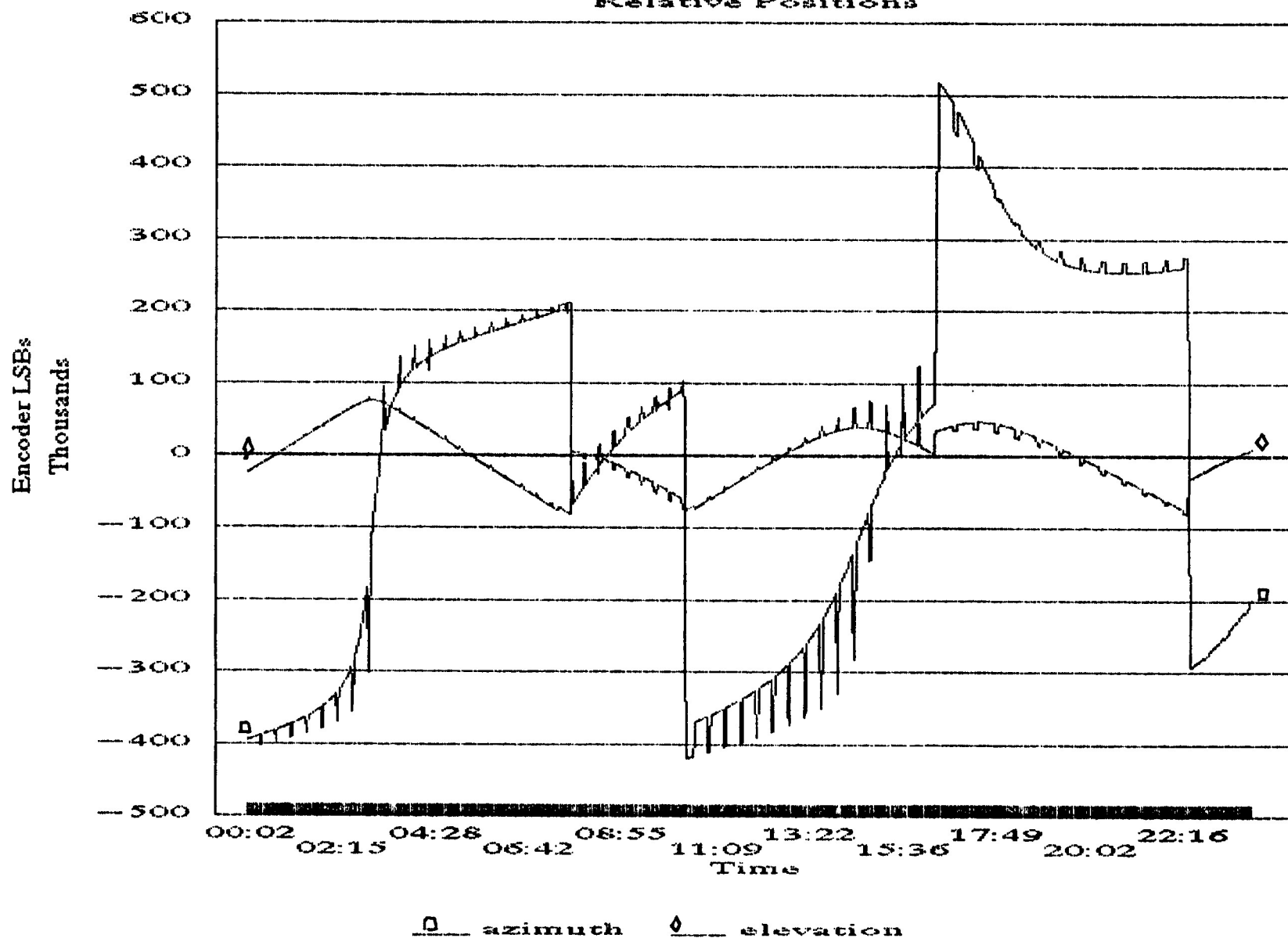


Dec 17, 1989  
C. Jones



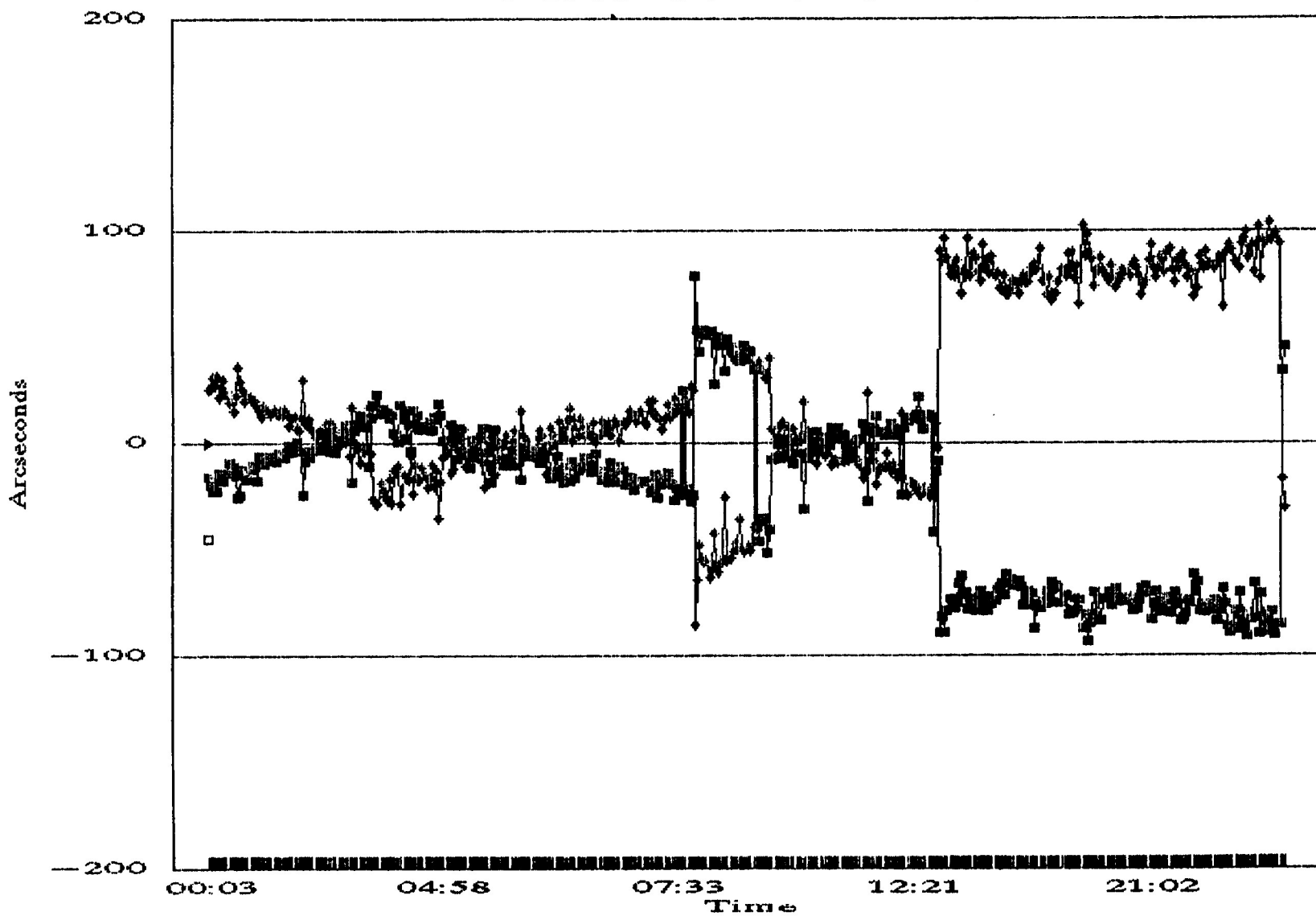
# Ant 6: Antenna Position

## Relative Positions



Dec 17, 1989  
C. Jones

# Ant 6: Y Tilts



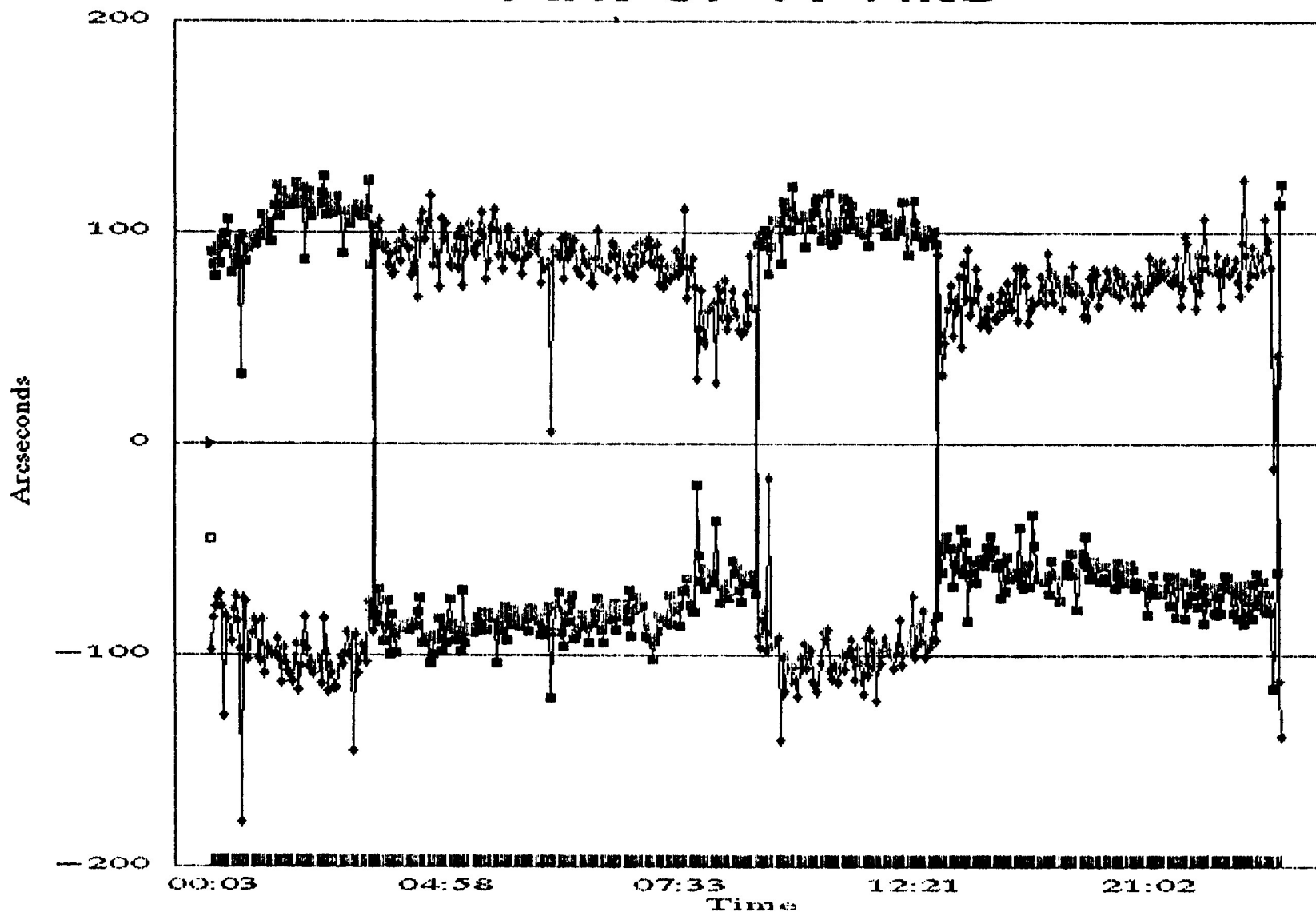
—■— Ey Tilt    —◆— Wy Tilt

Dec 17, 1989

C. Janez

*large telescope motions removed*

# Ant 6: X Tilts

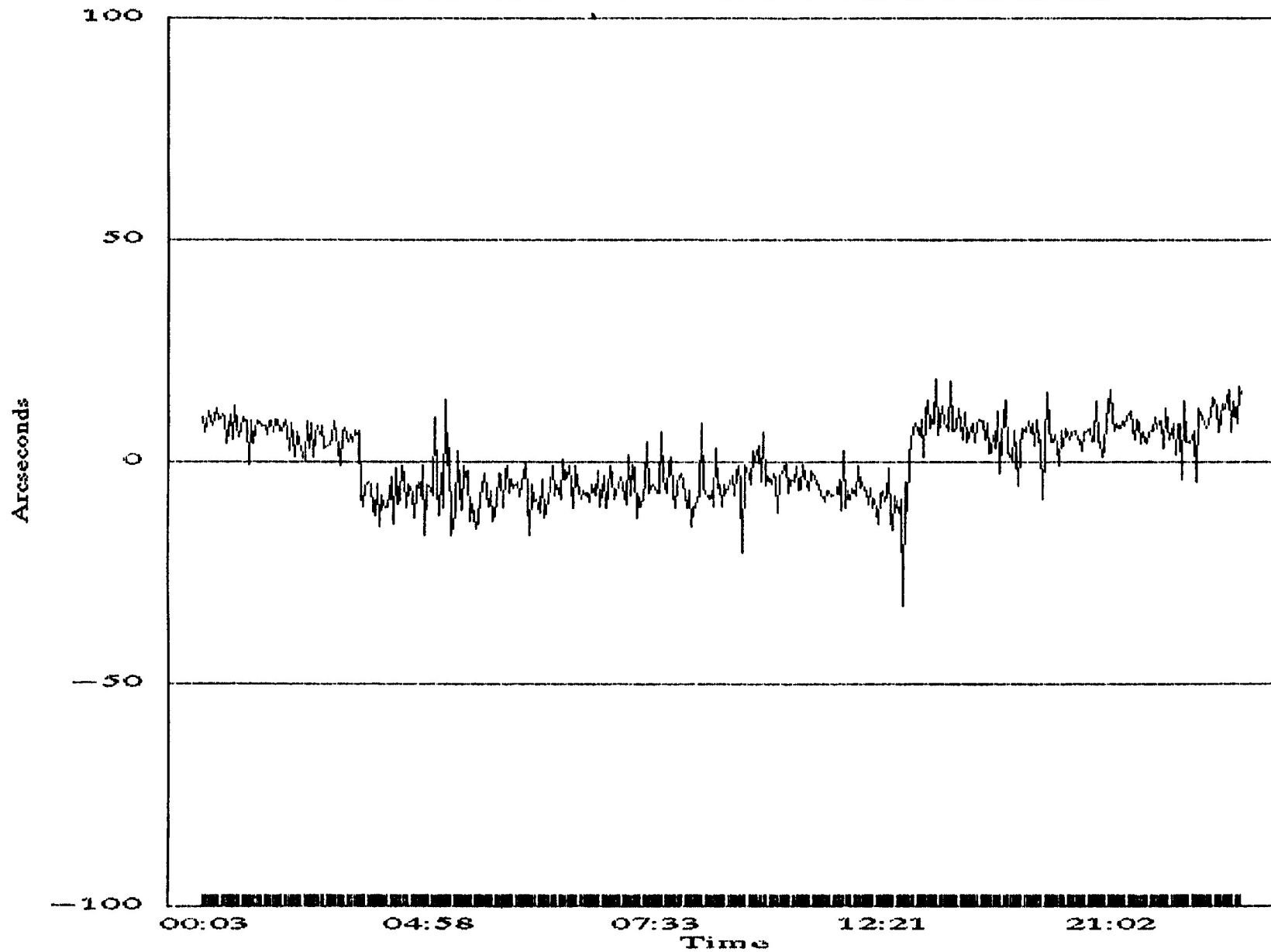


—■— Ex Tilts    —◆— Ws Tilts

Dec 17, 1969  
C. Jones

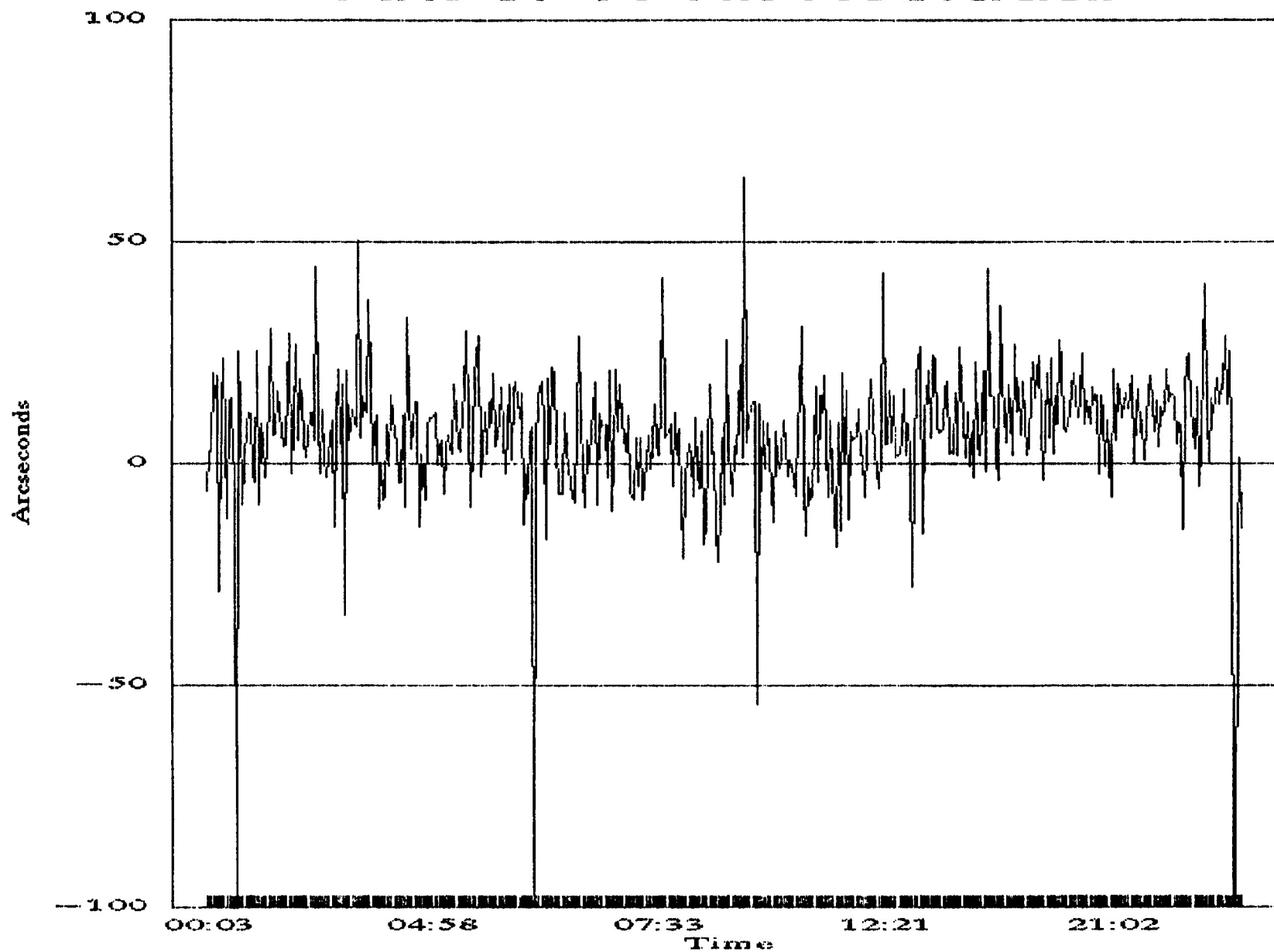
*Large telescope motions removed*

# Ant 6: Y Tilt Residual



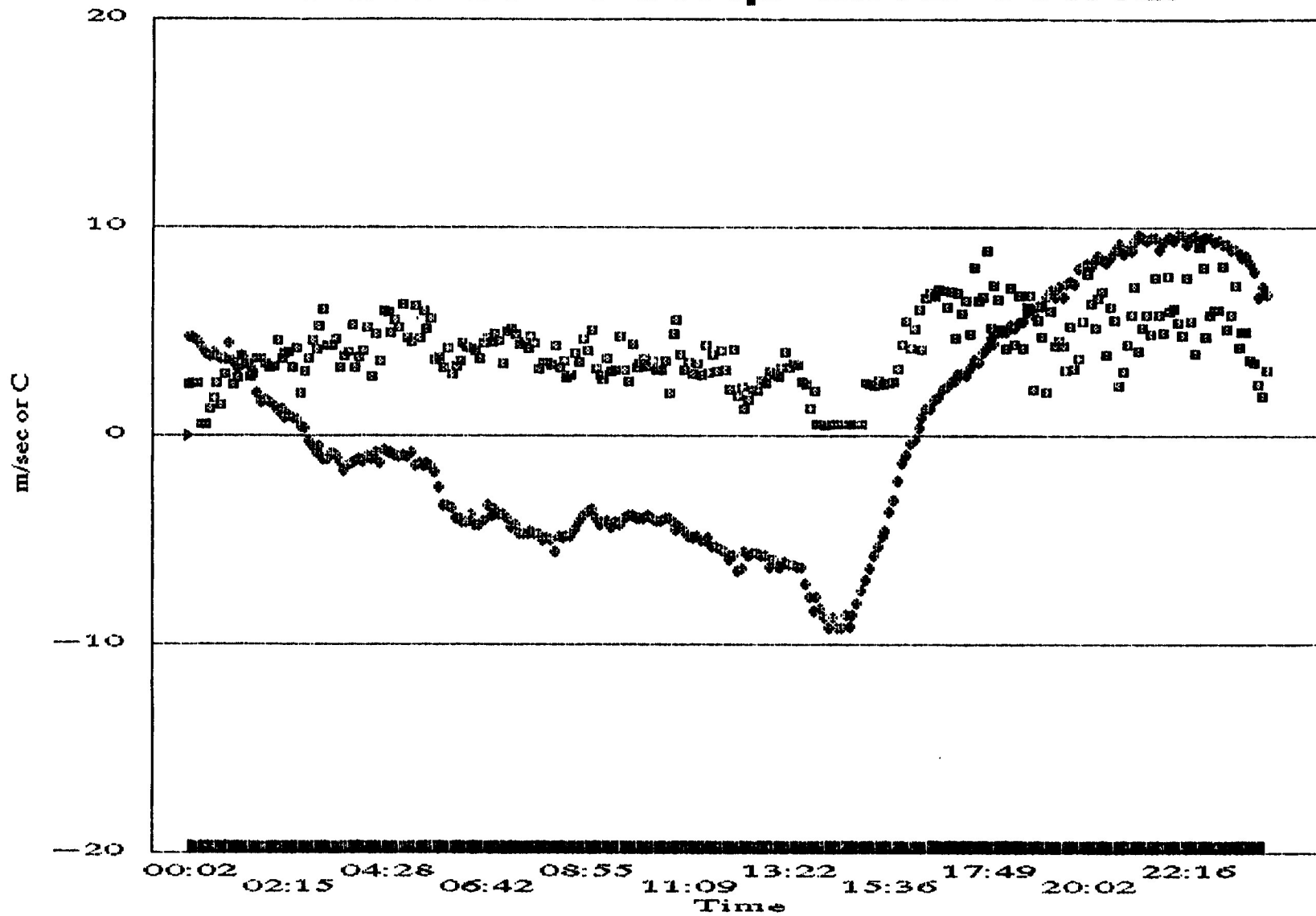
Large telescope motions removed  
C. Janes, Dec. 17, 1989

# Ant 6: X Tilt Residual



Large telescope motions removed  
C. Janes, Dec 17, 1989

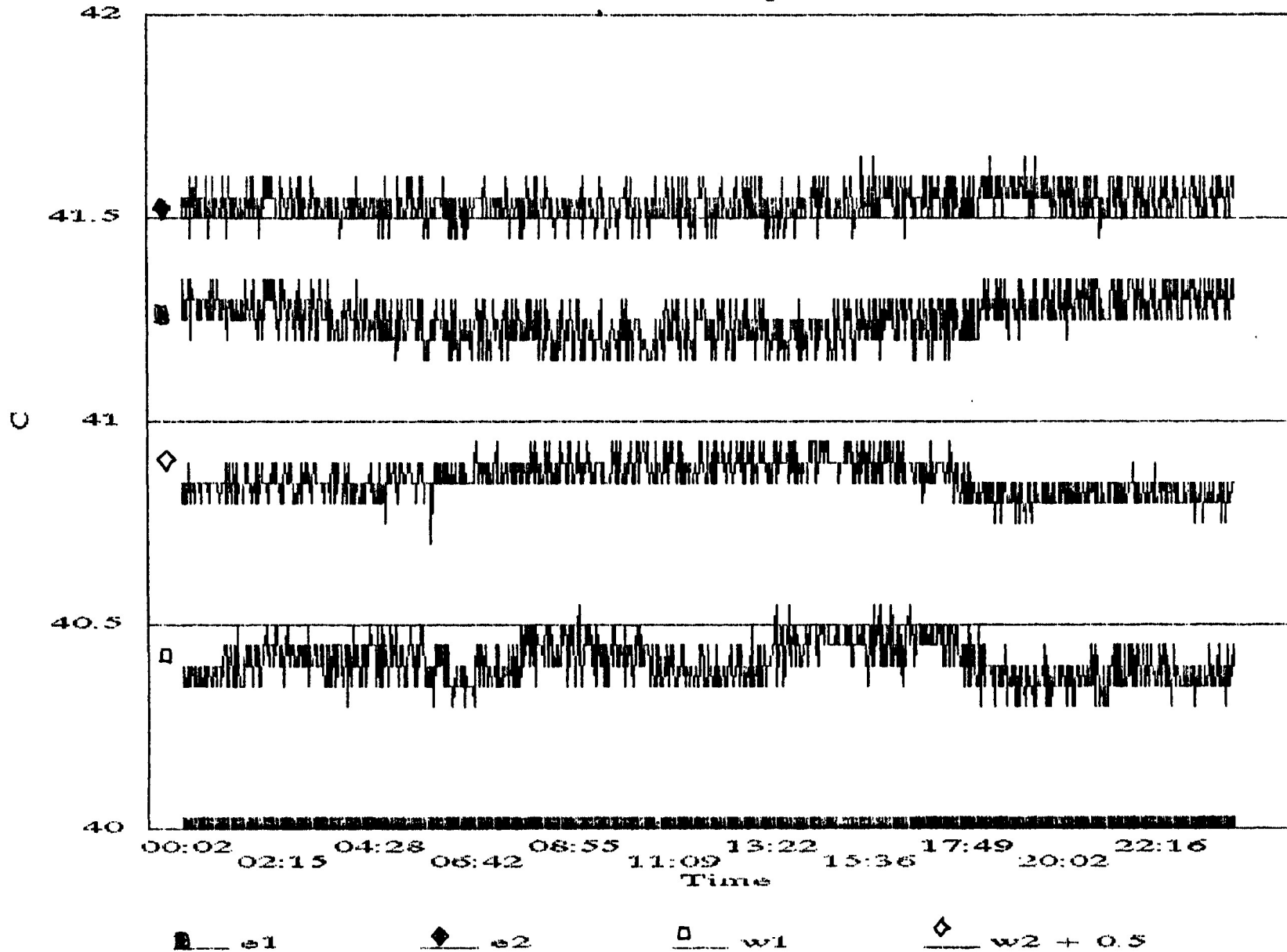
# Ant 6: Temp and Wind



■ Wind in m/sec    ● Temp in C

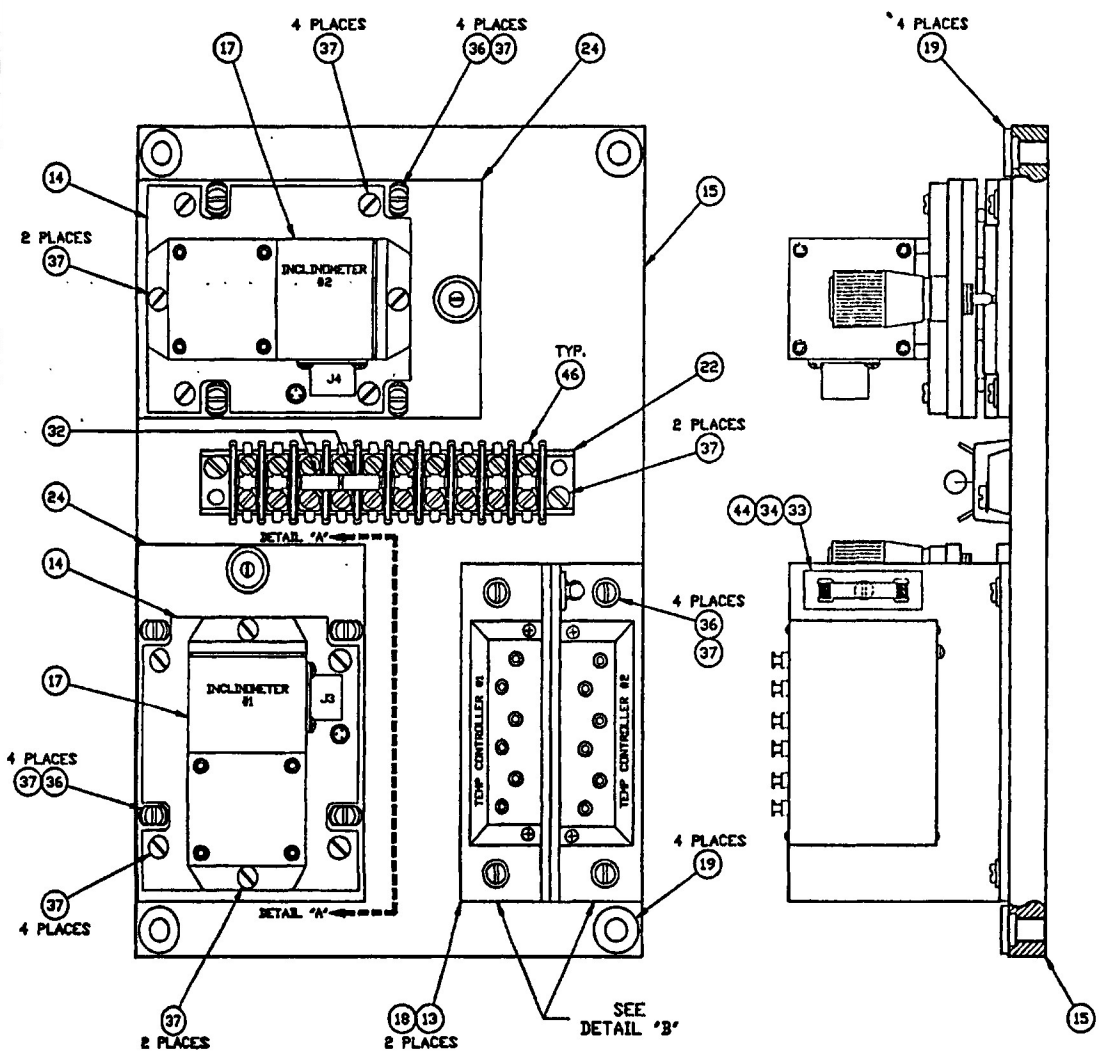
Dec 17, 1989  
C. Janes

# Ant 6: Temperatures



Temperature sensors (tilt meters)  
C. Janes, 17 Dec 89

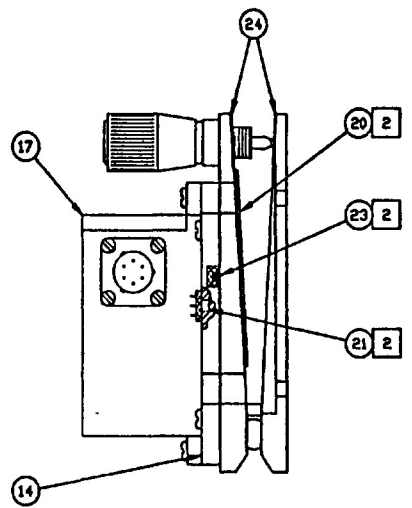
REV	DATE	DRAWN BY	APPRVD BY	DESCRIPTION
A	2-89	ANDREATTA		REDRAWN:



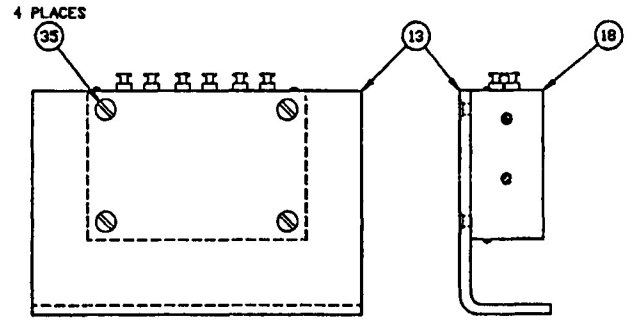
**BASEPLATE ASSEMBLY**  
SCALE 1/1

**NOTES :**

1. APPLY HEAT SINK COMPOUND BETWEEN THE TILT TABLE AND THE INCLINOMETER MOUNTING BASE AND BETWEEN THE INCLINOMETER MOUNTING BASE AND THE INCLINOMETER.
2. USE MINCO #6 RUBBER ADHESIVE TO INSTALL HEATERS (CONSTRUCTIONS ENCLOSED) AND TEMP SENSORS.



**DETAIL "A-A"**  
TYP. FOR BOTH INCLINOMETERS  
SCALE 1/1



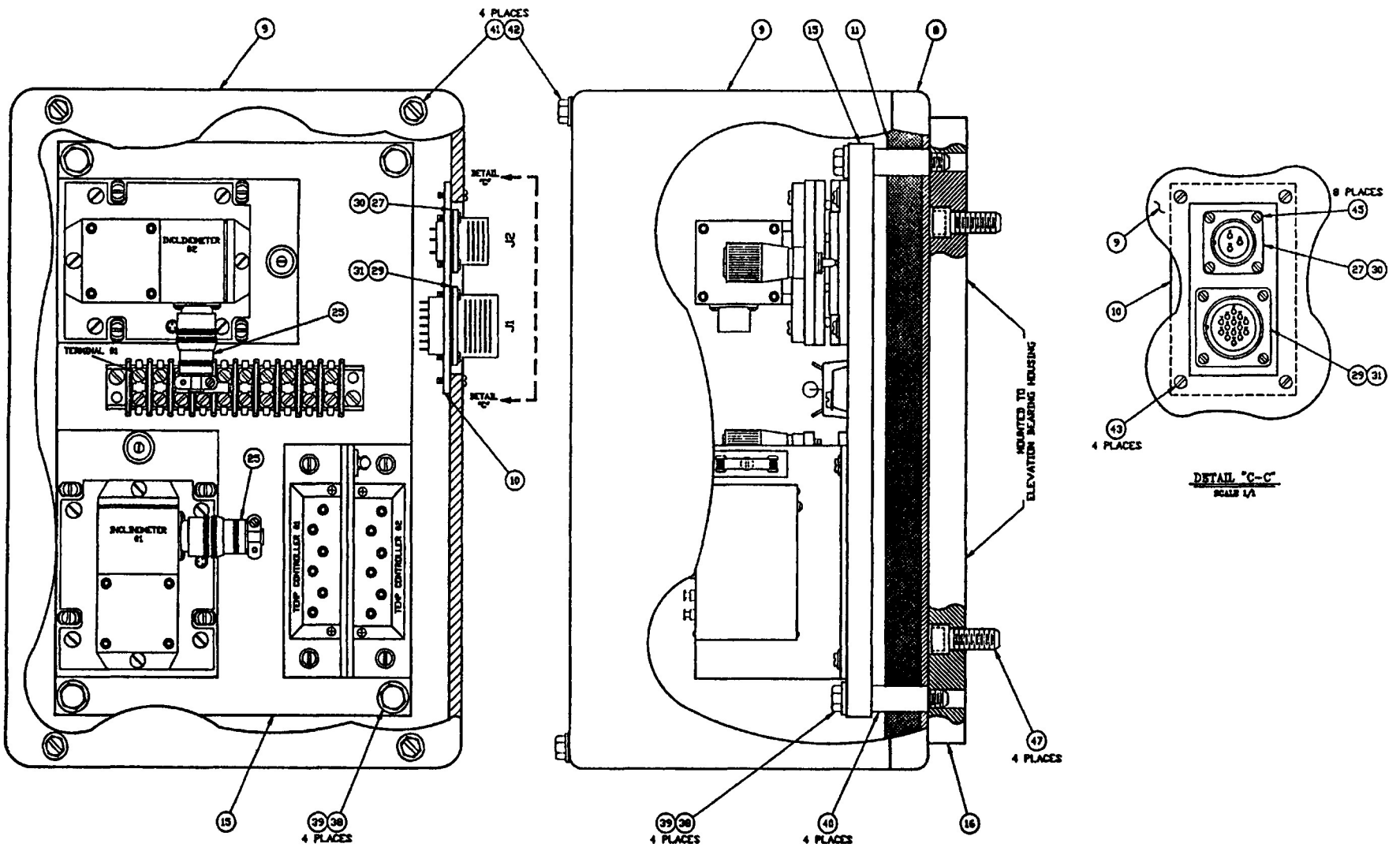
**DETAIL "B"**  
SCALE 1/1

BOM : #A13721Z08

UNLESS OTHERWISE SPECIFIED DIMENSIONS ARE IN INCHES TOLERANCES ANGLES & — 3 PLACE DECIMALS (.000) & — 2 PLACE DECIMALS (.00) & — FRACTIONS (1/32) & —	V L A	<b>TILTMETER</b>		<b>NATIONAL RADIO ASTRONOMY OBSERVATORY</b>	
		TILTMETER MOUNT ASSEMBLY		SOCORRO, NEW MEXICO 87801	
MATERIAL: _____		DRAWN BY ANDREATTA	DATE 10-87	DESIGNED BY KRISHNAN	DATE 10-87
FINISH: _____		APPROVED BY _____	DATE _____		
SHEET 1 of 2		DRAWING NUMBER D13721P88	REV. A	SCALE 1/1	



REV	DATE	DRAWN BY	APPR'D BY	DESCRIPTION
A	2-89	ANDREATA		REDRAWN

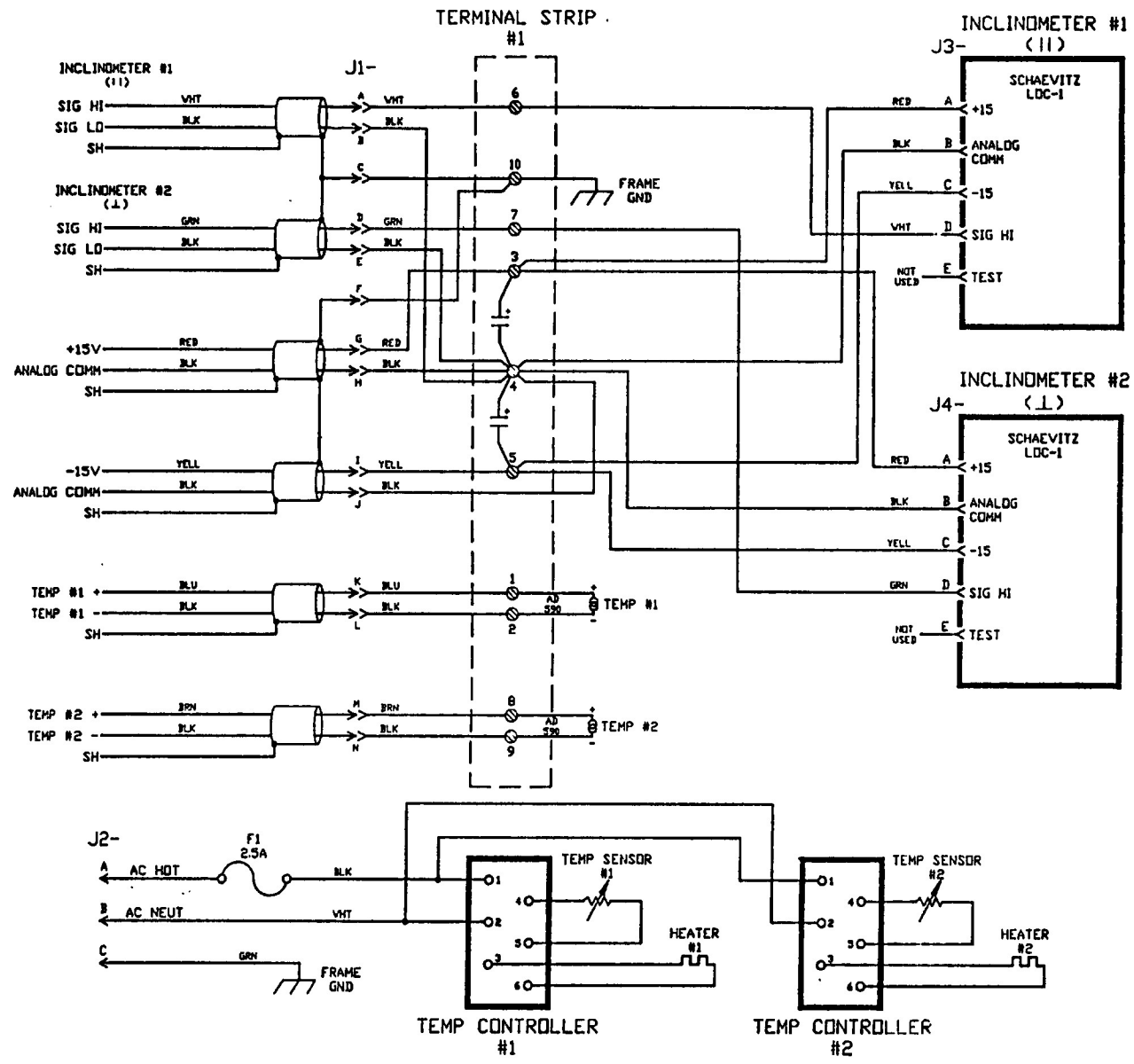


BOM : #A13721Z08

UNLESS OTHERWISE SPECIFIED DIMENSIONS ARE IN INCHES TOLERANCES: ANGLES ± _____ 3 PLACE DECIMALS (.000) ± _____ 2 PLACE DECIMALS (.100) ± _____ FRACTIONS (1/32) ± _____	V L A	TILTMETER	NATIONAL RADIO ASTRONOMY OBSERVATORY	
		TILTMETER MOUNT ASSEMBLY	SOCORRO, NEW MEXICO 87601	
MATERIAL: _____		DESIGNED BY ANDREATA	DATE 10-87	
FINISH: _____		DESIGNED BY KRISHNAN	DATE 10-87	
		APPROVED BY	DATE	
	3107 NUMBER 2 of 2	DRAWING NUMBER D13721P88	REV. A	SCALE 1/1

D  
C  
B  
A

D  
C  
B  
A



ACAD - INCLSKEM

NEXT ASSY	USED ON

UNLESS OTHERWISE SPECIFIED  
 DIMENSIONS ARE IN INCHES  
 TOLERANCES: ANGLES ± —  
 3 PLACE DECIMALS (XXX) ± —  
 2 PLACE DECIMALS (XX) ± —  
 1 PLACE DECIMALS (X) ± —

MATERIAL: \_\_\_\_\_  
 FINISH: \_\_\_\_\_

V L A	TILTMETER	NATIONAL RADIO ASTRONOMY OBSERVATORY SOCORRO, NEW MEXICO 87801	DATE 12-85
	TILTMETER SCHEMATIC		DESIGNED BY ZAMORA DATE 11-85
SHEET NUMBER 1 OF 1		DRAWING NUMBER C13720526	REV. SCALE —

DRAWING NO. 731-44272

D

D

C

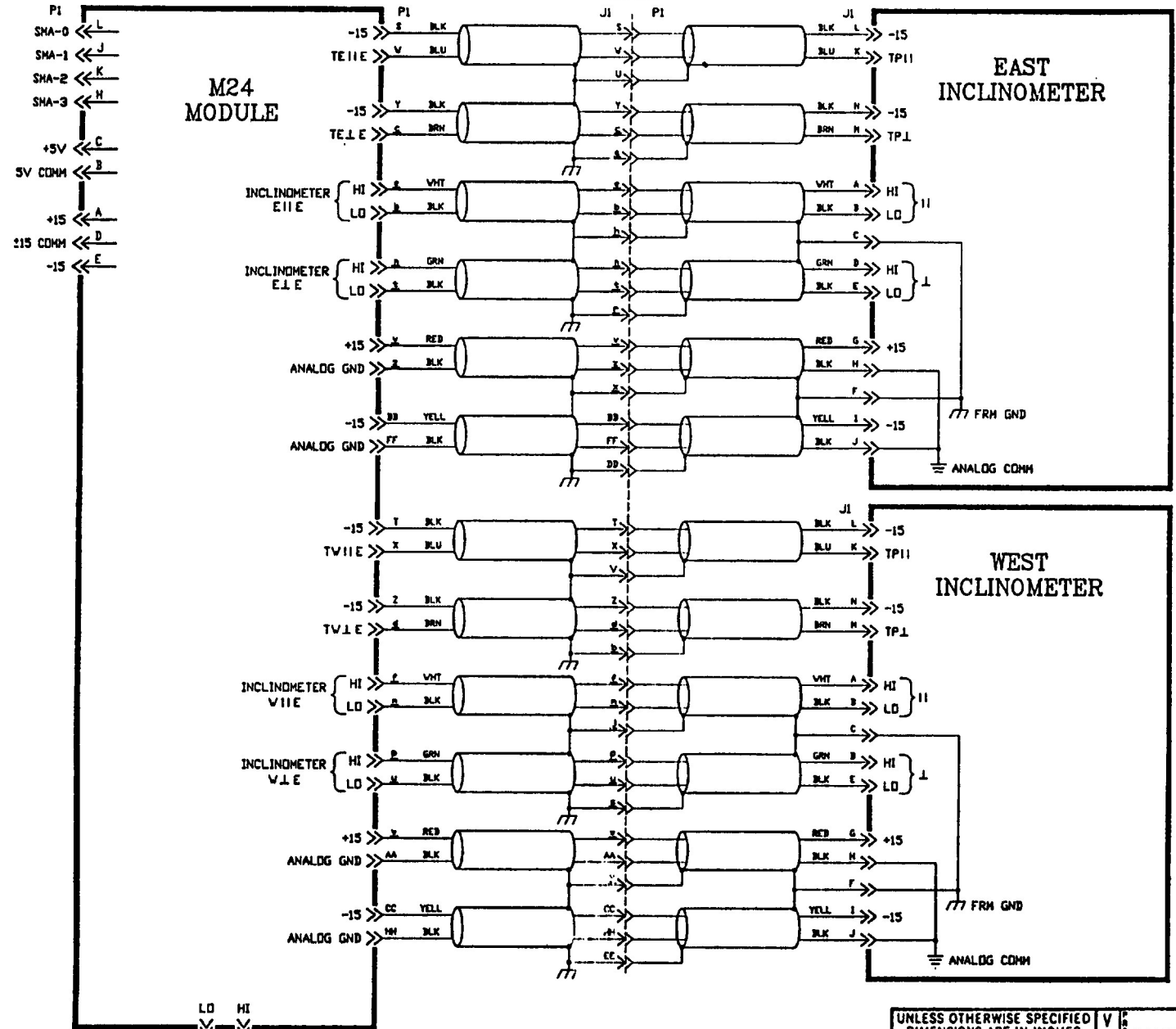
C

B

B

A

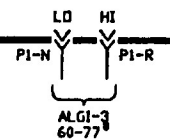
A



M24  
MODULE

EAST  
INCLINOMETER

WEST  
INCLINOMETER



ACAD INCLCABL

UNLESS OTHERWISE SPECIFIED  
DIMENSIONS ARE IN INCHES  
TOLERANCES: ANGLES ±  
3 PLACE DECIMALS (XXX) ±  
2 PLACE DECIMALS (XX) ±  
1 PLACE DECIMALS (X) ±

V L  
P  
O  
J  
E  
C  
T  
I  
C  
A  
INCLINOMETER  
CABLE  
WIRE DIAGRAM

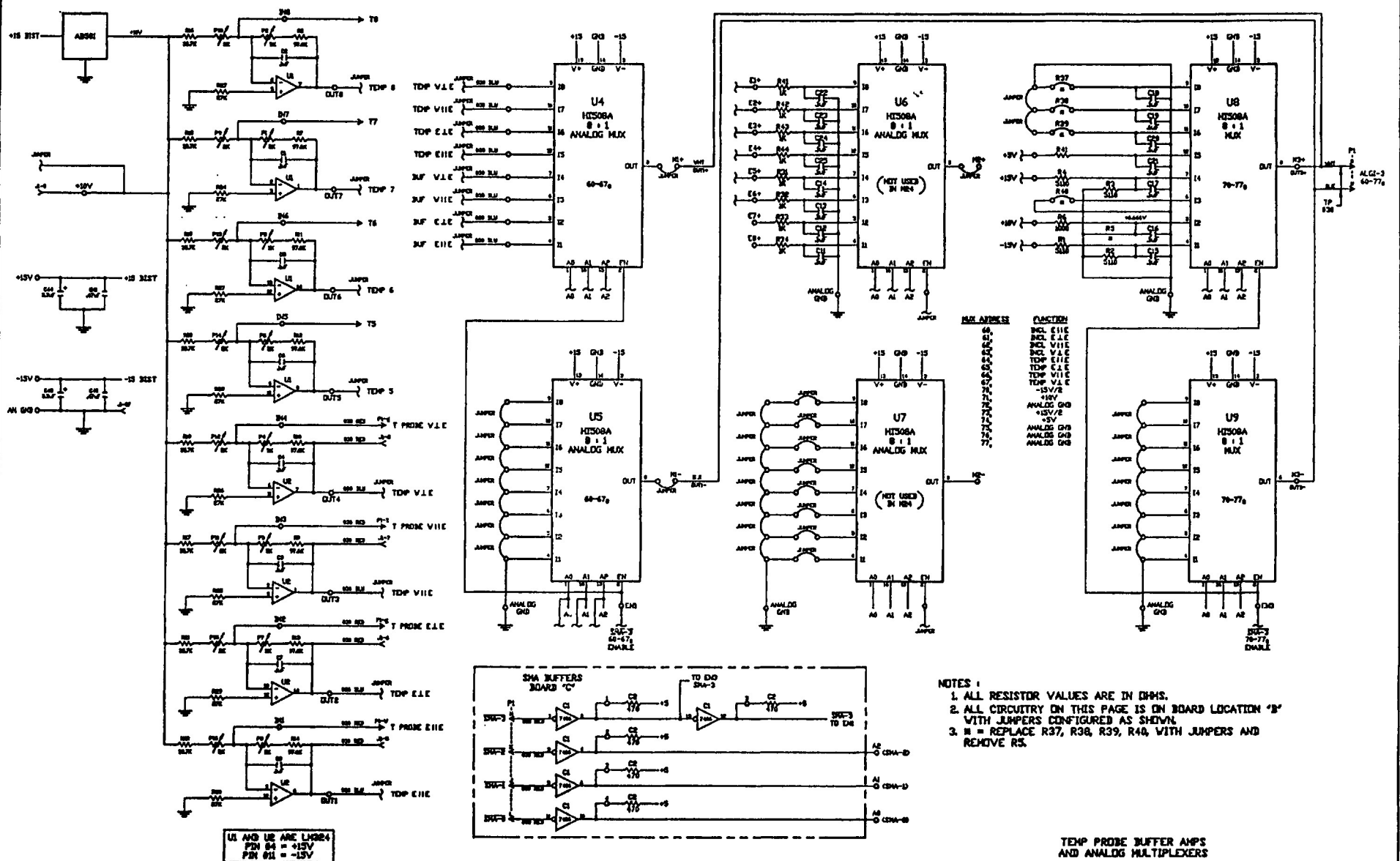
NATIONAL RADIO  
ASTRONOMY  
OBSERVATORY  
SOLICOND, NEW MEXICO 87801

DRAWN BY ANDREATA	DATE 4-89
DESIGNED BY WEBER	DATE 4-89
APPROVED BY	DATE

NEXT ASSY	USED ON

MATERIAL:  
\_\_\_\_\_  
FINISH:  
\_\_\_\_\_

REV	DATE	DRAWN BY	APPRVD BY	DESCRIPTION
A	12-89	ANDREATTA		REDRAWN WITH ACAD;

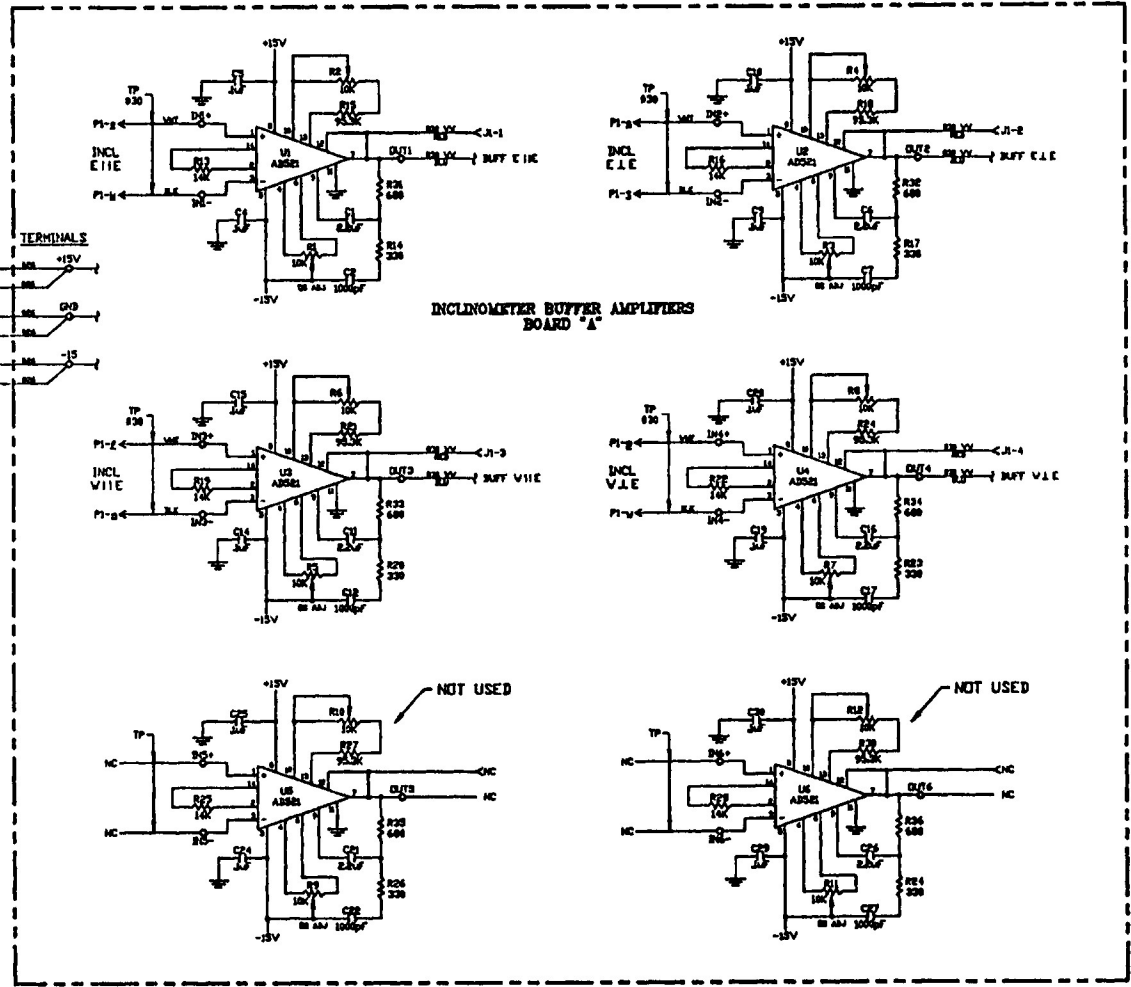
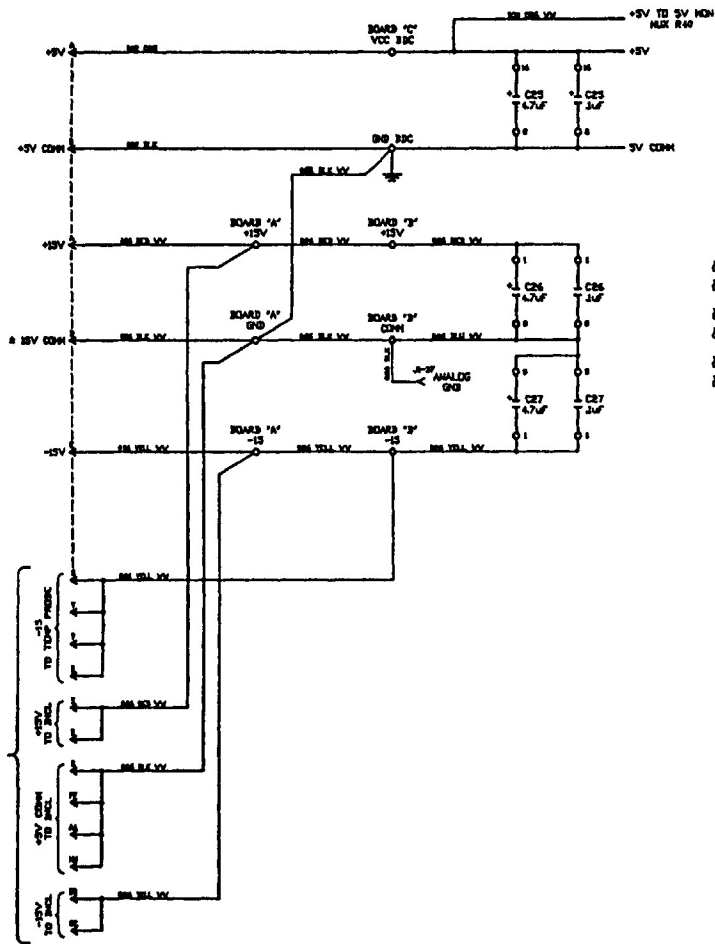


UNLESS OTHERWISE SPECIFIED DIMENSIONS ARE IN INCHES TOLERANCES ANGLES & 3 PLACE DECIMALS (.000) & 5 PLACE DECIMALS (.00000) & FRACTIONS (1/2) &	MATERIAL: _____ FINISH: _____	M24 INCLINOMETER INTERFACE SCHEMATIC	NATIONAL RADIO ASTRONOMY OBSERVATORY SOCORRO, NEW MEXICO 87801
			DRYEN BY WEBER DESIGNED BY WEBER APPROVED BY _____ DATE 3-89 DATE 3-89 DATE _____ REV. A SCALE

Sheet Number 1 of 2    Drawing Number D13720S29

REV	DATE	DRAWN BY	APPRVD BY	DESCRIPTION
A	12-89	ANDREATA		REDRAWN WITH ACAD;

**POWER DISTRIBUTION WIRING**



TO INCLINOMETER BUSES

**INCLINOMETER BUFFER AMPLIFIERS**

UNLESS OTHERWISE SPECIFIED DIMENSIONS ARE IN INCHES TOLERANCES: DIMENSIONS <math>0.125</math> & <math>0.250</math> & <math>0.375</math> & <math>0.500</math> & <math>0.625</math> & <math>0.750</math> & <math>1.000</math> & <math>1.250</math> & <math>1.500</math> & <math>1.750</math> & <math>2.000</math> & <math>2.500</math> & <math>3.000</math> & <math>3.500</math> & <math>4.000</math> & <math>4.500</math> & <math>5.000</math> & <math>5.500</math> & <math>6.000</math> & <math>6.500</math> & <math>7.000</math> & <math>7.500</math> & <math>8.000</math> & <math>8.500</math> & <math>9.000</math> & <math>9.500</math> & <math>10.000</math> & <math>10.500</math> & <math>11.000</math> & <math>11.500</math> & <math>12.000</math> & <math>12.500</math> & <math>13.000</math> & <math>13.500</math> & <math>14.000</math> & <math>14.500</math> & <math>15.000</math> & <math>15.500</math> & <math>16.000</math> & <math>16.500</math> & <math>17.000</math> & <math>17.500</math> & <math>18.000</math> & <math>18.500</math> & <math>19.000</math> & <math>19.500</math> & <math>20.000</math> & <math>20.500</math> & <math>21.000</math> & <math>21.500</math> & <math>22.000</math> & <math>22.500</math> & <math>23.000</math> & <math>23.500</math> & <math>24.000</math> & <math>24.500</math> & <math>25.000</math> & <math>25.500</math> & <math>26.000</math> & <math>26.500</math> & <math>27.000</math> & <math>27.500</math> & <math>28.000</math> & <math>28.500</math> & <math>29.000</math> & <math>29.500</math> & <math>30.000</math> & <math>30.500</math> & <math>31.000</math> & <math>31.500</math> & <math>32.000</math> & <math>32.500</math> & <math>33.000</math> & <math>33.500</math> & <math>34.000</math> & <math>34.500</math> & <math>35.000</math> & <math>35.500</math> & <math>36.000</math> & <math>36.500</math> & <math>37.000</math> & <math>37.500</math> & <math>38.000</math> & <math>38.500</math> & <math>39.000</math> & <math>39.500</math> & <math>40.000</math> & <math>40.500</math> & <math>41.000</math> & <math>41.500</math> & <math>42.000</math> & <math>42.500</math> & <math>43.000</math> & <math>43.500</math> & <math>44.000</math> & <math>44.500</math> & <math>45.000</math> & <math>45.500</math> & <math>46.000</math> & <math>46.500</math> & <math>47.000</math> & <math>47.500</math> & <math>48.000</math> & <math>48.500</math> & <math>49.000</math> & <math>49.500</math> & <math>50.000</math> & <math>50.500</math> & <math>51.000</math> & <math>51.500</math> & <math>52.000</math> & <math>52.500</math> & <math>53.000</math> & <math>53.500</math> & <math>54.000</math> & <math>54.500</math> & <math>55.000</math> & <math>55.500</math> & <math>56.000</math> & <math>56.500</math> & <math>57.000</math> & <math>57.500</math> & <math>58.000</math> & <math>58.500</math> & <math>59.000</math> & <math>59.500</math> & <math>60.000</math> & <math>60.500</math> & <math>61.000</math> & <math>61.500</math> & <math>62.000</math> & <math>62.500</math> & <math>63.000</math> & <math>63.500</math> & <math>64.000</math> & <math>64.500</math> & <math>65.000</math> & <math>65.500</math> & <math>66.000</math> & <math>66.500</math> & <math>67.000</math> & <math>67.500</math> & <math>68.000</math> & <math>68.500</math> & <math>69.000</math> & <math>69.500</math> & <math>70.000</math> & <math>70.500</math> & <math>71.000</math> & <math>71.500</math> & <math>72.000</math> & <math>72.500</math> & <math>73.000</math> & <math>73.500</math> & <math>74.000</math> & <math>74.500</math> & <math>75.000</math> & <math>75.500</math> & <math>76.000</math> & <math>76.500</math> & <math>77.000</math> & <math>77.500</math> & <math>78.000</math> & <math>78.500</math> & <math>79.000</math> & <math>79.500</math> & <math>80.000</math> & <math>80.500</math> & <math>81.000</math> & <math>81.500</math> & <math>82.000</math> & <math>82.500</math> & <math>83.000</math> & <math>83.500</math> & <math>84.000</math> & <math>84.500</math> & <math>85.000</math> & <math>85.500</math> & <math>86.000</math> & <math>86.500</math> & <math>87.000</math> & <math>87.500</math> & <math>88.000</math> & <math>88.500</math> & <math>89.000</math> & <math>89.500</math> & <math>90.000</math> & <math>90.500</math> & <math>91.000</math> & <math>91.500</math> & <math>92.000</math> & <math>92.500</math> & <math>93.000</math> & <math>93.500</math> & <math>94.000</math> & <math>94.500</math> & <math>95.000</math> & <math>95.500</math> & <math>96.000</math> & <math>96.500</math> & <math>97.000</math> & <math>97.500</math> & <math>98.000</math> & <math>98.500</math> & <math>99.000</math> & <math>99.500</math> & <math>100.000</math>	M24 INCLINOMETER INTERFACE	NATIONAL RADIO ASTRONOMY OBSERVATORY SOCORRO, NEW MEXICO 87801			
			MATERIAL:	DRAWN BY WEBER	DATE 3-89
			FINISH:	DESIGNED BY WEBER	DATE 3-89

# App A. Manufacturer's specs

Schaevitz LSOC-1

## INCLINOMETER DATA SHEET

DATE \_\_\_\_\_ TESTED BY: WBYGJ  
 MODEL NO. LSOC-1 APPROVED BY: G.M.  
 SERIAL NO. 24127 CUSTOMER INSP. \_\_\_\_\_  
 CUSTOMER \_\_\_\_\_ GOVT. INSP. \_\_\_\_\_  
 SALES NO. \_\_\_\_\_

CONNECTIONS - SCHAEVITZ DRAWING NO. Pg. 7  
 POWER SUPPLY VOLTAGE(S) ±15 volts  
 POWER SUPPLY CURRENT +10-14 ma  
 FREQUENCY RESPONSE (-3db) 3 cps  
 RANGE 1 degrees  
 FULL RANGE OUTPUT 4.984 volts  
 CROSS AXIS SENSITIVITY .500 volts/g  $6.1g$   
 NOISE .002 volts rms  $1.44\%$   
 LINEARITY 0.05 %  $3.10\%$   
 OUTPUT IMPEDANCE 16.8 K ohms  
 ZERO OFFSET +0.33 volts  
 SCALE FACTOR  
 TEMPERATURE COEFFICIENT .019 %/°C  $1.368\%$   
 NULL TEMPERATURE COEFFICIENT .035 %FS/°C  $2.52\%$   
 TILT APPLIED SO THAT CONNECTOR  
 END IS LOWER CAUSES OUTPUT  
 VOLTAGE TO BECOME MORE  
Pos.  
 MOUNTING DIMENSIONS 2550070-600

$$\frac{4.984V}{-10} = \frac{1.384mV}{1}$$

$$= \frac{0.7223\mu}{mV}$$

Resolution

$$.001\% FS = 0.072\mu$$

Repeatability

$$.01\% FS = 0.72\mu$$

# SPECIFICATIONS

(typical @ +25°C and  $V_S = +5V$  unless otherwise specified)

MODEL	AD590J	AD590K	AD590L
<b>ABSOLUTE MAXIMUM RATINGS</b>			
Forward Voltage (E+ to E-)	+44V	*	*
Reverse Voltage (E+ to E-)	-20V	*	*
Breakdown Voltage (Case to E+ or E-)	±200V	*	*
Rated Performance Temperature Range	-55°C to +150°C	*	*
Storage Temperature Range	-65°C to +175°C	*	*
Lead Temperature (Soldering, 10sec)	+300°C	*	*
<b>POWER SUPPLY</b>			
Operating Voltage Range	+4V to +30V	*	*
<b>OUTPUT</b>			
Nominal Current Output @ +25°C (298.2°K)	298.2μA	*	*
Nominal Temperature Coefficient	1μA/°C	*	*
Calibration Error <sup>1</sup> @ +25°C	±5.0°C max	±2.0°C max	±1.0°C max
Absolute Error <sup>1</sup> (-55°C to +150°C)			
Without External Calibration Adjustment	±9.0°C max	±3.8°C max	±2.4°C max
With +25°C Calibration Error Set to Zero	±2.0°C max	±1.0°C max	**
Nonlinearity <sup>1</sup> (-55°C to +150°C)	±2.0°C max	±0.5°C max	**
Current Noise	40pA/√Hz	*	*
Power Supply Rejection			
+4V ≤ $V_S$ ≤ +5V	0.5μA/V	*	*
+5V ≤ $V_S$ ≤ +15V	0.2μA/V	*	*
+15V ≤ $V_S$ ≤ +30V	0.1μA/V	*	*
Case Isolation to Either Lead	10 <sup>10</sup> Ω	*	*
Effective Shunt Capacitance	100pF	*	*
Electrical Turn-On Time <sup>2</sup>	20μs	*	*
Reverse Bias Leakage Current <sup>3</sup> (Reverse Voltage = 10V)	10pA	*	*

## NOTES:

<sup>1</sup> See error explanations page.

<sup>2</sup> Does not include self-heating effects; see page on explanation of these effects.

<sup>3</sup> Leakage current doubles every 10°C.

\*Specifications same as AD590J.

\*\*Specifications same as AD590K.

Specifications subject to change without notice.

# SPECIFICATIONS

(typical @  $V_S = \pm 15V$ ,  $R_L = 2k\Omega$  and  $T_A = 25^\circ C$  unless otherwise specified)

MODEL	AD521J	AD521K	AD521S
<b>GAIN</b>			
Range (For Specified Operation, Note 1)	1 to 1000	•	•
Equation	$G = R_4/R_G$ V/V	•	•
Error from Equation	( $\pm 0.25 - 0.004G$ )%	•	•
Nonlinearity (Note 2)	•	•	•
$1 \leq G \leq 1000$	0.1% max	•	•
Gain Temperature Coefficient	$\pm (3 \pm 0.05G)$ ppm/ $^\circ C$	•	$\pm (15 \pm 0.4G)$ ppm/ $^\circ C$
<b>OUTPUT CHARACTERISTICS</b>			
Rated Output	$\pm 10V$ , $\pm 10mA$ min	•	•
Output at Maximum Operating Temperature	$\pm 10V$ @ $5mA$ min	•	•
Impedance	$0.1\Omega$	•	•
<b>DYNAMIC RESPONSE</b>			
<b>Small Signal Bandwidth (<math>\pm 3dB</math>)</b>			
$G = 1$	$> 2MHz$	•	•
$G = 10$	$300kHz$	•	•
$G = 100$	$200kHz$	•	•
$G = 1000$	$40kHz$	•	•
<b>Small Signal, <math>\pm 1.0\%</math> Flatness</b>			
$G = 1$	$75kHz$	•	•
$G = 10$	$26kHz$	•	•
$G = 100$	$24kHz$	•	•
$G = 1000$	$6kHz$	•	•
<b>Full Peak Response (Note 3)</b>			
<b>Slew Rate, <math>1 \leq G \leq 1000</math></b>			
<b>Settling Time (any 10V step to within 10mV of Final Value)</b>			
$G = 1$	$7\mu s$	•	•
$G = 10$	$5\mu s$	•	•
$G = 100$	$10\mu s$	•	•
$G = 1000$	$35\mu s$	•	•
<b>Differential Overload Recovery (<math>\pm 30V</math> Input to within 10mV of Final Value) (Note 4)</b>			
$G = 1000$	$50\mu s$	•	•
<b>Common Mode Step Recovery (30V Input to within 10mV of Final Value) (Note 5)</b>			
$G = 1000$	$10\mu s$	•	•
<b>VOLTAGE OFFSET (may be nulled)</b>			
<b>Input Offset Voltage (<math>V_{OS1}</math>)</b>			
vs. Temperature	$3mV$ max ( $2mV$ typ) $15\mu V/^\circ C$ max ( $7\mu V/^\circ C$ typ)	$1.5mV$ max ( $0.5mV$ typ) $5\mu V/^\circ C$ max ( $1.5\mu V/^\circ C$ typ)	**
vs. Supply	$3\mu V/\%$	•	•
<b>Output Offset Voltage (<math>V_{OS0}</math>)</b>			
vs. Temperature	$400mV$ max ( $200mV$ typ) $400\mu V/^\circ C$ max ( $150\mu V/^\circ C$ typ)	$200mV$ max ( $30mV$ typ) $150\mu V/^\circ C$ max ( $50\mu V/^\circ C$ typ)	**
vs. Supply (Note 6)	$0.005V_{OSN}/\%$	•	•
<b>INPUT CURRENTS</b>			
<b>Input Bias Current (either input)</b>			
vs. Temperature	$80nA$ max $1nA/^\circ C$ max	$40nA$ max $500pA/^\circ C$ max	**
vs. Supply	$2\%/V$	•	•
<b>Input Offset Current</b>			
vs. Temperature	$20nA$ max $250pA/^\circ C$ max	$10nA$ max $125pA/^\circ C$ max	**
<b>INPUT</b>			
<b>Differential Input Impedance (Note 7)</b>			
<b>Common Mode Input Impedance (Note 8)</b>			
<b>Input Voltage Range for Specified Performance</b>			
<b>Maximum Voltage without Damage to Unit, Power ON or OFF Differential Mode (Note 9)</b>			
<b>Voltage at either input (Note 10)</b>			
<b>Common Mode Rejection Ratio, DC to 60Hz with 1k<math>\Omega</math> source unbalance</b>			
$G = 1$	$70dB$ min ( $74dB$ typ)	$74dB$ min ( $80dB$ typ)	**
$G = 10$	$90dB$ min ( $94dB$ typ)	$94dB$ min ( $100dB$ typ)	**
$G = 1000$	$100dB$ min ( $104dB$ typ)	$104dB$ min ( $114dB$ typ)	**
$G = 1000$	$100dB$ min ( $110dB$ typ)	$110dB$ min ( $120dB$ typ)	**
<b>NOISE</b>			
<b>Voltage RTO (p-p) @ 0.1Hz to 10Hz (Note 10)</b>			
<b>RMS RTO, 10Hz to 10kHz</b>			
<b>Input Current, rms, 10Hz to 10kHz</b>			
<b>REFERENCE TERMINAL</b>			
<b>Bias Current</b>			
<b>Input Resistance</b>			
<b>Voltage Range</b>			
<b>Gain to Output</b>			
<b>POWER SUPPLY</b>			
<b>Operating Voltage Range</b>			
<b>Quiescent Supply Current</b>			
<b>TEMPERATURE RANGE</b>			
<b>Specified Performance</b>			
<b>Operating</b>			
<b>Storage</b>			

\*Specification same as AD521J.

\*\*Specification same as AD521K.

Specifications and prices  
subject to change without notice.



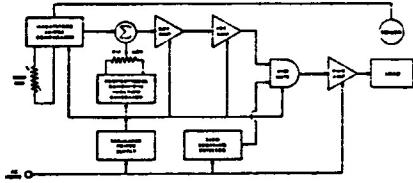
## GENERAL DESCRIPTION

Oven Industries' full proportional, indicating Temperature Controller Series is insensitive to environmental temperature changes and line fluctuations on the control circuit. These units provide excellent temperature control of resistive heaters ranging from 1 ampere to 40 amperes. All 5C5 models are capable of maintaining the desired set temperature to  $\pm 0.05^\circ\text{C}$ . at the probe and 5CX models will maintain  $\pm 0.1^\circ\text{C}$ . at the probe.

The circuit design employed in this series will maintain a set point stability of  $\pm 0.005^\circ\text{C}/^\circ\text{C}$ . with ambient change on the controller over a  $-20^\circ\text{C}$ . to  $+70^\circ\text{C}$ . range. The set point stability with respect to input line change is  $\pm 0.0025^\circ\text{C}/\text{volt}$  of line change between 100VAC and 140VAC or 200 and 240VAC.

Temperature can be adjusted precisely with the ten-turn counting knob with locking device. 1000 numerical increments are available for rapid set temperature change and a calibrated temperature chart may be established for a particular thermal system.

Radio frequency interference is virtually eliminated by the zero voltage firing circuit. Users may operate heater loads supplied from AC sources that also supply other sensitive instruments. Complete solid state design and rugged mechanical construction assures reliable performance and freedom from shock and vibration damage in either shipping or installation.



## THEORY OF OPERATION

All controllers are completely solid state with adequate derating to ensure high reliability and long field service. Referring to the simplified schematic diagram, a thermistor sensor is used in a constant resistance bridge network with a precision potentiometer for set temperature adjustment. The sensing bridge signal is fed to a differential amplifier and then to a variable gain preamplifier and power stage. Zero crossing information is combined with the temperature control signal and this combined signal causes the triac to conduct as the line voltage passes through zero.

These true proportional controllers have the ability to supply fixed power to the load without temperature change at the sensor. Proportioning bandwidth is accomplished by generating a sawtooth signal and summing this signal with the sensor information in a manner which enables the controller to establish the necessary power to the load for each individual time base period. By providing an internal time base of approximately one (1) second, the "on" time is varied as a percent of the total time base which gives the ability to apply as little as one half ( $\frac{1}{2}$ ) cycle out of 60. Thus, the controller will proportion the correct number of "on" cycles and "off" cycles out of every individual time base.

The controller's power resolution of 0.8% is further enhanced by its ability to vary the number of "on" cycles in each successive time base period. (i.e., 35 on, 37 on, 34 on, etc.). A mathematical analysis of this type system will conclude that any level of power between 0% and 100% is possible. End item control temperatures can be as small as  $\pm 0.05^\circ\text{C}$ . with proportional control.

## SPECIFICATIONS

**Accuracy:** \*to  $\pm 0.1^\circ\text{C}$ . of set point at the probe for 5CX models  
to  $\pm 0.05^\circ\text{C}$ . of set point at the probe for 5C5 models

**Control Range:** \*From  $-65^\circ\text{C}$ . to  $+550^\circ\text{C}$ . ( $-85^\circ\text{F}$ . to  $+1000^\circ\text{F}$ .) for 5CX Models  
From  $-20^\circ\text{C}$ . to  $+110^\circ\text{C}$ . ( $-4^\circ\text{F}$ . to  $+230^\circ\text{F}$ .) for 5C5 Models

**Bandwidth Control:** Adjustable from  $0.25^\circ\text{C}$ . to  $10^\circ\text{C}$ .

**Temperature Set Point:** Ten turn counting potentiometer provides 1000 numerical increments of adjustment.

**Circuit Mode:** Full Proportional Zero Voltage Firing

**Voltage and Power Ratings:** Single Phase 50/60 Hz. (for 400 Hz. operation - see derating curve).

LINE VOLTAGE	MAXIMUM POWER	MAXIMUM CURRENT	MECHANICAL FIGURE	PROBE SERIES	MODEL NUMBER	PRICE
117 VAC	1.75 KW	15 amps	1	TX	*5CX-220	\$109.00
117 VAC	1.75 KW	15 amps	1	TP	5C5-220	109.00
117 VAC	2.92 KW	25 amps	2	TX	*5CX-222	125.40
117 VAC	2.92 KW	25 amps	2	TP	5C5-222	125.40
117 VAC	3.51 KW	30 amps	2	TX	*5CX-224	134.20
117 VAC	3.51 KW	30 amps	2	TP	5C5-224	134.20
117 VAC	4.68 KW	40 amps	2	TX	*5CX-226	159.50
117 VAC	4.68 KW	40 amps	2	TP	5C5-226	159.50
208/230VAC	3.45 KW	15 amps	1	TX	*5CX-230	115.50
208/230VAC	3.45 KW	15 amps	1	TP	5C5-230	115.50
208/230VAC	5.75 KW	25 amps	2	TX	*5CX-232	137.50
208/230VAC	5.75 KW	25 amps	2	TP	5C5-232	137.50
208/230VAC	6.90 KW	30 amps	2	TX	*5CX-234	146.30
208/230VAC	6.90 KW	30 amps	2	TP	5C5-234	146.30
208/230VAC	9.20 KW	40 amps	2	TX	*5CX-236	170.50
208/230VAC	9.20 KW	40 amps	2	TP	5C5-236	170.50

NOTE: (\*) Specifications apply to models similarly marked.